The role of α2δ-3, a subunit of voltage gated calcium channels, in somatosensation and chronic pain.

Dissertation

zur Erlangung des Grades eines Doktors
der Naturwissenschaften

der Mathematisch-Naturwissenschaftlichen Fakultät
und
der Medizinischen Fakultät
der Eberhard-Karls-Universität Tübingen

vorgelegt
von

Florian Mayer

aus Tübingen, Deutschland

Januar-2016

Tag der mündlichen Prüfung: 09.05.2016

Dekan der Math.-Nat. Fakultät: Prof. Dr. W. Rosenstiel
Dekan der Medizinischen Fakultät: Prof. Dr. I. B. Autenrieth

1. Berichterstatter: Dr. J. Hu
2. Berichterstatter: Prof. Dr. M. Knipper

Prüfungskommission: Prof. Dr. M. Knipper
Prof. Dr. J. Engel
Dr. Jing Hu
Prof. Dr. B. Antkowiak

I hereby declare that I have produced the work entitled: “The role of α2δ-3, a subunit of voltage gated Calcium channels, in somatosensation and pain.”, submitted for the award of a doctorate, on my own (without external help), have used only the sources and aids indicated and have marked passages included from other works, whether verbatim or in content, as such. I swear upon oath that these statements are true and that I have not concealed anything. I am aware that making a false declaration under oath is punishable by a term of imprisonment of up to three years or by a fine.

Tübingen, 09.05.2016

Table of Content:

I. Abstract

The α2δ-3 subunit was first discovered as an auxiliary subunit of voltage gated calcium channels. Recently it has been shown that a deficit in the *Cacna2d3*-gene leads to a reduction in heat pain sensitivity in drosophila, mice and humans [1]. The mechanism underlying this phenomenon, however, is not clear yet.

Here we describe that the deficit in heat sensitivity is caused by alterations in the peripheral and central part of the somatosensory system. Mice deficient in α2δ-3 show a reduced sensitivity in the hot plate test. With X-gal staining we show that the subunit is expressed in most large cells (Aβ-fibers) and a subpopulation of small cells (C- and Aδ-fibers) in the dorsal root ganglion (DRG). In the spinal cord (SC), staining was found in the dorsal and the ventral horn. We further confirmed expression in DRG and SC with qRT-PCR. With ex-vivo skin-nerve recordings we were able to show deficits in signal transduction in the periphery. C-fibers of deficient mice show a reduction in spike frequency after thermal stimulation and an increased heat-threshold. The population of Aδ-fibers responding to heat is diminished in these animals. In calcium imaging experiments a reduced calcium influx upon heat stimulation was found. Interestingly, the data from whole cell patch experiments show that the voltage gated calcium currents are not affected in the deficient mice. However, the inward current, respectively the sodium current, is reduced in cells from deficient mice. Further the heat and capsaicin induced currents are smaller. This shows clearly that the loss of α2δ-3 leads to deficits in heat-pain transduction at the periphery, namely that less input from the periphery reaches the spinal cord.

Surprisingly, the deficient animals show a second phenotype. In the Hargreaves test the animals show a higher sensitivity compared to wild type (WT) littermates. Same was found for the mechanical von Frey test. We further found an increased sensitivity after induction of chronic pain, like neuropathic or chronic inflammatory pain. Under chronic pain condition the increased sensitivity is not restricted to thermal stimulation and occurs for tactile as well. The subunit is down-regulated in neuropathic pain but recovers, same as the behavioral phenotype. Therefore this phenotype quite likely is a result of a reduced input onto inhibitory interneurons that in the end leads to a faster reflex. This input is mainly carried by Aβ-fibers, which are highly positive for α2δ-3.

Altogether these data show a contribution of the α2δ-3 subunit of voltage gated calcium channels in the somatosensory system, in acute and chronic pain. Heat-pain or better burning pain can be a tough burden to suffer of, especially for chronic pain patients. The knowledge acquired here might help to improve the understanding of heat-pain perception mechanisms and might lead to new strategies for therapy and treatment, maybe even serve as a new target for pharmaceutical investigations.

II. Abbreviations

AP	action potential
AUC	area under the curve
BOLD	blood oxygen level dependent
CCI	chronic constriction injury
CFA	complete Freund's adjuvant
CNS	central nervous system
CoIP	co-immuno precipitation
DRG	dorsal root ganglion
E-Coli	Escherichia coli
EGFP	enhanced green fluorescent protein
ER	endoplasmic reticulum
fMRI	functional magnetic resonance imaging
GPI	Glycosylphosphatidylinositol
HRP	Horseradish peroxidase
MIDAS	metal ion dependent adhesion site
MβCD	Methyl-β-cyclo-dextrine
NGS	normal goat serum
PAGE	poly acrylamide gel electrophoresis
PBS	phosphate buffered saline
PCR	polymerase chain reaction
PFA	para formaldehyde
PKC	protein kinase C
PNS	peripheral nervous system
qRT-PCR	quantitative real time PCR
RT	room temperature
RT-PCR	reverse transcriptase PCR
SC	spinal cord
SDS	sodium dodecyl sulfonate
TBE	tris borate EDTA-buffer
TBS	tris buffered saline
TRP	transient receptor potential
TRPV1	transient receptor potential vaniloid 1
TTX	Tetrodotoxin
VWA	von Willebrandt-Factor
YFP	yellow fluorescent protein

III. Figures

IV. Tables

1. Introduction:

1.1. The somatosensory system

As „Somatic sensation“ we refer five different modalities: touch, proprioception, thermal sensation, itch and nociception. Touch enables us to detect the surface and texture of things, which is very important for discrimination. Proprioception is needed to get feedback about the body position and movement. Thermal sensation enables us to detect warmth and cold. Itch and Nociception is very important to keep the body integrity and avoid harmful stimuli.

The somatosensory system involves the primary afferent nerve-fibers, with their somata in the dorsal root ganglion (DRG), the spinal cord (SC), the brainstem and higher brain areas such as the thalamus and the somatosensory cortex (Figure 1).

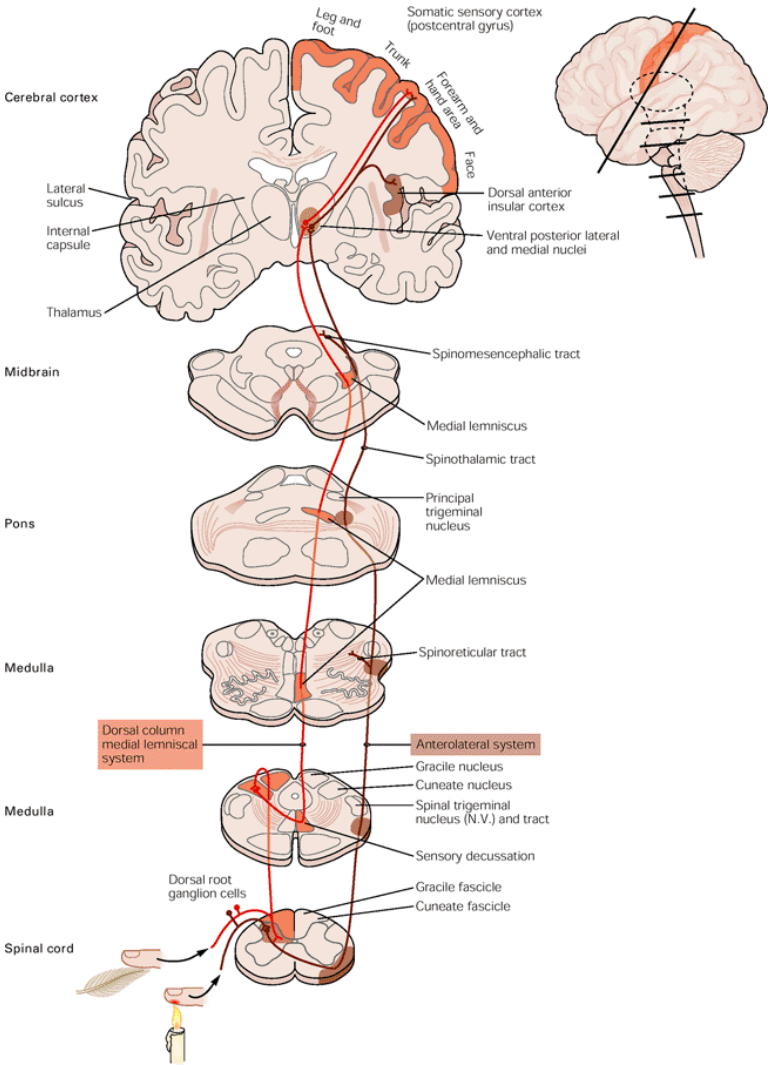

Figure 1: The somatosensory system. The system contains both, peripheral and central parts. The primary afferent fibers of the DRG's transduce the different stimuli into electrical signals and transmit these to the spinal cord. From here, normal touch sensations are projected via the dorsal column medial lemniscal system through the thalamus to the somatosensory cortex (orange pathway). Nociceptive input is projected via the anterolateral system through the thalamus to the cortex and the insula (brown pathway). (From Kandel, principles of neural science (4th edition)[2])

In principle each sensory system detects four characteristics of stimuli: modality, location, intensity and timing. Modality is set by the stimulus energy an encoded by a labeled line code. Stimulus transduction happens in specialized receptors that convert the different modalities of stimuli into electrical signals.

The mechanoreceptors for touch sensation are located in the skin (hairy and glabrous). There are specialized organs that transduce the mechanical stimuli. These organs are the Meissner corpuscle (stroking, fluttering), the Merkel disc receptor (pressure, texture), the Pacinian corpuscle (vibration) and the Ruffini endings (stretch). Beside these specialized organs for sensing mechanical stimuli there are free nerve endings in the skin, which are capable of sensing temperature and responsible for painful stimuli and transduce them through nerve fibers to the DRG, where the somata of these neurons are [2].

The DRG neurons are pseudo unipolar neurons, they have only one process (axon) that bifurcates at a T-junction into a peripheral and a central branch. The DRG fibers connect to the spinal cord via the dorsal root to the dorsal horn of the spinal cord. The fibers can be differentiated according to the size of their cell bodies and the degree of myelination. Small cells (in mice < 20 μm) have unmyelinated fibers and are called “C-fibers”, the medium sized (in mice between 20 and 25 μm) and light myelinated fibers are called “Aδ-fibers”. The big cells (in mice >25 μm) are highly myelinated and termed “Aβ-fibers”. The C- and Aδ-fibers are the dominant ones in detecting and transducing nociceptive stimuli. These can be mechanical, thermal or chemical stimuli. The Aβ -fibers are more for light and gentle touch. According to the grade of myelination the fibers can be differentiated according to the conduction-velocity of electrical signals [3].

The spinal cord is comprised of the inner grey matter, which is made up by the nuclei of the cells and surrounded by the white matter, which manly contains the fibers of the cells. It receives input from the muscles, the skin and the joints. Further it gives output via motor neurons to the muscles for conscious or unconscious (reflex) movements. The grey matter with its shape of the letter “H” or a “butterfly” has four structures called horns, the left and right, dorsal and ventral horns. The dorsal horns receive inputs from the periphery and the ventral horns give output to the muscles for movement. The spinal cord not only gets information from the skin but also from muscles and inner organs. In the ventral horn the motor neurons are not specially organized or clustered. But in the dorsal horn the sensory neurons form structures of clusters that organize the cell bodies to different layers with different properties and function (Figure 2).

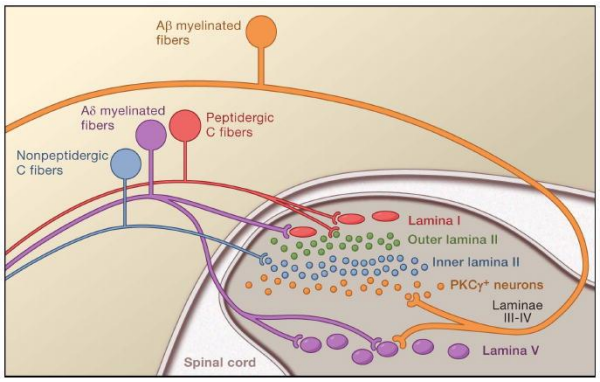

Figure 2 Spinal dorsal horn organization. The different fiber types project to different lamina in the spinal dorsal horn. The peptidergic C-fibers (red) and Aδ-fibers (purple) project to the outer most lamina I where they synapse onto the large projection neurons (red). The non-peptidergic C-fibers (blue) synapse onto small interneurons (blue) in inner Lamina II. The non-nociceptive input from Aβ fibers targets a special group of neurons positive for PKCγ (yellow). In Lamina V a additional set of projection neurons is target of input from Aδ and Aβ fibers. (From Basbaum et al., Cell 2009 [4])

In these clustering, interneurons are involved, that additional receive descending input from higher brain areas. So the interneurons can modulate the incoming sensory inputs before giving the output to the motor neurons. The white matter can also be subdivided in smaller structures. There is the dorsal column (between the two dorsal horns), the ventral column (between the two ventral horns) and the two lateral columns (between dorsal and ventral horn, left and right). For the ventral and lateral columns, they contain ascending and descending fibers. The dorsal column exclusively contains ascending fibers. The projections to the brain cross the midline on the level of the medulla, from where they run through the medial lemniscus to the thalamus. They terminate in the Cortex, where all the body parts are represented in a somatotopic map. This somatotopy is kept from the very beginning, when the nerves first time reach the spinal cord. Our right body parts are represented in the left cortex and vice versa.

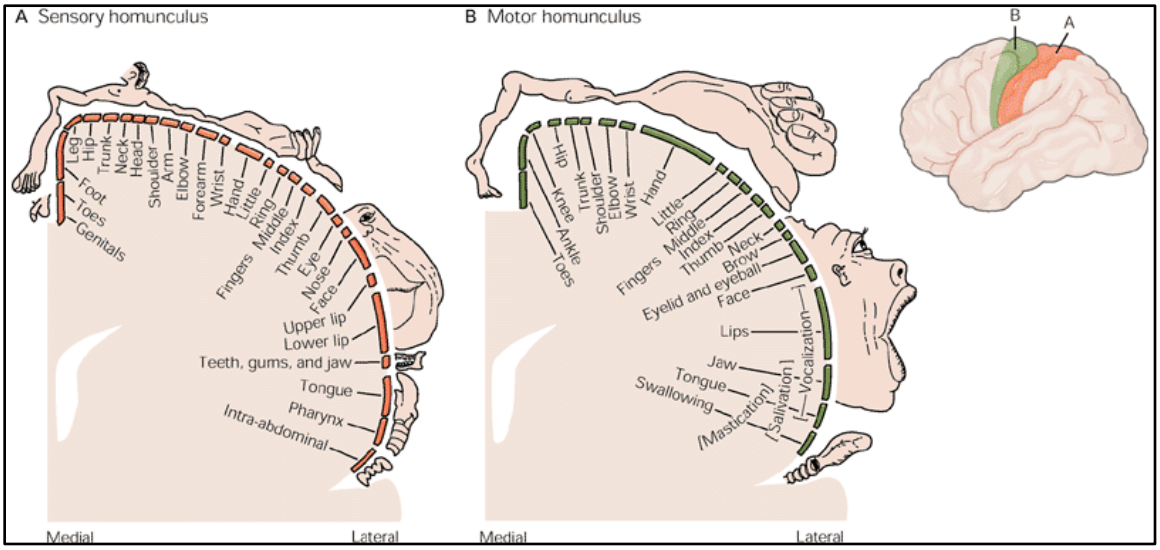

Figure 3 Homunculus: Re-presentations of the body parts in the somatosensory cortex, for sensation (A) and the motor output (B). The size of the representation in the cortex is not related to the real size of the body part represented, but the degree of innervation. (From Kandel, principles of neural science (4th edition)**[2]**)

All parts of the body are represented in the somatosensory and the motor cortex (Figure 3). The more sensitive body parts are, the more space they occupy in the somatosensory cortex.
The somatosensory system is quite complex thus including the biggest "organ" humans have, the skin. The more research is done on this system and its single components, the more complex it turns out to be. Overall there are three steps of integration of signals. The DRG is the peripheral one, which a lot of people in the field wouldn't count for integrative aspects. But that's a question of definition. So to my opinion already at the free nerve-endings in the skin there is some signal integration happening, especially under pathological conditions such as chronic pain. The both central relays of integration are the SC and the brain, and for sure the interplay between activation of high and low threshold receptors as well as the psychological condition are going to influence the output very much.

1.2. Normal and pathological pain

Pain is by definition of the international association for the study of pain (IASP): "An unpleasant sensory and emotional experience associated with actual or potential tissue damage, or described in terms of such damage". Pain saves our body integrity, because whenever there is a potentially harmful stimulus the pain would elicit a behavior that tries to avoid this stimulus.
There are several ways of pain classification. A common concept is to classify it into three different kinds of pain. First there is **nociceptive pain**. It is the pain that occurs upon intense stimuli (mechanical, temperature or chemical) and serves as the warning signal for potential disruption of body integrity. Second there is **inflammatory pain,** caused by inflammatory mediators such as prostaglandins, interleukins and many others. This pain normally occurs after tissue damage, when disrupted cells release their content and therefore activate the immune system. This pain is needed to enable wound healing. Infections can also lead to inflammatory pain. Both mentioned pain forms can be regarded as normal pain, because both have protective functions. Nevertheless chronic inflammation can lead to pathological pain states. The last type of pain is the most problematic, because it is maladaptive rather than protective. **Pathological pain** can have many causes. It shouldn't be considered as a symptom but as a disease state. Two further distinctions can be made. If the pain occurs from any kind of nerve damage it's called **neuropathic pain**. If there is no such kind of nerve damage or inflammation it's called **dysfunctional pain** (Figure 4). The treatment of pathological pain is a big issue in clinical medicine, because a lot of people suffer from it,

but effective therapies and treatments available are rare and often cause severe side effects [5].

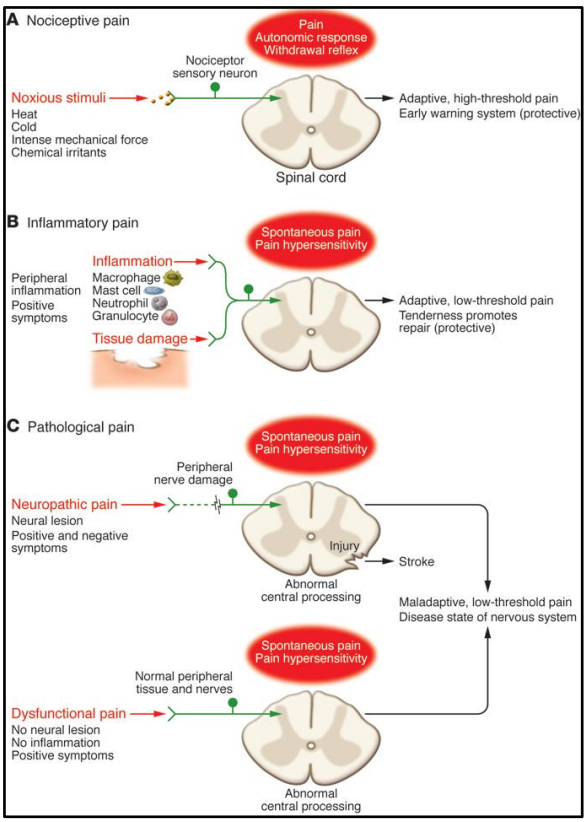

Figure 4: Schematic pain classification. The normal, while protective pain is shown in A and B. Nociceptive pain (A) keeps the body integrity and induces fast behavior (reflexes) to avoid the potentially harmful stimulus. Inflammatory pain (B) is needed for wound healing, to protect the injury side from further damage and too much movement. The both pathological pain states are shown in C. None of it has a protective function and therefore can be regarded as a disease state in itself. (From Woolf et al., the journal of clinical investigations 2010 **[5]**)

To have a closer look on how pain is transduced and transmitted we have to go to the molecular level. In the free nerve endings of the primary afferent fibers, which are processes of the peripheral branch of the DRG axon, a lot of ion channels and receptors are located. These proteins are responsible for the transformation of painful stimuli into a transmittable electrical signal. The main ion-channels involved are sodium, potassium, calcium and chloride ion channels. These channels can either be voltage activated or ligand gated as well as leak-channels (background). Other channels involved are acid sensing ion channels and the transient receptor potential (TRP) channels. Three sodium channels, namely $Na_V1.7$, $Na_V1.8$ and $Na_V1.9$ are found to be the most important in pain signaling. The $Na_V1.7$ is expressed preferentially in peripheral neurons but here along the whole DRG process including the central branch onto the spinal cord. This channel is responsible for setting the gain of the nociceptors due to slow closed-state inactivation and a relatively hyperpolarized voltage dependence [6]. The importance of this channel maybe seen in the effects genetic mutations can have. The inherited erythromelalgia (IEM) is such a type of mutation in the *SCN9A* gene, encoding for $Na_V1.7$. In this case it's

an example for a gain-of-function mutation. People carrying this mutation experience extreme burning pain upon mild warming of the skin [7]. There are loss-of-function mutations as well. The channelopathy-associated insensitivity to pain is an example. These people don't feel pain according to for example bone fractures, tooth extraction and burn [8]. The $Na_V1.8$ channel is mostly expressed in nociceptive DRG neurons and shows a unique feature in displaying a depolarized voltage-dependence causing a relative resistance to inactivation [9]. $Na_V1.9$ channels are expressed in the DRG as well, having slow kinetics and therefore do not really participate in action potential (AP) upstroke. These channels are more for the enhancement of small depolarizations [10]. A pain therapy with sodium channel blockers is difficult because of severe side effects, regarding the potential blocking of any AP.

Potassium channels are very important for repolarization of neurons and for establishing and keeping the membrane potential. The potassium channel family can be subdivided into voltage-gated- , ion activated- , two-pore-potassium channels and inward rectifiers. G-protein coupled inwardly rectifying potassium (GIRK) channels are well known for their role in pain sensation. It has been shown that they are involved in opioid analgesia [11]. Voltage gated potassium channels like most of other potassium channels are down regulated in animal models of pain. Neuronal hyperexcitability as a consequence of this decrease contributes to the behavioral phenotype. For therapeutic issues it would be very important to selectively target isoforms that are specific for the pain signaling [12].

There is a huge variety of channels that are permeable for calcium. Some of them are known to be involved in nociception, including voltage gated calcium channels, NMDA-receptors, purinergic receptors, transient-receptor-potential (TRP) channels and acid sensing channels. The voltage gated calcium channels are discussed in detail in the next section, so the others are briefly described here.

NMDA-receptors are expressed in the soma as well as the central and the peripheral part of DRG. After nerve injury or inflammation these receptors are up regulated [13-15]. Treatment with NMDA inhibitors lead to a reduction of pathological pain, leaving the basal, normal pain transmission unaffected [16].

The purinergic receptors like P2X3 are preferentially expressed in nociceptive neurons [17]. There are P2X receptors which are ionotropic, non-selective cation channels and metabotrobic, G-protein coupled P2Y receptors. Several of these receptors are involved in pain signaling. The already mentioned P2X3 receptor for example is known to act in inflammatory, neuropathic and bone cancer pain, as it was shown that pharmacological blockage or knockdown attenuate the mentioned pain types [18, 19].

The last group that's mentioned here is the transient-receptor-potential (TRP) channel family. These channels have a wide range in response to different chemical substances, as well as temperature (Figure 5). There are 7 subgroups in the TRP-family. The TRPC

(canonical), the TRPV (vaniloid), the TRPA (ankyrin), the TRPM (melastatin), the TRPP (polycystin), the TRPML (mucolipin) and the TRPN (NOMPC = no mechanoreceptor potential C). Except the TRPN all of them are expressed in mammals. In all subfamilies there are several isoform so that there are 27 different TRP-Channels expressed in mammals. For pain research the most interesting ones are the TRPV1, the TRPM8 and the TRPA1 [20].

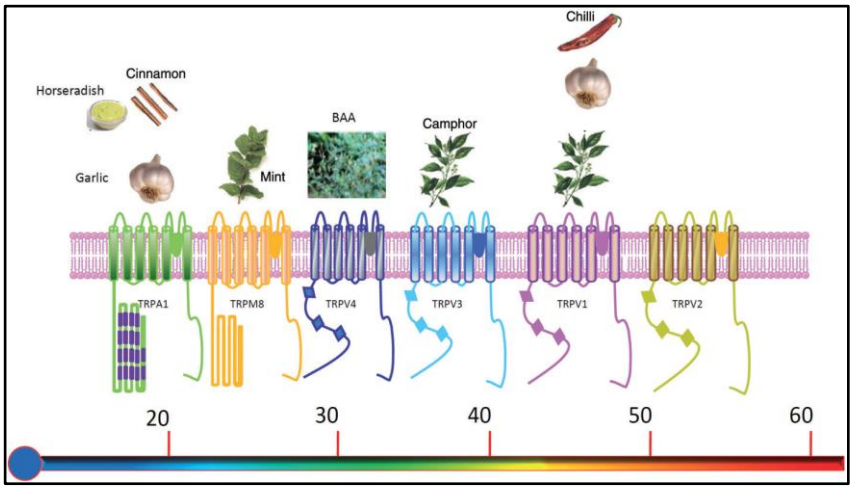

Figure 5: Scheme of the most studied TRP-channels in mammals. The structure of the channels is similar, containing 6 transmembrane domains. Both, the C- and the N-terminus are located intracellular. They differ in the activating temperature range and the chemicals that can act as agonists. (From Vay L. et al. **[21]**)

The TRPV1 channel is the first channel that was described to act as a thermo sensor [22]. Most of research has been done on this channel. The TRPM8 is thought to be mainly for the detection of non-painful cold stimuli, but also known to be co-expressed with TRPV1 in some DRG neurons. There is also evidence for a participation in pain mechanisms [23]. For TRPA1 the involvement in pain processing seems to be quite clear, because of the noxious cold range it can detect. It is expressed in nociceptors (small diameter neurons) and ablation in mice leads to deficits in nocifencive behavior according to cold stimuli [24, 25]. Like most of the TRP channels TRPM8 and TRPA1 can be also activated by several chemical compounds like menthol and inflammatory mediators can influence their properties[20].

As already mentioned the TRPV1 receptor is the most popular channel in this family, as it was the first one discovered. Its expression is restricted to most of fiber-types that are regarded as nociceptors, namely C- and part of the Aδ-fibers. But not only heat can activate the channel there are plenty of substances like vanilloids and low pH that can activate the channel. The most famous substance is capsaicin that makes the chillies spicy. If the temperature rises over 42-43°C the channel is activated [22]. This temperature is roughly the threshold for humans when heat gets painful. During tissue injury or inflammation the released pro inflammatory mediators can sensitize the channel and lower the threshold for activation. Low pH can either sensitize the channel

(until pH 6.4) or directly activate it (pH < 6)[21]. In mouse-models of inflammatory pain the TRPV1 knock-out mice showed clear deficits in generation of thermal hyperalgesia but surprisingly show a quite normal acute heat-pain behavior. This could be explained with the fact that there are some other channels that respond to heat (Figure 5), meaning there could be compensation for the loss of TRPV1 [26]. So whenever there is a heat phenotype in a new knock-out mouse line people might first think of possible involvement of the TRPV1 channel. Several studies showed protein-protein interactions of TRPV1 with other proteins like Tubulin, TRPV2, protein kinase A anchoring protein 150 (AKAP150) or the phosphatidylinositide-binding protein Pirt [27-30]. Recently a study showed that the voltage gated K^+ channel β-2 (Kvβ2) subunit serves as an interaction partner of TRPV1. With Co-IP it was shown that there is a direct interaction of the two proteins. A cell surface biotinylation protocol showed that co-expression of Kvβ2 increases the cell surface expression of TRPV1 in a cell-line system [31]. All this studies show that there is a huge variety of potential interaction partners for TRPV1.

1.3. Neuronal voltage gated calcium channels

The voltage gated calcium channels in the nervous system are the ion channels that mediate the calcium entry after depolarization. Therefore they are very important for signal transduction, because the calcium entry can lead to a variety of alterations in the corresponding part of the neuron. At the synapse for example the calcium entry after depolarization leads to vesicle fusion and neurotransmitter release.

The intracellular Calcium concentration is rather low (around 0,1 µM) and outside the cell rather big (around 1 mM) so that there is a large concentration gradient along which the calcium ions can flow inside the cell. This influx can be very local, like in the synapses and therefore specifically act on proteins that are close. But beside this action calcium can act as a signaling molecule that triggers a variety of other pathways. Gene transcription in general for example can be calcium dependent as well as neurite outgrowth. There are also calcium dependent enzymes that are activated upon calcium increase, for example calmodulin-dependent protein kinase II and protein kinase C (PKC). A prolonged increase in Calcium concentration can have toxic effects, so the mechanisms that open and close the calcium permeable channels are rather tightly controlled.

There are several types of neuronal voltage gated calcium channels (Table 1). At first they can be separated according to the voltage dependence into high- and low-voltage-activated channels [32]. The low-voltage-activated calcium channels are called T-type or Ca_V3 channels and in mammalians 3 isoforms exist ($Ca_V3.1$, $Ca_V3.2$ and $Ca_V3.3$). These channels consist of one $Ca_V\alpha1$ subunit. Different from that the high-voltage-activated

(HVA) channels are heteromers of a $Ca_V\alpha1$, a $Ca_V\beta$ and a $Ca_V\alpha2\delta$ subunit. There is even a $Ca_V\gamma$ subunit but the function of it is still under debate [33]. The $Ca_V\alpha2\delta$ subunits are discussed in the next section in further detail.

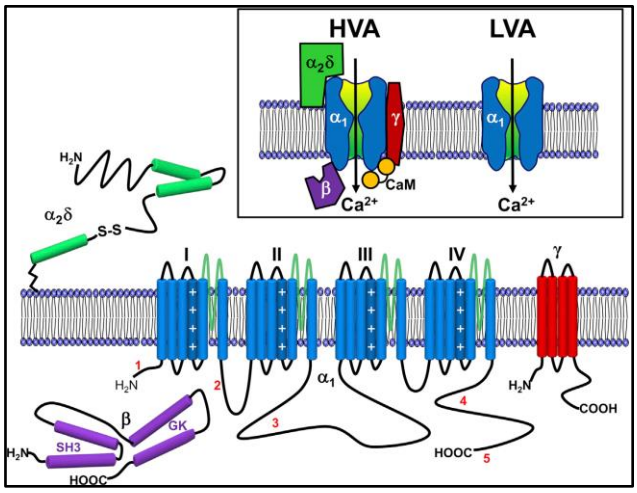

Figure 6 Scheme of voltage gated calcium channels and their subunits. The high voltage activated (HVA) channels are heteromers of up to 4 subunits. The low voltage activated (LVA) channels are monomers. The α1 subunit is the pore forming one, consisting of 4 transmembrane domains. The γ subunit is supposed to be a transmembrane protein too. β-subunits are soluble proteins in the cytosol. The α2δ-subunits are thought to be membrane bound via a GIP anchor, and extracellular. (From Simms & Zamponi, Neuron 2014 [34])

There are 7 isoforms of $Ca_V\alpha1$ for HVA channels. Four Isoforms for the L-type channels ($Ca_V1.1$, $Ca_V1.2$, $Ca_V1.3$ and $Ca_V1.4$) as well as P/Q-type ($Ca_V2.1$), N-Type (Ca_V 2.2) and the R-Type ($Ca_V2.3$). All the isoforms share the common topology as depicted in Figure 6. For differentiation specific pharmacological properties like agonists or blockers could be used. They also differ in their cellular and sub-cellular distribution.

There are 4 isoforms of the $Ca_V\beta$ subunits known (β1 - β4). These auxiliary subunits have effects on the gating properties of the $Ca_V\alpha1$ subunits but even more efficient, they influence their trafficking [35]. $Ca_V\gamma$-subunits are known to be part of mostly L-type channel complexes and seven potential isoforms have been identified so far. Nevertheless it's still under debate if they should be considered as calcium channel subunits because some of the isoforms have profound effects on the whole cell current density [36].

Most of the voltage gated calcium channels have a role in pain signaling, that's known. N-type channels for example lead to pain-hyposensitivity if knocked out. Therefore treatment with ω-Conotoxin, a toxin from a snail that acts as an antagonist can reduce pain. But nevertheless there are severe side effects like dizziness, blurred vision, hypotension and memory problems [37]. T-Type channels participate as well in pain processing, shown by analgesic effects of blockers in rodent experiments [38]. The other types of calcium channels (R, P/Q and L) play only minor roles in pain signaling. The following Table 1 gives an overview:

Table 1: Different isoforms of neuronal voltage gated calcium channels. (Modified from Catteral et al.[39])

channel	$Ca_V\alpha1$	type	localization	specific antagonists	cellular function
$Ca_V1.1$	α_{1S}	L	skeletal muscle; transverse tubules	Dihydropyridines; phenyl-alkyl amines; benzodiazepines	excitation-contraction coupling
$Ca_V1.2$	α_{1C}	L	Cardiac myocytes; smooth muscles; endocrine cells; neurons	Dihydropyridines; phenyl-alkyl amines; benzodiazepines	excitation-contraction coupling; hormone release; transcription regulation; synaptic integration
$Ca_V1.3$	α_{1D}	L	Endocrine cells; neuronal; cardiac atrial myocytes and pacemaker cells; cochlear hair cells	Dihydropyridines; phenyl-alkyl amines; benzodiazepines	Hormone release; regulation of transcription; synaptic regulation; cardiac pace making; hearing; neurotransmitter release from sensory cells
$Ca_V1.4$	α_{1F}	L	Retinal rod and bipolar cells; spinal cord; adrenal gland; mast cells	Dihydropyridines; phenyl-alkyl amines; benzodiazepines	Neurotransmitter release from photoreceptors
$Ca_V2.1$	α_{1A}	P/Q	Nerve terminals and dendrites; neuro-endocrine cells	ω-Agatoxin IVA	Neurotransmitter release; dendritic Ca2-transients; hormone release
$Ca_V2.2$	α_{1B}	N	Nerve terminals and dendrites; neuro-endocrine cells	ω-Conotoxin-GVIA	Neurotransmitter release; dendritic Ca2-transients; hormone release
$Ca_V2.3$	α_{1E}	R	Neuronal cell bodies and dendrites	SNX-482	Repetitive firing; dendritic calcium transients
$Ca_V3.1$	α_{1G}	T	Neuronal cell bodies and dendrites; cardiac and smooth muscle myocytes	None	Pacemaking; repetitive firing
$Ca_V3.2$	α_{1H}	T	Neuronal cell bodies and dendrites; cardiac and smooth muscle myocytes	None	Pacemaking; repetitive firing
$Ca_V3.3$	α_{1I}	T	Neuronal cell bodies and dendrites	None	Pacemaking; repetitive firing

1.4. The α2δ-Subunits

There are four different genes for α2δ-subunits. For each there is only one protein translated that is post-translationally cleaved into the α2- and the δ-part. These two parts are reconnected via disulfide bonds. The δ-part was first thought to enable transmembrane anchoring. But more recent data show that the subunits are bound to membrane by glycol-phosphatidyl-inositol (GPI) anchors [40].

The *CACNA2D1* gene encodes for the α2δ-1 subunit, which is the best studied while first described. It is ubiquitously expressed in muscles and neuronal tissues. Associated pathologies with this subunit are cardiac dysfunction and neuropathic pain. *CACNA2D2*,

encoding α2δ-2 is exclusively expressed in neurons of the central nervous system (CNS), most prominent in the cerebellum. That's why dysfunction of α2δ-2 can lead to cerebellar ataxia, but also epilepsy [41]. The α2δ-3 subunit is encoded by the *CACNA2D3* gene and not as prominent as the first two described here. A recent publication showed that it's exclusively expressed in the CNS and neither in the SC nor the DRG. Additionally it was shown that this subunit is involved in heat nociception, in higher brain areas among different species, including humans. Finally it was point out that this gene (*CACNA2D3*) is the first one shown to be involved in synesthesia [1]. *CACNA2D4* encodes for the last known subunit α2δ-4. It's mainly expressed in endocrine tissue but also present in retinal cells, leading to retinal dystrophy and night blindness if disrupted [41]. All the isoforms show some common structural features shown in Figure 7.

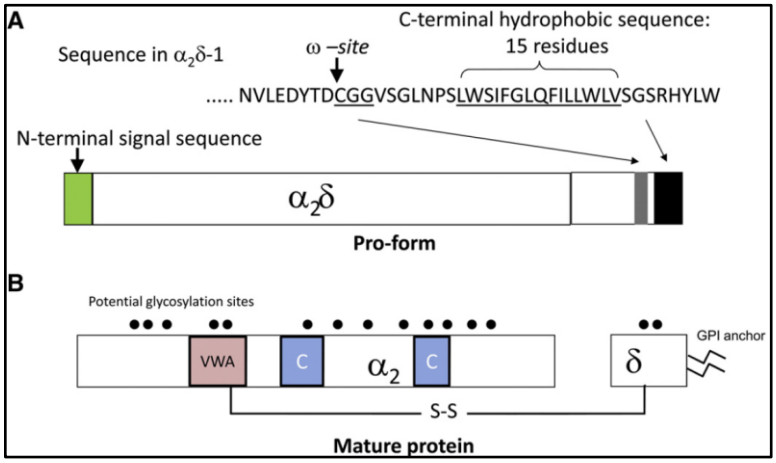

Figure 7: Scheme of the common α2δ structure. The preform (A) is post-translationally cleaved and reconnected via disulfide bonds (B). Black dots showing glycosylation sites. The preform has a hydrophobic sequence that in principle could enable the subunit to insert into the membrane. But there is a cleavage site as well, that more likely shows that the subunit is membrane bound via a GPI anchor. VWA: von Willebrandt factor type A; C: Cache domain (From Dolphin et al. [41])

The α2 part is completely extracellular and the δ part shows a GPI-anchoring motif. The N-terminal signal sequence is co-translationally cleaved and directs the protein into the endoplasmic reticulum (ER). The proteolytical cleavage is supposed to occur post ER. Many cysteine residues are potential candidates to form the disulfide bonds. For the α2δ-1 subunit the pair of cysteines making the disulfide bond recently has been identified [42]. All the four isoforms contain a von Willebrandt-Factor (VWA) domain which is important for protein-protein interactions. This domain-type is also found in proteins like integrins, collagens and laminin. It contains a metal ion dependent adhesion site (MIDAS) via which the interaction is possible. Divalent cations like Ca^{2+} or Mg^{2+} are coordinating this interaction. Additionally there are Cache-domains (C) in the protein downstream to the VWA domain. This domain type is normally found in bacteria where it is needed for chemotaxis [43]. All isoforms are found in the neuronal processes and only to minor degree in the soma. The α2δ-1 subunit is known to be transported into the peripheral and the central branch of the axon in DRG [44]. Subcellularly they

locate mostly in lipid rafts suggesting that this localization is important for proper function of the subunits [40].
Plenty of studies showed that one function of the α2δ-subunits is to act on trafficking of the α1 pore forming subunits, meaning more α2δ leads to more channels in the membrane. Other effects reported upon co-expression of different α1- and α2δ-subunits are increased channel expression and increased current amplitude. Most probably the α2δ proteins do all this according to interactions with their VWA-domains. Investigators have been all the time in search for specific combinations of α2δ and α1 isoforms, but so far none of these are known. A possible role for the Cache-domain could be the binding to endogenous ligands that are not known so far. For the α2δ-1 and -2 subunits it is known that they have a binding site for gabapentinoid drugs that are used as anti-epileptic drugs and for treating neuropathic pain. According to this aspect the α2δ-1 and -2 subunits have been intensively investigated [41]. α2δ-1 was even shown to act as a receptor for thrombospondin, a protein family that is involved in extracellular signaling and synaptogenesis [45].

For the α2δ-3 subunit in mice not much literature is available. The most popular publication already cited, was done by Neely et al. [1]. In a drosophila screening the homolog gene (*straightjacket, stj*) was found to be involved in heat sensation. Drosophilas missing this gene are not able to avoid high temperatures (46°C) and die. A mouse-line where the *CACNA2D3* was disrupted by insertion of a LacZ-cassette was created and phenotyped (2.1). The impairment of the gene doesn't lead to any obvious deficits in the animal's behavior, but these mice are less sensitive for high temperatures in the hot-plate-test. In this study the protein in mice was only found in brain. Although in drosophila it is expressed in the sensilla, a peripheral sensory organ [1]. Others showed that the protein is needed for proper synaptic morphogenesis in neuro muscular junctions in drosophila [46]. Even some single nucleotide polymorphisms (SNP) were found in humans that lead to less heat-induced pain. Because there was no protein found in the SC or the DRG the cause of this behavioral phenotype was thought to locate in the brain. Therefore noninvasive functional magnetic resonance imaging (fMRI) was performed, using the blood oxygenation level-dependent (BOLD) signal. An impaired transmission from the thalamus to the cortex was observed. As well as a sensory cross-activation, meaning the heat or tactile stimuli not only activated the somato sensory- but also visual- and auditory-cortex in mutant mice. Leading to suggestions this gene (*CACNA2D3*) might be the first one shown to be involved in synesthesia [1]. Beside this study others showed that the subunit is expressed in DRG [44, 47, 48]. In the study from Neely et al. they detect the protein in Drosophila in the sensilla of the leg, a sensory organ for sensing taste [49]. This result shows already that

in this species the subunit is involved in the periphery of a sensory system, same as we would expect for the somato-sensory system in mice.
The α2δ-3 subunit seems to be involved in other disease like psychiatric disease like for autism spectrum disorders [50] and cancer [51].
A2δ-3 was also shown to be involved in auditory processing. It is expressed in the spiral ganglia and the deletion results in impaired auditory processing. The mutant mice show a reduced acoustic but increased tactile startle. Furthermore the mutant mice show reduced presynaptic calcium channel levels and smaller terminals of auditory nerve fibers [52]. Overall it seems that α2δ-3 has a role in different sensory systems among different species, maybe even independent from its influence on calcium channels.
Further evidence for α2δ-3 acting especially in the periphery of the somatosensory system was given by scientists quite recently. Altered startle responses in α2δ-3 deficient mice according to either acoustic or tactile stimulation have been investigated. Following acoustic stimulation the startle response in the deficient mice was reduced in meanwhile upon tactile stimulation the startle response was increased [52]. The opposing results the gene deletion elicits in the two different sensory systems point on alterations in peripheral cells, because obviously central relay stations are shared for both (Figure 8).

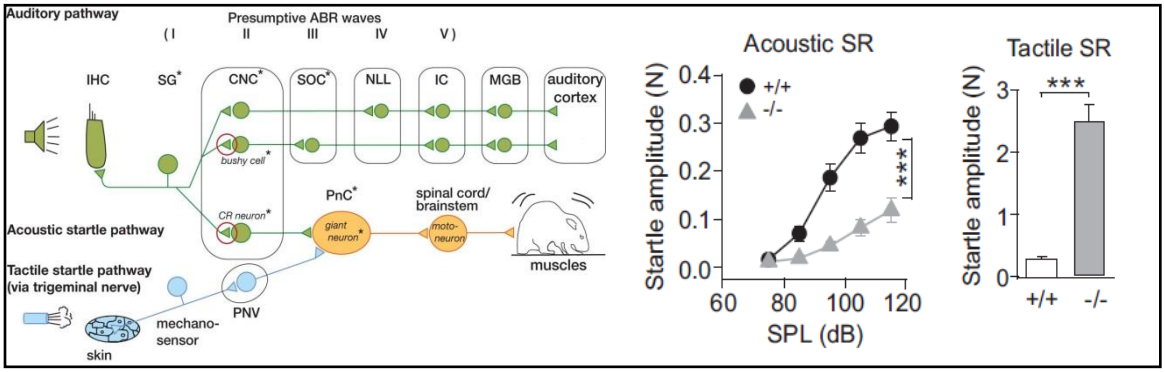

Figure 8: Scheme of auditory and trigeminal-tactile startle pathways. The acoustic startle pathway (green) and the tactile startle pathway (here trigeminal) share some parts. Both pathways involve giant neurons in the caudal pontine reticular formation (PnC) and the motor output pathway. The red circles in the acoustic startle pathway mark synaptic boutons which are reduced in size in α2δ-3 deficient mice. Therefore the activation of the bushy cells and the cochlear root (CR) neurons in the cochlear nuclear complex (CNC) via these smaller boutons might be less effective, which could explain the reduced acoustic startle response (Acoustic SR). Giving the fact that the tactile startle response is increased (Tactile SR), there should be a difference in the peripheral part of the pathways. Black asterisks mark cells that express α2δ-3. Spiral ganglion (SG), superior olivary complex (SOC), inferior colliculus (IC), nuclei of the lateral lemniscus (NLL), medial geniculate body (MGB), auditory brainstem response (ABR). (From Pirone et al. [52])

The peripheral parts of the pathways are formed by specific ganglion cells. For the acoustic pathway it is the spiral ganglion cells (SG) which in the same study have been shown to form smaller synaptic boutons at the contact side to the giant neurons which are the first relay station in the acoustic startle pathway.

Therefore we assume that in the peripheral part of the somatosensory system which is formed by DRG neurons the loss of α2δ-3 can lead to the alterations described above. Maybe mainly via reduced input on neurons which drive the inhibitory effect?

1.5. Working hypothesis/Aims

According to the literature published so far, we thought that the α2δ-3 subunit of voltage gated calcium channels has a function in heat-perception in the somatosensory system. The yet unclear mechanism was the main point of interest.
One aim was to investigate the peripheral part, the primary afferents and the DRG to see if α2δ-3 is needed for proper heat reception in this part of the pathway. The second aim was to look into the SC, which belongs to the central part of the somatosensory system. Here the processing and integration of the signals from the periphery happens and a loss of α2δ-3 might alter that.
For the two above mentioned aims we not only wanted to investigate differences between naïve WT and KO animals, we further wanted to see effects under chronic pain conditions.

Over all this study should shed more light onto the mechanisms of heat perception in mice in general and under chronic pain conditions. This knowledge could be useful in regard of treatments or therapies of disease which cause deficits in heat-pain perception.

2. Materials and Methods

2.1. Mouse lines

The used mouse line is the B6.129P2-*Cacna2d3*^{tm1Dgen}/J (Stock Number: Jackson Lab: 5780). This mouse has a *LacZ*-insert in the *Cacna2d3* gene, coding for the α2δ-3 subunit of voltage gated calcium channels. Therefore the mouse is deficient for this subunit and the *LacZ*-gene, coding for a β-galactosidase is driven by the endogenous α2δ-3 promoter. X-gal staining (2.3.2) which is a standard method to investigate β-galactosidase activity can be used to look for cells were the α2δ-3 promoter is active.

We created a new mouse line by crossing the B6.129P2-*Cacna2d3*$^{tm1Dgen/J}$ line with an EGFP-reporter-mouse line: FVB-Tg(GadGFP)45704$^{Swn/J}$. This reporter mouse line expresses the enhanced green fluorescent protein (EGFP) under the promoter of the glutamate decarboxylase GAD 67, which is a marker for inhibitory interneurons in the spinal cord.

2.2. Molecular Biology

2.2.1. DNA/RNA extraction

DNA/Plasmid extraction was done using an extraction Kit from Quiagen. The whole procedure was done according to the manual. RNA extraction was done by use of the RNeasy kit (Quiagen), according to the manual.

2.2.2. PCR

PCR's were performed, if not explicitly mentioned using the MyTaq red mix (Bioline). All steps have been performed according to the manual.
To check the expression of the different proteins, the following primers have been used:
α2δ-1 subunit mouse:

forward:	GCACCAAGGGAATACTGCAATGA
reverse:	CCACCATCATCTAGAATGACACAGT

α2δ-2 subunit mouse:

forward:	GCATGATTGACGGCGACAAAG
reverse:	AATGCCCGTGTCCAGAATCAAG

α2δ-3 subunit mouse:
forward: TACATTGACAGCACCCTCCC
reverse: GCATTTCGTAACACATCATCCC

α2δ-4 subunit mouse:
forward: TCCTCTAGCCACAACCAAGACC
reverse: AAGAAACTCAGCTCCCAGCTCC

This PCR-Program was used:

1. 94°C 3 min
2. 94°C 20 sec
3. 72°C 30 sec
4. 94°C 20 sec
5. 66°C 30 sec (decreased by 1°C each cycle)
6. 72°C 30 sec

Back to step 4, 5 times

7. 94°C 20 sec
8. 61°C 30 sec
9. 72°C 30 sec

Back to step 7, 28 times

10. 72°C 5 min

2.2.3. RT-PCR

The RNA isolation was already described above (2.2.1). For the reverse transcription the "SuperScript III First-Strand Synthesis System for RT-PCR" (Invitrogen) was used. The whole procedure was done according to the manual.

2.2.4. qRT-PCR

The quantitative real-time-PCR was done using the TaqMan protocol. Therefore the TaqMan Gene Expression Assays had to be designed in advance. This was done by the Obermair lab at the medical University Innsbruck, Austria [53]. The samples were pipette into a 96-well plate according to the following protocol:

10 µl TaqMan Universal PCR Mastermix (2x)
1 µl TaqMan Gene Expression Assay
X µl cDNA (20ng)
9 – X µl water (Mili-Q)

the total volume was set to 20 µl. The plates were put into a cycler from Applied Biosystems (7500 Fast-Realtime PCR system). The 7500 software V.2.0.3 was used.

2.2.5. Genotyping

For genotyping, the Phire animal tissue direct PCR kit (Biozym) was used. All steps were done according to the manual. The primer sequences were taken from the Jackson Laboratory (5' – 3'):

Forward: GCA GAA GGC ACA TTG CCA TAC TCA C
Reverse: TAG AAA AGA TGC ACT GGT CAC CAG G
Mutant: GGG CCA GCT CAT TCC TCC CAC TCA T

The same PCR program as in 2.2.2 was used.

2.2.6. Western-Blot

After collection, the tissue was put into lysis buffer (2.9.1.3) and grinded in a potter. Afterwards sample was centrifuged (2000rpm, 10min) and the supernatant taken. Than protease inhibitor was added as well as the loading buffer (BoltTM, LDS sample buffer 4x, NOVEX by life technologies). This mixture was heated in a water bath for 10min at 100°C. Thereafter the sample was stored until usage at -20°C.
The SDS-Gel was prepared according to the recipe (2.9.1.4). First the running gel was prepared and 45 min later the stacking gel was put on top of it. After another 45 min the gel was put into the MINI-Protean tetra system (BioRad) filled with running buffer (1x) (2.9.1.5). Up to 30 µl sample was loaded on the gel and run 40min at 80mV and 1h at 120mV. Afterwards the upper stacking gel was cut away and the running gel was put into transfer buffer (2.9.1.6). For blotting a PVDF membrane (Roche) was used as well as blotting-paper (PROTEAN XL, BioRad) in a semi dry manner. The plot was done for 1h at 15mV.

2.2.7. Transformation and clone picking

For the transformation competent E-Coli cells have been used. 100 µl of these cells have been mixed with Plasmid (1-10 ng/l) and incubated for 30 min on ice. Afterwards the cells were heat-shocked for 1,5 min at 42°C (water bath) and thereafter kept on ice for another 1,5 min. 300 ml LB-Medium was added and the cells were incubated for 40 min at 37°C. Than 50 – 100 µl have been put on an agar-plate containing the corresponding antibiotic (most cases Ampicillin or Kanamycin). The plates were incubated over night at

37°C upside-down. Thereafter few clones were picked and put into 6 ml of LB-Medium. The incubation was done again over night at 4°C. On the next day a cloning-PCR was performed (protocol like 2.2.2, with 1. Step expansion to 5 min).

2.2.8. Co-immuno precipitation (CoIP)

CoIP was performed using the "Dynabeads Protein G Immuno precipitation Kit" from life technologies. The whole procedure was done according to the manual. HEK cells were transfected as described in 2.4.3. A α2δ-3-HA tagged construct as well as a TRPV1-YFP construct have been used. For co-Transfection in a 9 cm Petri dish 7,5 µg (15µg in total) of protein were transfected to the HEK cells. After 2 days incubation the cells were harvested and lysed as like for western-blot (2.2.6).

2.3. Histochemistry

2.3.1. Immunostaining

The tissue was fixed with 2% PFA and 15% Picric acid, overnight at 4°C. For cryo-section the tissue was additionally incubated with 30% sucrose overnight at 4°C. If not specifically mentioned the tissue was put into Tissue-Tek (O.C.T.^{TM} compound) and cut at the cryostat at 12µm. Cell culture samples were fixed with 2% PFA for 10 minutes on ice. Afterwards the cells were incubated with PBS at RT. Then the cells were incubated with 100mM Glycine for 15 min at RT. For all the antibodies a standard immuno-protocol was used (if not especially mentioned). The slices were washed for 10min with PBS (0.1 % Triton). Afterwards the Incubation with blocking solution (2.9.2.1) for 1h at room temperature (RT) was done, followed by the Incubation with primary antibody in blocking solution over night at 4°C or for 2h at RT. After another 3 times washing for 5 min with PBS the secondary antibody was added and incubated for 1h at RT. Thereafter again the washing (3 times for 5 min with PBS) happened and the tissue was sometimes additionally stained with Höchst (1:1000) for 5 min at RT. Afterwards the slices were mounted with vecta-shield (Linaris) and stored at 4°C. If not particularly mentioned each staining was at least repeated 3 times.

2.3.2. X-gal staining

The Tissue was fixed like described (2.3.1). For the staining the stock solution (2.9.2.3) and the X-gal had to be mixed 1:30. The solution was applied directly to the tissue and incubated for at least 20 h at 37°C. During the incubation the tissue was protected from light.

2.4. Cell culture

2.4.1. Primary DRG culture

One day before the cell culture the coverslips had to be coated. Therefore the coverslips have been put for 30 sec in a surface plasma generator (Diener, Femto). Afterwards poly-L-Lysine (500 µg/ml) was put on the coverslips overnight (37°C). Next day the coverslips were washed 3 times with PBS and then Laminin (0.4 µg/ml) was put on it and incubated at least 1h (37°C).

The animals were sacrificed and the dorsal root ganglions (DRG) were taken out. The tissue was put into PBS on ice. After collection the PBS was sucked off and collagenase (10 µg/ml) was added and incubated for 30 min at 37°C in the water bath. Than the collagenase was removed and trypsin (0,05%) was added (incubated for 30 min at 37°C in the water bath). Afterwards the digestion was stopped removing the trypsin and adding DRG-medium (2.9.3.1). The cells were careful triturated and centrifuged (5 min 800 rpm). The Medium was removed, new medium added and triturated again. Then the coverslips with the Laminin were washed 3 times with PBS and one time with DRG-medium (2.9.3.1). Thereafter the cell suspension was put onto them (120µl per cover slip). After 4 h the cells settled down and the whole petri dish could be flooded with Medium.

2.4.2. HEK 293 culture

HEK-293 cells were unfrozen (from -80°C) and put into Medium (2.9.3.2). Incubation was done at 37°C and 5% CO_2. When the cells reached confluence they were removed with Trypsin (0,05%) and washed with medium. Afterwards the cells were split and the passage was counted.

2.4.3. Transfection of HEK cells

Transfections in HEK-cells were done with Lipofectamine-2000 (Invitrogen). 2 µl Lipofectamine were pipetted into 100 µl of OptiMEM reduced medium and incubated at RT for 5 minutes. 1 µg DNA was put into 100 µl OptiMEM mixed and put into the Lipofactamine-OptiMEM solution. This mixture was incubated for 20 min at RT. The coverslips (50-60% confluence) with the cells were 2 times washed with OptiMEM and put into 12-well plates. The mixture was put into the wells plus additional 200 µl OptiMEM to cover the whole well with solution. After 6 h incubation (37°C, 5% CO_2) the OptiMEM was removed and normal Medium (with serum) was added. The cells were incubated overnight (37°C, 5% CO_2).

2.5. Electrophysiology

2.5.1. Patch

The DRG's for patch clamp recording have been cultured as described (2.4.1). Fire-polished glass electrodes have been used with a resistance of 3-7MΩ. The extracellular and intracellular solutions used here are described in 2.9.4.1 and 2.9.4.2. For amplification of membrane current and voltage an EPC-10 amplifier from HEKA was used. For monitoring and analysis of the experiments an AxioObserver A1 (Zeiss) microscope and the Patchmaster and Fitmaster (HEKA) software have been used. For drug application a WAS 02 (Ditel) gravity driven perfusion system was used.

2.5.2. Ex-Vivo skin nerve recordings

For the skin nerve preparation the animal is killed and the skin from the hind paw is removed very carefully [54]. The saphenous nerve has to stay intact as well as the free nerve Endings in the skin. During the whole preparation the tissue is kept wet with the synthetic interstitial fluid (SIF-buffer, 2.9.4.7). Before cutting the nerve it has to be ligated with a thread. The nerve should never be touched, but the thread. After putting the skin nerve preparation in the recording chamber the thread can be removed. The nerve is put in mineral oil and has to be freed from the surrounding epineurium. Thereafter the splitting of the nerve into smaller fibers could be performed. This step is necessary to ideally get single unit recording. The recording is done with a silver wire (electrode) the split nerve is put on. During the recording the signal was monitored using an oscilloscope (Tektronix). For recording and analyzing the LabChart 6 Pro software (ADIntruments) was used. This device was also used for giving heat stimuli.

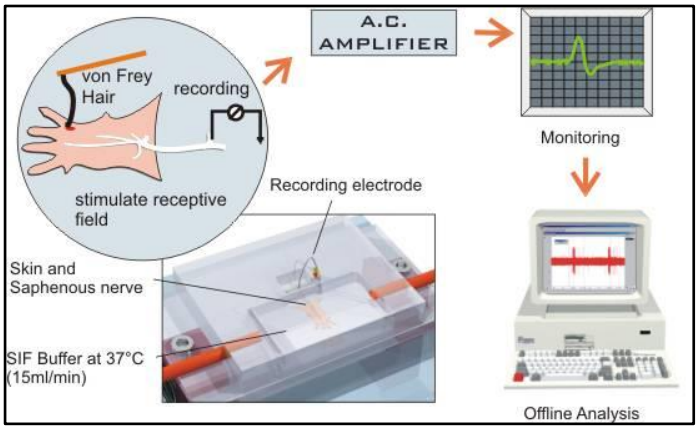

Figure 9: Ex-vivo skin nerve recording. The skin removed from mouse hind paw is put into a chamber upside down and perfused with SIF buffer. The intact nerve is put into the recording chamber filled with mineral oil. The nerve has to be split into smaller segments to achieve single unit recordings. Stimuli as heat, cold, chemicals and mechanical force can be applied to the skin. The properties of the units can be checked with electrical stimulation. According to conduction velocity and response shape the unit can be classified into the fiber types. (Picture was kindly provided by Dr. Jing Hu)

2.6. Calcium imaging

2.6.1. DRG and HEK-Cells

The Cells were cultured as described (2.4.1 or 2.4.2). Before the calcium imaging the cells were loaded with a calcium sensitive dye, Fura-2. Therefore the cells were washed 3 times with extracellular solution (2.9.4.1) incubated with Fura-2 (500µl; 1:250) for 30 min in the dark (37°C, 5% CO_2). Afterwards the cells were washed with extracellular solution and again incubated for another 30 min in the dark. Adjacent to that the cells were put into the perfusion chamber at the microscope for performing the experiments. The setup used for calcium imaging was the same as under 2.5.1.
The stimulation protocol consisted of several chemical stimuli (KCl 40mM, capsaicin 100nM and capsaicin 1µM) and different heat stimuli of the following composition:

- fast 43°C = 37°C for 10 s; heat ramp till 43°C in 0,5s; hold 43°C for 1s; hold 37°C for 2s
- slow 43°C = 37°C for 10 s; heat ramp till 43°C in 5s; hold 43°C for 1s; hold 37°C for 2s
- fast 53°C = 37°C for 10 s; heat ramp till 53°C in 2s; hold 53°C for 1s; hold 37°C for 2s
- slow 53°C = 37°C for 10 s; heat ramp till 53°C in 20s; hold 53°C for 1s; hold 37°C for 2s

2.7. Behavior

All animal tests were done according to the German animal protection law. All animal experiments had to be approved by the Regierungspräsidium Tübingen and were strictly controlled.

2.7.1. Von Frey-test

Automatic von Frey

For the von Frey test the animals were habituated in the behavioral setup (Ugo Basile, Dynamic Plantar Aesthesiometer). This consists of a metal grit and transparent boxes with lids as well as a controlled apparatus with a blunt needle. For testing the blunt needle was put under the hind paw of the animal. The needle is pressed against the hind paw with increasing force, feeling pain, the animal removes the paw, and the time (latency) and the force is measured. For each animal the hind paw was tested 3 times.

Manual von Frey

For the manual von the animals have been habituated in the same way and set up as for the automatic von Frey. Here filaments in different strength (0.008, 0.02, 0.04, 0.07, 0.16, 0.4, 0.6, 1.0, 1.4 and 2.0 g) were pressed against the hind paw. Each filament was

tested 5 times at each paw at each time point. Did the animal show 3 or more times pain behavior (shaking or licking of the paw) the result was rated as positive for this filament.

2.7.2. Hargreaves-test

In this thermal test the animals have been habituated like in 2.7.1 in the setup (Ugo Basil, Plantar Test). The setup consists of a glass plate and transparent boxes as well as a device with a controlled infrared light source to heat up the skin at the hind paw of the animals. The infrared intensity normally was chosen as 20 or 80 (99 is the maximum). The device was put under the hind paw of the animal and started, so that the skin was heated up. Whenever the animal feels pain it removes the paw and the device stops heating and measures the time (latency). For each animal and each time point every hind paw was measured 3 times.

2.7.3. Hot plate-test

In the hotplate test the animals are put onto a plate that has a temperature range from 2 – 66°C (Ugo Basil, Hot/Cold Plate). The plate was heated up to a certain temperature (50° or 53°C) and the animal was put on the plate, that's surrounded by a transparent cylinder. As soon as the animal touches the plate, the timer was started and as soon as the animal showed any kind of pain behavior (shaking, liking, jumping) the timer was stopped and the animal immediately removed from the plate.

2.7.4. Capsaicin-test

In this test the animals were injected with 5 µl Capsaicin solution (2.9.5.1) [55]. For the injection the animals were put into a towel and the hind paw carefully fixed with the hand. Immediately after the injection a timer was started and the time, the animal spent for licking was measured. Additionally the shaking was counted. The animal was observed for 10 min, as long as the Capsaicin seems to act.

2.8. Pain-models

2.8.1. Chronic constriction injury (CCI)

In this model the sciatic nerve is ligated to induce neuropathic pain [56]. Therefore the animals had to be anesthetized (Isoflurane) and shaved at the incision spot. After

disinfection the skin was opened and with a blunt separation of the muscle (musculus gluteus superficialis) the sciatic nerve was exposed. The ligature was done using a sterilized thread (FST). 4 ligatures were made in close vicinity along the nerve. Each ligature was fixed with 2 knots. The force the first knot was done with was set by observation of a slight movement of the corresponding hind paw. Afterwards the ligated nerve was put to the original position and the skin was closed. During the whole procedure the body temperature of the animal was kept and the exposed nerve was perfused with pre-warmed saline.

2.8.2. CFA-Model

For the Injection of the complete Freund's adjuvant (CFA) (2.9.6.1) [57] the animal was anesthetized. 20µl of the emulsion have been injected on one of the hind paws. After the injection the paw width was measured to monitor the edema formation. Paw measurement was done taking photos of the paw on a gridded ground, to later analyze the distance digitally.

2.9. Solutions and recipes

Chemicals were in general used from Sigma-Aldrich.

2.9.1. Molecular Biology

2.9.1.1. Phosphate-buffered-saline (**PBS**)

NaCl	137,0 mM
KCl	2,7 mM
Na_2HPO_4	10,0 mM
KH_2PO_4	1,8 mM

The pH is adjusted to 7,4

2.9.1.2. Tris-Borate-EDTA-buffer (**TBE**)

Tris Base	90 mM
Boric acid	90 mM
EDTA	20 mM

2.9.1.3. Lysis buffer:

0,61 g Tris (50 mM)
0,87 g NaCl (150 mM)
0,19 g EDTA (5 mM)
1% Triton (or 0,5% NP40)
Fill up with water to 100 ml

2.9.1.4. SDS-Gel:

running Gel:

Water	2,0 ml
Tris 1,5 mM pH8	1,25 ml
30% Bis/Acrl	1,7 ml
10% SDS	50 µl
10% AP	25 µl
TEMED	2,5µl

stacking gel:

Water	1,2 ml
Tris 0,5 mM pH8	0,5 ml
30% Bis/Acrl	266 µl
10% SDS	20 µl
10% AP	10 µl
TEMED	1 µl

2.9.1.5. Running buffer (5x):

15,2 g Tris Base
72,0 g Glycine
5,0 g SDS
fill up with water to 1 L

2.9.1.6. Transfer buffer (1x):

3,03 g Tris Base (250 mM)
14,4 g Glycine (2500 mM)
200 ml Methanol (20%)
filled up with water to 1L

2.9.1.7. Tris-buffered-Saline (10x) (**TBS**):

87,66 g NaCl (1,5 M)
12,1 g Tris (100 mM)
set the pH to 8,0
fill up with water to 1L

2.9.2. Histochemistry

2.9.2.1. Blocking solution normal

NGS	2,5%
donkey serum	2,5%
Triton X-100	0,1%

Diluted in pre-warmed PBS.

2.9.2.2. Blocking solution **TRPV1**

NGS	3%
BSA	1%
Triton X-100	0,1%

Diluted in pre-warmed PBS.

2.9.2.3. X-Gal stock solution:

The X-gal substrate was received from PeqLab.
10% X-gal were diluted in N,N-dimethylformamide.

2.9.2.4. X-Gal staining solution:

1,8 ml of	0,2 M Na_2HPO_4	[890 mg in 25 ml]
0,7 ml of	0,2 M NaH_2PO_4	[690 mg in 25 ml]
1,5 ml of	5,0 M NaCl	[7,3 g in 25 ml]
50 µl of	1 M $MgCl_2$	[5,07 g in 25 ml]
3 ml of	50 mM $K_3[Fe(CN)_6]$	[412 mg in 25 ml]
3 ml of	50 mM $K_4[Fe(CN)_6]$	[527 mg in 25 ml]

Filled up with water to 50 ml total volume. pH has to be adjusted to 8. Immediately before use, the X-Gal stock solution and the staining solution were mixed 1:30 (30µl X-Gal stock + 870 µl X-Gal staining solution).

2.9.3. Cell-culture

2.9.3.1. DRG-Medium:

DMEM	42,5 ml
Horse serum	5,0 ml (10 %)
Glutamine 2mM	0,5 ml
Glucose 8 mg/l	1,0 ml
Pen/Strep 100 µg/ml	1,0 ml

2.9.3.2. HEK-Cell-Medium:

DMEM	42,5 ml
FCS	15,0 ml (15 %)
Glutamine 2mM	1,0 ml
Pen/Strep 100 µg/ml	1,0 ml

2.9.4. Electrophysiology

2.9.4.1. Extracellular solution (Patch and calcium imaging)

NaCl	140 mM
KCl	4 mM
$CaCl_2$	2 mM
$MgCl_2$	1 mM
Glucose	4 mM
HEPES	10 mM

the solution has to be adjusted to pH = 7,4 with NaOH

2.9.4.2. Intracellular solution (Patch)

KCl	110 mM
NaCl	10 mM
MgCl2	1 mM
EGTA	1 mM
Hepes	10 mM

the solution has to be adjusted to pH = 7,4 with KOH

2.9.4.3. Calcium channel extracellular solution (Patch)

TEA-Cl	135 mM
KCl	40 mM
$CaCl_2$	2 mM
$MgCl_2$	1 mM
Glucose	10 mM
HEPES	10 mM

the solution has to be adjusted to pH = 7,3 with TEA-OH

2.9.4.4. Calcium channel intracellular solution (Patch)

CsCl	126 mM
EGTA	10 mM
EDTA	1 mM
HEPES	10 mM
Mg-ATP	4 mM

the solution has to be adjusted to pH = 7,3 with TEA-OH

2.9.4.5. High KCl-solution (Calcium imaging)

NaCl	115 mM
KCl	40 mM
$CaCl_2$	2 mM
$MgCl_2$	1 mM
Glucose	10 mM
HEPES	10 mM

the solution has to be adjusted to pH = 7,4 with NaOH

2.9.4.6. Capsaicin solution (Calcium imaging)

The capsaicin was received from Cayman chemicals.

High concentration:

Capsaicin	1 µM

Dissolved in extracellular solution (2.9.4.1)

low concentration:

Capsaicin	100 nM

Dissolved in extracellular solution (2.9.4.1)

2.9.4.7. Synthetic interstitial fluid (**SIF**-Buffer)

$CaCl_2$	2,0 mM
Glucose (Roth)	5,5 mM
HEPES (Roth)	10,0 mM
KCl	3,5 mM
$MgSO_4$	0,7 mM
NaCl	123,0 mM
NaH_2PO_4	1,5 mM
Na-gluconate	9,5 mM
Saccharose	7,5 mM

2.9.5. Behavior

2.9.5.1. Capsaicin solution (Capsaicin test)

Saline	730 µl
Capsaicin (10mM)	200 µl
Tween80	70 µl

2.9.6. Pain-models

2.9.6.1. Complete Freund's adjuvant

The complete Freund's adjuvant was mixed (1:1) with sterile saline and

2.10. Antibodies

Table 2: Antibodies used for Histochemistry

	Species	**company**	**dilution**
TRPV1	rabbit	D. Julius lab	1:1000
NF-200	mouse	SIGMA	1:1000
β-gal	chicken	Abcam	1:250
β-gal	mouse	Promega	1:250
V-Glut 1	guinea pig	Synaptic systems	1:1000
V-Glut 2	rabbit	Synaptic systems	1:1000
V-Glut 3	rabbit	Synaptic systems	1:1000
CGRP	guinea pig	Peninsula	1:500
α2δ-3	goat	Santa Cruz	up to 1:200
α2δ-3	rabbit	Novus	up to 1:200
α2δ-3	rabbit	Abcam	up to 1:200
α2δ-3	rabbit	SIGMA	up to 1:100
c-fos	goat	Santa cruz	1:500
GAD 67	mouse	Millipore	1:500
PGP 9.5	rabbit	Abcam	1:500
HA-Tag	mouse	Covance	1:1000
GFP	goat	Genetex	up to 1:200
T7	goat	Abcam	up to 1:200

2.11. Constructs

The TRPV1 construct was a kind gift of the group of Dr. P. Heppenstall from Italy.
The T7 tagged α2δ-3 construct was a kind gift of Dr. Akiyama from Japan.
The HA tagged α2δ-3 construct was a kind gift of Dr. G. Obermair from Austria.

2.12. Software

Table 3: Software

Software name	Version	Company
LabChart 6 Pro	6	ADInstruments
MATLAB	R2014b	Mathworks
Graph-Pad-Prism 6	6	Graph-Pad Software
Axio Vision	SE64 Rel. 4.9.1	Zeiss
Image J	1.49 n	Wayne Rasband (NIH)

3. Results

This study was aimed to investigate the role of the α2δ-3 subunit in the somatosensory system, especially in the peripheral part including the primary afferents, the DRG and the first central part, the SC. Some studies already showed involvement of the subunit in heat-perception or chronic pain conditions, but a mechanism for the effects in periphery and SC was never proposed.

3.1. Phenotyping

As a lot of genomes of the known species are sequenced these days, now the function of all the genes that have been discovered is of great interest. Therefore several strategies have been invented to determine protein function. As a kind of gold standard, the knock out technic has been established. In this technic the gene of interest is just simply deleted or mutated in a way that the protein, which the gene codes for, is not produced anymore or at least loses its functionality. Various species can be used to knock out genes, but the mouse model serves as the “closest to humans” one. Since genetic alterations in mice are a standard procedure nowadays, there are knockout mice for a huge variety of genes. Another advantage is the good and rather fast progeny of mice.

After the gene deletion in mouse, it has to be carefully phenotyped. The alterations according to wild type (WT) animals are directly linked to the gene function. For the mouse model, most of the common investigations that need to be done for phenotyping are standardized, which is another big advantage.

Therefore we thought the knock-out (KO) mouse would be the model of choice to discover the function of the α2δ-3 subunit in the somatosensory system.

Mice lacking the α2δ-3 subunit of voltage gated calcium channels have been shown to exhibit altered startle response according to acoustic or tactile stimulation. The acoustic evoked startle response is reduced compared to wild-type (WT) animals but the tactile evoked startle is enhanced [52]. These two startle pathways share most of their central parts, demonstrating that the opposing phenotypes are due to alterations in periphery.

In another study the α2δ-3 subunit was also shown to be involved in heat sensation. In a drosophila screening, designed for identification of genes participating in heat perception this subunit was found. Further studies showed that not only in flies but also in mice and humans this protein takes part in the process of heat pain sensation. Interesting in this study is the fact, that all the described alterations in heat pain sensation are regarded as supra spinally provoked effects. This conclusion was based on the lack of evidence for the protein to be expressed in periphery [1].

For us the aforementioned results of the startle experiments were very striking and we therefore wanted to investigate the role of the α2δ-3 subunit in the somatosensory system.

3.1.1. The α2δ-3 subunit is expressed in DRG and spinal cord

First we investigated the expression of the subunit in the DRG and SC. The mouse-line we used (2.1) has a *LacZ-casette* inserted into the *Cacna2d3* gene disrupting its proper expression and function. Instead of α2δ-3 a β-galactosidase enzyme is expressed, under the α2δ-3 promoter. This enzyme can be detected via X-Gal, a synthetic substrate of the enzyme showing its activity, producing a blue colored precipitate.
At first we did reverse transcription PCR (RT-PCR) and quantitative real-time-PCR (qRT-PCR, was done by the Obermair Group in Innsbruck) for all the four subunits in the tissues of interest, whereas brain tissue served as a control [53] (Figure 10).

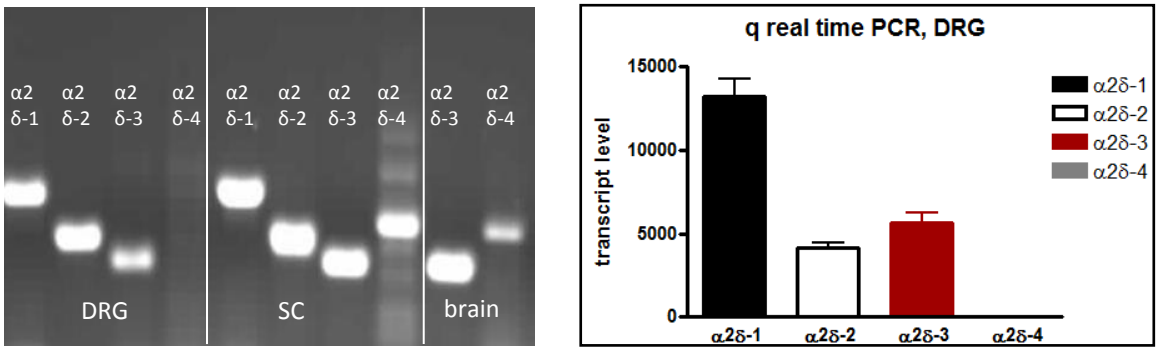

Figure 10: RT-PCR and qRT-PCR of the isoforms. The RT-PCR (left) was performed in different tissues, dorsal root ganglion (DRG), spinal cord (SC), and brain. The qRT-PCR (right) was performed in DRG tissue (data kindly provided by G. Obermair, Innsbruck). Each experiment was repeated three times. Error bars indicate standard error (SEM).

In the RT-PCR we found m-RNA of α2δ-3 in all tissues tested. Same was true for α2δ-1 and -2 (not shown for brain tissue). The α2δ-4 subunit seems not to be expressed in DRG tissue (Figure 10, left). The data of qRT-PCR from the Obermair group in Innsbruck acquired for DRG tissue confirmed the findings of the RT-PCR (Figure 10, right). Interestingly, the transcription level of α2δ-3 seems to be higher than the one of α2δ-2. To further investigate the distribution of a2d3 in DRG, we took the advantage that the mouse line we used has a lac-Z insert, we went for X-Gal staining in cryo sections of DRG and SC tissue.

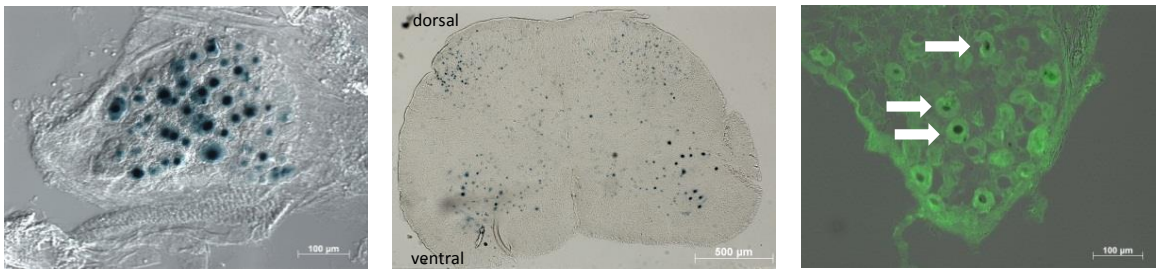

Figure 11: X-Gal staining in fixed tissue. DRG (left and right) and SC (middle, dorsal horn up). The tissue was fixed as described (2.3.2). Expression of α2δ3 is indicated by the blue colored cells. Co-staining with NF-200 (right, green) indicates myelination of α2δ3 positive cells (white arrows). Animal Numbers WT = 3; KO = 5. The staining was repeated 3 times for each animal.

The α2δ-3-subunit is expressed in the dorsal root ganglion (DRG) and the spinal cord (SC) (Figure 11, left: DRG, middle: SC). In the DRG most of the X-gal positive, meaning α2δ-3 expressing cells are positive for NF-200 a neurofilament that marks myelinated cells (Figure 11, right), which is consistent with observations from other laboratories [47]. In the SC α2δ-3 is expressed in the dorsal horn, where the nociceptors terminate and the ventral horn, where the motor neurons locate. Therefore alterations in the behavioral output can be caused by both, deficits in the dorsal (touch and pain) and the ventral (motor function) part. Tests for motor function like the rota-rod test can elicit possible deficits, the lack of α2δ-3 in the ventral horn can cause.
These results are in line with other studies, reporting α2δ-3 m-RNA expression in DRG in rat and mice [44, 47]

Next we investigated which cells in DRG express the α2δ-3 subunit. In DRG cells can be differentiated according to the size of the cells. C-fibers, mainly responsible for pain perception are smaller than 20 µm, A-δ-fibers, responsible for pain and normal temperature, are between 20 and 25 µm and the A-β fibers, responsible for normal touch are bigger than 25 µm.

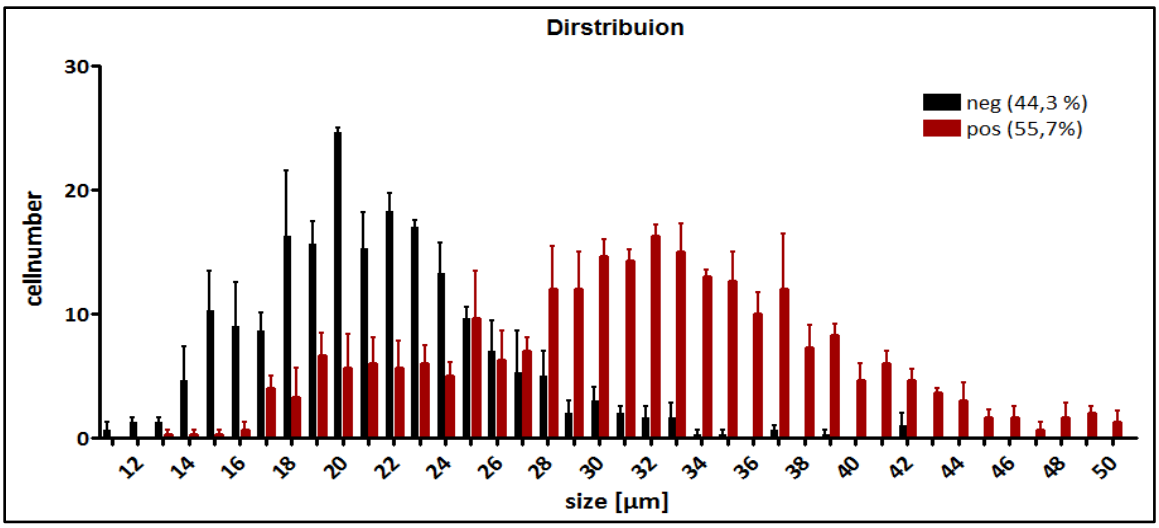

Figure 12: Cell-size distribution. The cell size was measured using Axio-vision (Zeiss) software. Same slices as in Figure 11 have been used. Two measures per cell were done and the mean was taken to plot the size-distribution. For each genotype 3 animals were used and DRGs of lumbar parts L3, L4 and L5 taken. More than 300 cells per group have been measured. Error bars indicate standard error (SEM).

The α2δ-3-positive cells are manly in the range of big, meaning non-nociceptive cells (>25 µm). But there are as well a lot of medium-sized (20 – 25 µm) and small cells (<20 µm) that express α2δ-3 subunit. Overall 55,7% of DRG neurons are positive for the subunit (Figure 12). This finding fits as well with a recent study using transcriptional profiling for differentiation of cells. In this study the α2δ-3 was mainly found in cells that are more responsible for normal touch sensation, but there was also a small subpopulation of nociceptors found expressing the subunit [47].

For a further specification of cells that express our protein of interest we wanted to do immuno-histo-chemistry. We checked plenty of commercially available α2δ-3 antibodies, with poor success. It is known that there can be three different sizes of the protein 59, 113, 123 kDa (Santa Cruz) expected. We tried three antibodies in western-blot but in our hand there was never a clear difference between KO and WT animals. The first experiments were performed with samples from brain as a positive control and samples from spinal cord (SC) and dorsal root ganglion (DRG) from WT animals.

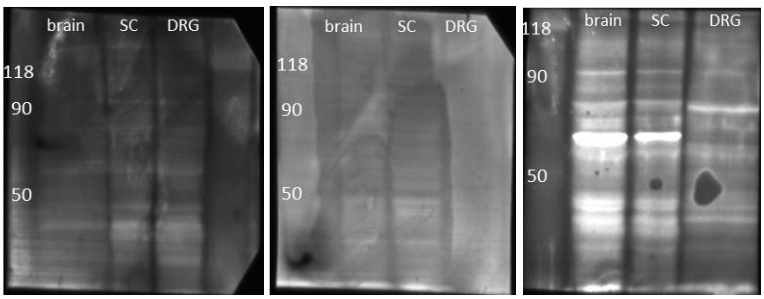

Figure 13: Western-blots. Left: AB from Abcam (ab81000), middle: AB from Novus (NBP1-20111), right: AB from Santa Cruz (sc-99324). Dilution was 1:500. No Bands for abcam and Novus AB. The Santa Cruz antibody showed some unexpected bands, especially for the DRG sample.

As shown in Figure 13 the commercially available antibodies weren't that promising. The only one showing clear bands was the one from Santa Cruz. All antibodies have been tried several times in different dilutions. In case of the Santa Cruz antibody the bands deviate from the expected size. Additionally they only appear in SC and brain, not in DRG.

In lack of a working commercially available antibody for the α2δ-3 subunit we wanted to create an own. Together with the help of Dr. Hubert Kalbacher from the "Medizinisch-Naturwissenschaftliches Forschungszentrum" of the University of Tübingen we immunized rabbits with 3 peptides chosen from the α2δ-3 subunit sequence. All of the peptides are supposed to be behind the insertion site of the lacZ-cassette. This is important because we don't know if parts of the α2δ-3 protein located before the insertion site are still transcribed and therefore present in the KO mouse.

First we tried western blot for checking the new antibody. The first western-blot was done using the antibody mixture of all three peptides that have been used for immunization of the rabbit.

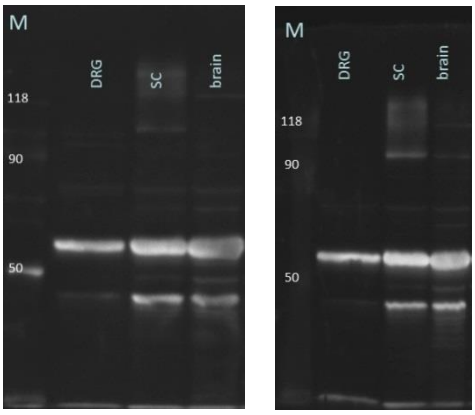

Figure 14: Western-blot with α2δ-3 antibody from Kalbacher. Here the antibody mixture (against all three peptides) was used in a dilution of 1:5000. Left shows the WT and right the KO. Prominent bands were higher than 50 kDa, probably 59 kDa, a band that can be expected. In brain and spinal cord (SC) there is an additional band lower than 50 kDa which was not expected. This band is not present in dorsal root ganglion (DRG). There are more bands but much weaker than the mentioned ones. There seem to be no difference between WT and KO. The experiment was repeated 3 times.

The western-blot doesn't show any difference between WT and KO animals (Figure 14). Expected bands with the size of 59 kDa appeared in WT but also in the KO where it should be absent. For further investigation we used an affinity purified antibody (against peptide YEEGKKRRKPNYSSVDLSEV). We selected this peptide because this didn't show any similarity with the α2δ-4 subunit in sequence, as the other both peptides did.

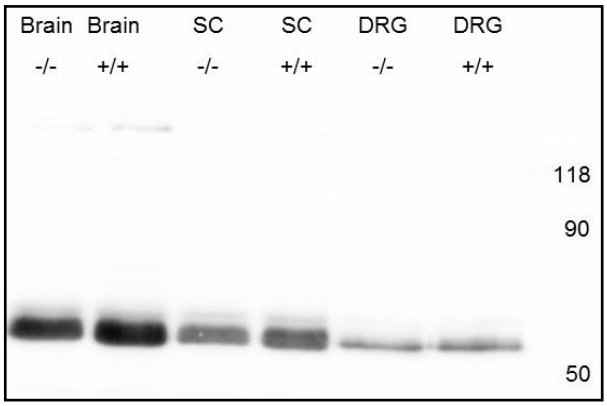

Figure 15: Western-blot with purified antibody. Kalbacher-antibody after affinity purification to the peptide (YEEGKKRRKPNYSSVDLSEV). The most prominent band is a bit higher than 50 kDa. This band probably is the 59 kDa band we can expect. Antibody dilution was 1:7500. Experiment was repeated 3 times.

For the affinity purified antibody the picture was very much the same (Figure 15). The most prominent band at 59 kDa is still present but also in the knockout animal. The very weak band (123 kDa) that only shows up in the brain sample of wild-type animals showed never up again, even when increasing the protein concentration, so it's most probably unspecific.

To check whether the prominent band contains the α2δ-3 subunit we cut it out, separated in an upper-, middle- and lower band and sent it for mass-spectrometry analysis to the Kalbacher lab.

	Accession	Mass	Score	Description
1.	gi|92911770	23896	109	XTP3TPA-transactivated protein 1 [Homo sapiens]
2.	gi|221045918	46936	90	unnamed protein product [Homo sapiens]
3.	gi|2119276	49362	88	beta-tubulin - human (fragment)
4.	gi|7106439	50095	87	tubulin beta-5 chain [Mus musculus]
5.	gi|18088719	50096	87	Tubulin, beta [Homo sapiens]
6.	gi|338695	50240	87	beta-tubulin [Homo sapiens]
7.	gi|189069169	50264	87	unnamed protein product [Homo sapiens]
8.	gi|4507729	50274	87	tubulin beta-2A chain [Homo sapiens]
9.	gi|21746161	50377	87	tubulin beta-2B chain [Mus musculus]
10.	gi|27227551	50283	87	class II beta tubulin isotype [Homo sapiens]

Figure 16: Part of protein summary report of the Mascot Search results. These first 10 hits show that the band mostly contains tubulin or tubulin associated proteins. The protein summary report was kindly provided by the Kalbacher lab.

The protein report from the mass-spectrometry didn't show any α2δ-3 in the band (Figure 16) but tubulin and tubulin-associated proteins show up. With this result it could still be possible that α2δ-3 occurs in the band, but if it shares the same size than tubulin protein it would be impossible to detect α2δ-3 because tubulin is expressed in much higher amounts than α2δ-3.

As a further experiment we used HEK cells transfected with a α2δ-3 construct that contains a T7-tag. This construct was a kind gift of Dr. Akiyama from the Medical and Dental University of Tokyo. We tested the purified Kalbacher antibody and a T7 antibody (Abcam ab9138) to compare three groups of cells. Naïve HEK cells without any transfection which should express no T7, a group with a control transfection (empty vehicle) and the group with the transfected construct.

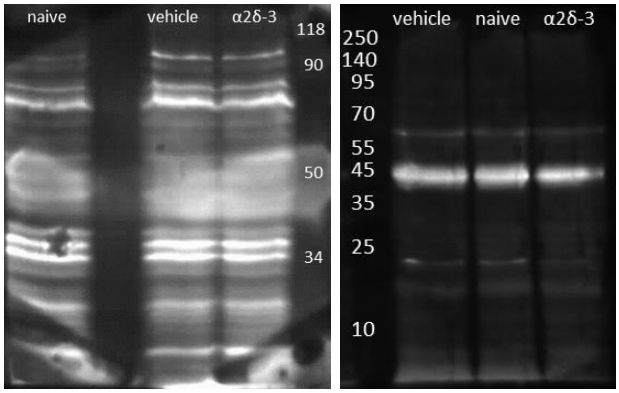

Figure 17: Western-blot of transfected HEK-cells. Left is the T7-antibody (1:2000) on the right the purified Kalbacher antibody (1:2500). The T7-antibody doesn't seem to work, because there is no difference. HEK cells do express the α2δ-3 intrinsically in low amounts, that's why we expected bands in all three groups. But in the α2δ-3 transfected group we would have expected a much broader band showing more protein. The expected band size is 59 kDa were a weaker band occurs. The more prominent band at 45 kDa was unexpected.

In the HEK-cell culture system both, the T7-antibody and the purified Kalbacher antibody didn't seem to work (Figure 17). For the α2δ-3 antibody we would have expected bands in all three samples, because HEK-cells intrinsically express low amounts of the subunit [58]. But the transfected sample should show a much stronger signal, because of overexpression of α2δ-3. The T7-antibody didn't show any difference in the samples. Here we would only expect a band in the transfected group with the construct (T7-α2δ-3). So far we haven't been able to find and/or create a proper α2δ-3 antibody.

Having the possibility of transcriptional profiling for the known Ca_V1 and 2 subunits as well as the auxiliary β- and α2δ-subunits by qRT-PCR, we looked for the developmental expression of the mentioned proteins in DRG of WT mice. The experiments were done by the applicant in the Obermair Lab at the medical university of Innsbruck. DRG-tissue from animals at postnatal day P0, P3, P7, P14, P28 and adult (> P56) was taken to perform the qRT-PCR profile.

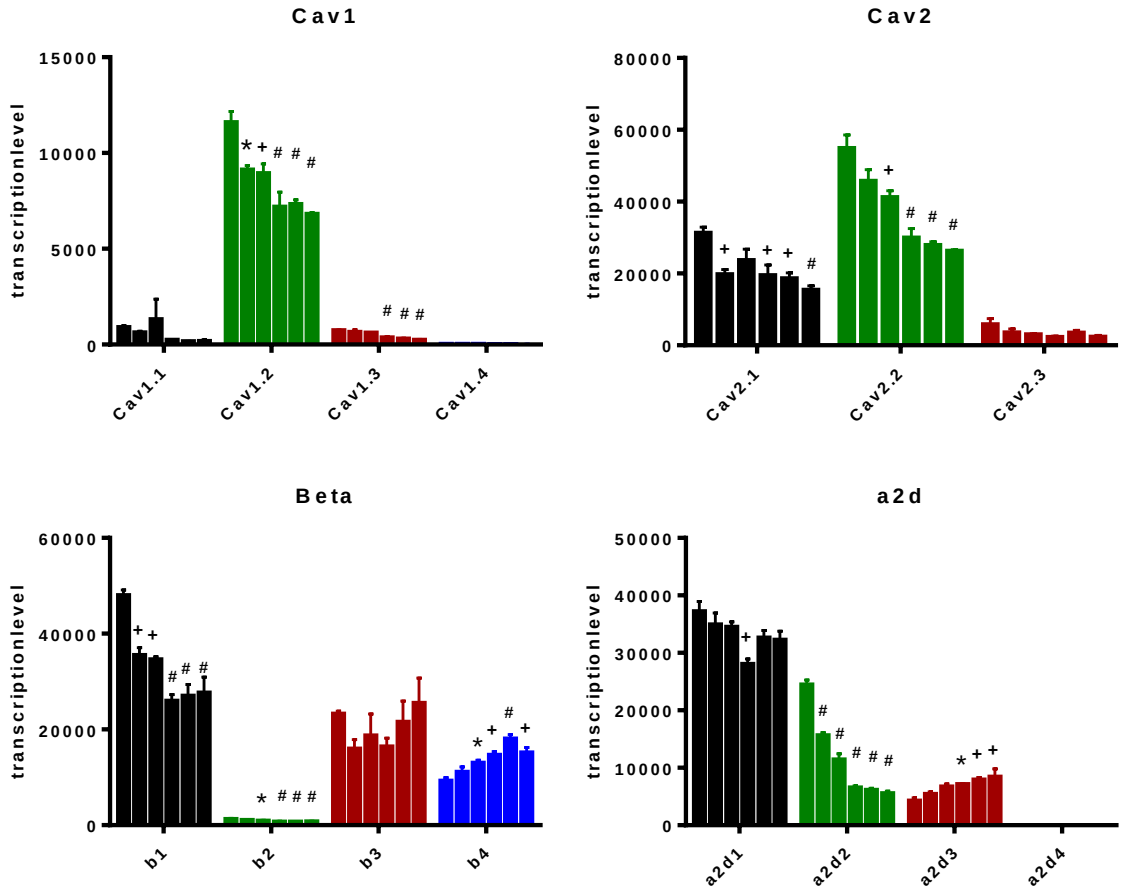

Figure 18: qRT-PCR of DRG neurons. The bars indicate different time points in development (from left to right: P0, P3, P7, P14, P28 and adult). The Ca_V1 channels (upper left) are also called L-Type channels. The Ca_V2 channels (upper right) are also called PQ-Type (Ca_V 2.1), N-Type (Ca_V 2.2) and R-Type (Ca_V 2.3) channels. The β- (lower left) and the α2δ-subunits (lower right) are supposed to be auxiliary subunits of the pore forming Ca_V proteins. Experiments have been measured as triplicates and repeated 3 times. Error bars indicate standard error (SEM). For Statistics one-way-ANOVA was used (Ca_V 1.2, 1.3 and 2.2, β1, 2 and 4, α2δ-2 = $p < 0.001$; Ca_V 2.1 and α2δ-3 = $p < 0.01$; α2δ-1 = $p < 0.05$), significances vs. P0 are indicated (* = $p < 0.05$; + = $p < 0.01$; # = $p < 0.001$).

The qRT-PCR data shows the transcription levels of the different genes. For the Ca_V1 or L-Type channels the highest expressed in DRG is the $Ca_V1.2$ (Figure 18, upper left). The highest expression level of all transcripts is shown by the $Ca_V2.2$ or N-Type channel (Figure 18, upper right). The time course of the pore forming Ca_V units seems to be the same, as they decrease during development (Ca_V 1.2, 1.3, 2.1 and 2.2 significantly). The auxiliary subunits β1 and 2 as well as α2δ-1 and -2 are significantly down regulated during development.

Interestingly the time course of the β-4 subunit (Figure 18 lower left) shows a significant up-regulation. Same accounts for the α2δ-3 subunit (Figure 18, lower right).

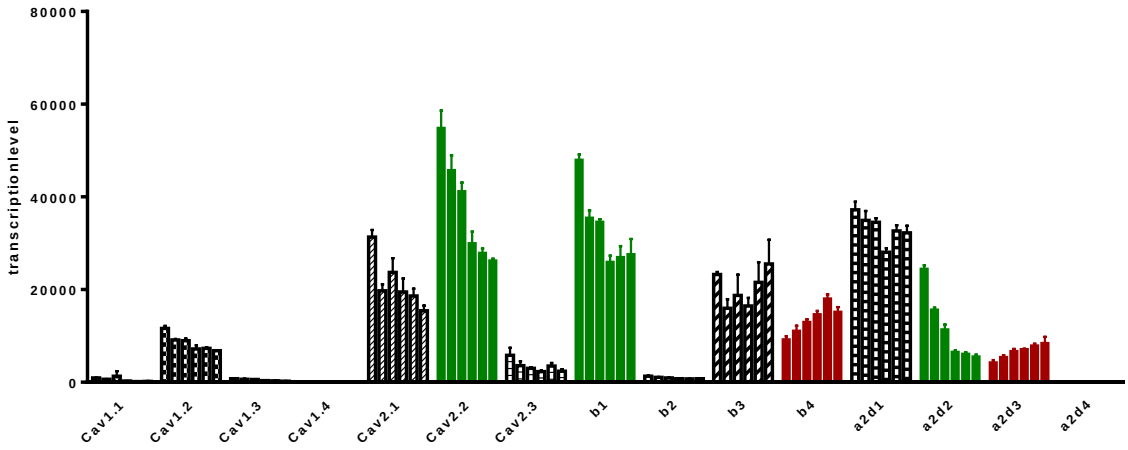

Figure 19: Overview of all transcripts checked. The colors indicated proteins that share similar expression profiles. The different bars are time points in development of the animals (from left to right: P0, P3, P7, P14, P28 and adult). In red the two transcripts that are up-regulated during development. In green three transcripts that decay very fast in younger animals. Tissue from 3 animals was used, each measurement was 3 times repeated.

In the overview (Figure 19) it's again quite obvious that there are only two transcripts (red) that are clearly up-regulated during development. Another interesting point is the fact, that the $Ca_V2.2$, the β-1 and the α2δ-2 (green) are extremely down-regulated during development. Unexpectedly again we found that in adult animals the transcript-level of α2δ-3 is even higher as the one of α2δ-2. To our knowledge this is the first time such kind of profiling is shown for DRG in mice.

3.1.2. Deficient mice show a prominent heat phenotype

Behavioral phenotyping is of extraordinary importance in the mouse model. It shows the functional consequence, which might be altered upon gene deletion. Here we did some classical tests for acute thermal and mechanical pain, regarded to the aforementioned studies that show an increased tactile startle response and a reduced sensitivity for heat pain.

In the Hot-plate test the animal is put on a plate that is heated to a defined temperature (53° and 50°C) and the latency is measured until any kind of pain behavior, like paw shaking or liking, or jumping in order to escape from the plate, occur. In this test the response of the animal reflects an integrated process that needs higher, supra spinal areas to elicit the corresponding behavior [59].

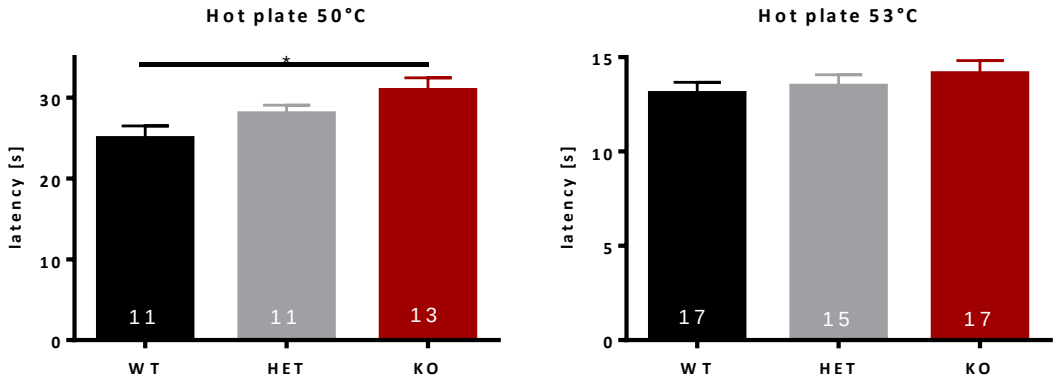

Figure 20: Hot plate-test. Test was performed with two temperatures. The animals were put on the plate and time until the first pain behavior measured. Animal numbers are indicated within the bars. Error-bars indicate standard error (SEM). For statistics one way ANOVA with Dunn's multiple comparison test was used(* = $p < 0.05$).

The deficient animals show a significant higher latency time at 50°C (Figure 20). At a higher temperature (53°C) the tendency is the same, but no significance appeared. This phenotype was published from another group soon after our first observation [1].

Next we performed a mechanical acute pain test, the automatic von Frey test (Figure 21). In this test the animal is put on a metal grid and a blunt needle is put under the hind paw. During the test, the needle is pushed against the paw with increasing force. If the animal feels pain it removes the paw and the latency-time and force is measured. This pain induced movement of the hind-paw is regarded as a spinal reflex [59].

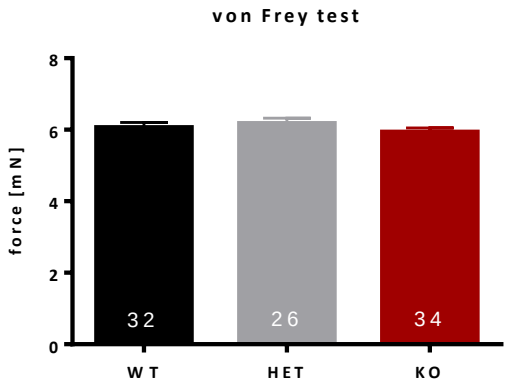

Figure 21: Automatic von Frey test. In the von Frey test each animal was tested 3 times at the same hind paw. For analyses all data from same animals were pooled. Animal numbers are indicated in the bars. Error-bars indicate standard error (SEM). Statistics was done using one way ANOVA with Dunn's multiple comparison test (WT vs. KO, n.s.).

There was no significant difference in the automatic von Frey test observed. This is in line with the results from the previous study by Neely et al., were no deficits in mechanical pain have been reported too.

Given the fact that there is a prominent α2δ-3 expression in the ventral horns of the SC (Figure 11), where the motor-neurons locate, we performed the Rota-Rod test as a classical test for motor function. This test was performed in order to investigate possible deficits in the motor output that could in the end cause the delayed response in the hot plate test. The animals are placed on a rotating tube and trained to walk there at a low velocity. For the test the velocity is increased over time and the time is measured until they cannot follow the rotation any more. Animals with problems in motor-function are expected to fail at lower velocities than intact animals.

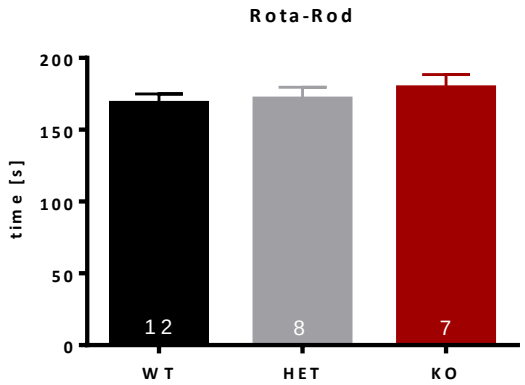

Figure 22: Rota-rod test. For rotarod Each animal was trained for 2 days, followed by 3 subsequent days of testing with 3 repetitions per day. For analyses all data from same animals were pooled. Animal numbers are indicated in the bars. Error-bars indicate standard error (SEM). Statistics was done using one way ANOVA with Dunn's multiple comparison test (WT vs. KO,n.s.).

We did not see a significant difference in the rota-rod test (Figure 22). This confirms that there are no deficits in motor-function in the KO mice.

3.2. Mechanisms

3.2.1. Deficient mice show alterations in fibers at the very periphery. (Experiments done by Dr. Jing Hu)

Our aforementioned results on α2δ-3 expression in peripheral tissue (DRG and SC) as well as the behavioral phenotypes, showing deficits especially in thermal pain perception lead us to several possible mechanisms that can cause the findings.
With ex-vivo-skin nerve recording (Figure 23) we are able to investigate alterations in the most peripheral part of the PNS, even before the cell soma in the DRG. With this approach possible changes in the pain transmission pathway can be elucidated. The Focus in this set of experiments was on fiber responses according to heat stimuli.

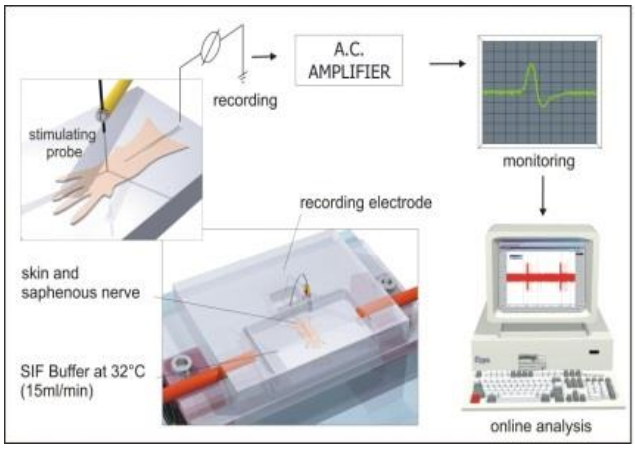

Figure 23: Scheme of the ex-vivo-skin-nerve recording. The skin of the hind-paw is carefully removed keeping the nerve intact. It is perfused with oxygenized synthetic interstitial fluid (SIF). The nerve has to be split into smaller fibers, as small as possible. These fibers are put onto the recording electrode. The skin part can be stimulated with mechanical, thermal or chemical stimuli. An oscilloscope shows the response shape that can be later used to classify the recorded fiber. Conduction velocity and mechanical threshold can as well serve as markers for classification. (This scheme was kindly provided by Dr. Jing Hu).

For thermal stimulation a ramp was chosen, starting at 32°C, heating up to 56°C, holding for 5s and then cooling down to 32°C again. An example trace is shown in Figure 24.

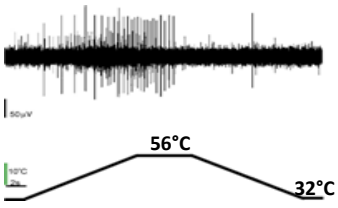

Figure 24: Example trace of the thermal stimulation. The lower scheme shows the heating ramp. The upper one shows the response of a nerve fiber according to the thermal stimulation. During the heating phase the firing of the fiber is most prominent. During the heat plateau (56°C) it stops firing. There is no response in the cooling phase of the stimulus. (This example trace was kindly provided by Dr. Jing Hu).

The analysis of the data was done according to the different fiber types. Therefore specific parameters like the conduction velocity and the mechanical threshold was

measured. We concentrated on C- and Aδ-fibers, because these are supposed to be thermo sensitive.

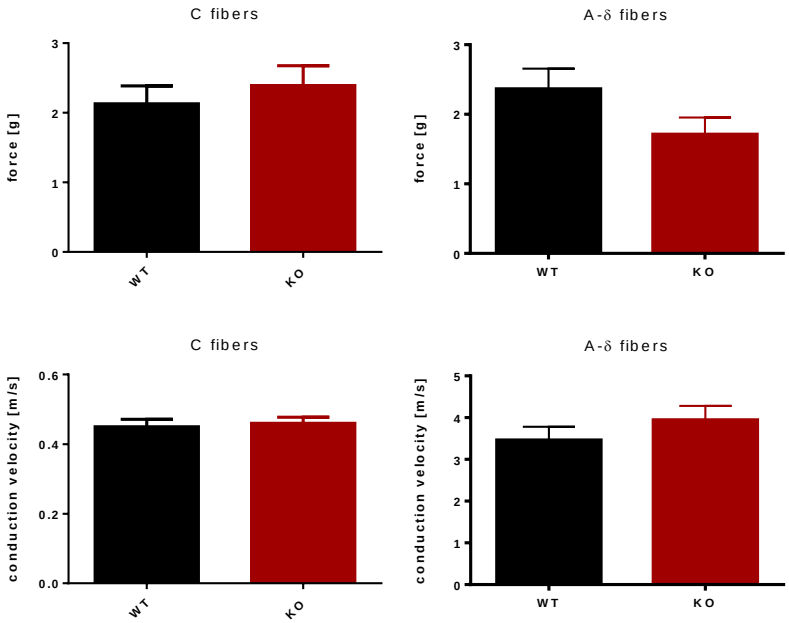

Figure 25: Mechanical threshold and conduction velocity. To differentiate between the different fiber types these parameters are measured. Mechanical threshold was determent with von Frey Filaments of different strength. The conduction velocity was measured using electrical stimulation. For WT 44 fibers were measured for KO 34. For statistics t-test was used (n.s.).

Dr. Hu did not observe any significant difference, neither for the mechanical threshold nor the conduction velocity (Figure 25), showing that the fibers in the mutant mice still have the same basic properties as WT fibers. The mechanical threshold is quite comparable for both fiber-types, ranging around 2 g. As already mentioned in the introduction the C-fibers are much slower in signal transmission because they lack of myelin sheets. So the Aδ-fibers are almost 10 times faster. But anyway no difference between WT and KO fibers was observed.

Next Dr. Hu measured the responses caused by thermal stimulation. Here the firing rate was determined (Figure 26).

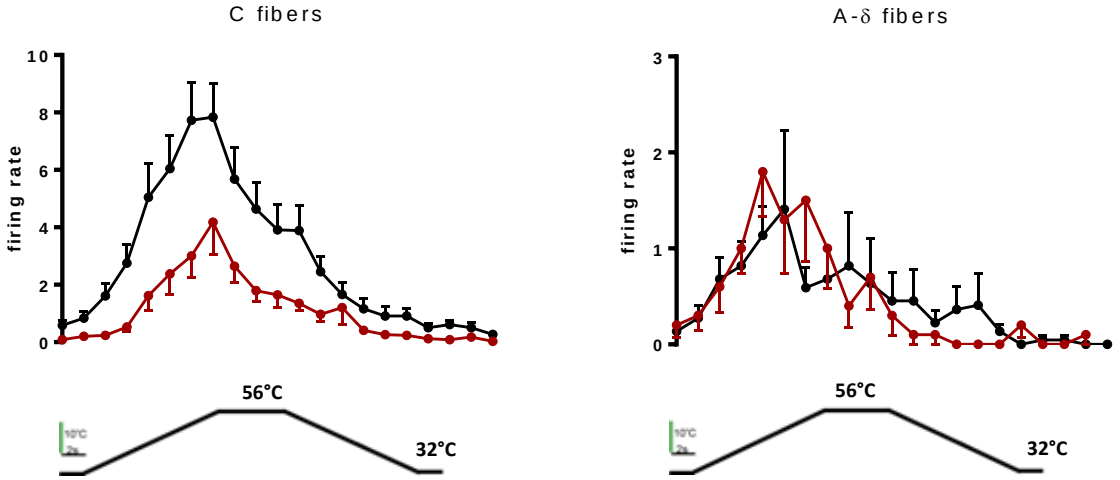

Figure 26: Firing rate of C- and Fibers. The upper graph shows the firing rate (WT in black, KO in red), the lower scheme shows the heating stimulus that was used. The firing rate is reduced in C-fibers but not in Aδ-fibers in the α2δ-3 deficient mice. The heating ramp was 2.4°C per second. The Numbers of recorded fibers are WT: 44 and KO: 34. For statistics two-way ANOVA was used (C-fibers: WT vs. KO $p < 0.01$; Aδ-fibers: n.s.). The graph was kindly provided by Dr. Jing Hu.

In the C-fibers there was a significant reduction in the firing rate observed. This was not found in Aδ-fibers (Figure 26). For both fiber types the firing rate increases upon heating and peaks approximately when the ramp reaching the terminal temperature.
A reduction in the firing rate could be one explanation for the reduced sensitivity in the hot plate test, mentioned earlier.
From the data recorded for the firing rate the thermal threshold could be calculated.

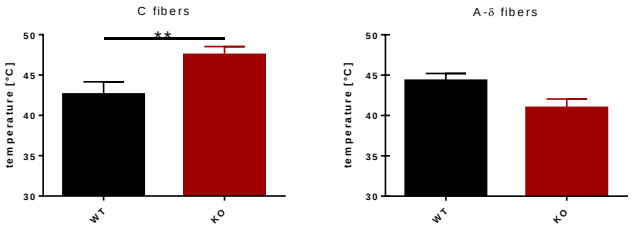

Figure 27: Heat-threshold of C-fibers. The threshold in C-fibers of the α2δ-3 deficient mice is significantly increased. The threshold was regarded as the temperature when the C-fibers start to fire according to the heating-stimulus. For significance testing t-test was used (** = $p < 0.01$). The data was kindly provided by Dr. Jing Hu.

The heat threshold was found to be increased only in C-fibers, not in Aδ-fibers (Figure 27). This can be an explanation for the reduced firing rate found in C-fibers. For Aδ-fibers the threshold seems to be a bit reduced, but not significant.

For further analysis the population of heat-responding fibers within the different fiber types was determined. Most of C-fibers are regarded as heat sensitive as well as about 50% of Aδ-fibers.

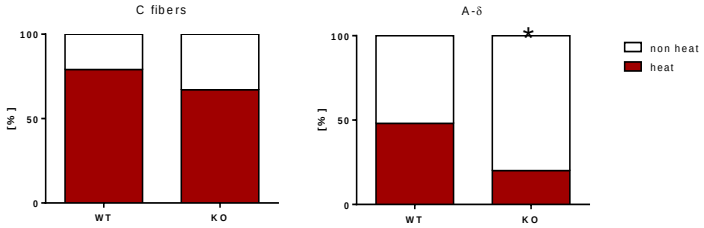

Figure 28: Population of heat responding fibers. The population of heat responding Aδ-fibers is significantly reduced. For significance testing the Fisher's-exact-test was used. Asterisks indicating significant difference: * = $p < 0.05$. The data was kindly provided by Dr. Jing Hu

As expected much more C-fibers respond to heat than Aδ-fibers. But only for the Aδ-fibers there was a significant reduction in heat-responding fibers detected. Therefore the different fiber types show up with different strategies to reduce the input to the DRGs and SC upon thermal stimulation. C-Fibers have reduced firing rates and an increased heat threshold and less Aδ-fibers respond to heat at all. Both strategies lead to the same consequence, less input from the periphery, which could be a nice explanation for the reduced sensitivity in the hot plate test.

3.2.2. Calcium influx after thermal and capsaicin stimulation is altered

From the previous experiment we know that there is already a change in the nerve fibers, carrying the signals to the DRG somas and the SC. With the next experiment we wanted to investigate the properties of the soma of DRG neurons and therefore used calcium imaging.

Calcium imaging is a common method to investigate what kind of substances or other stimuli lead to calcium influx into neuronal cells and additional what kind of treatment alters these responses. Because of the thermal phenotype we focused on heat stimuli of different ramps and different final temperatures as well as capsaicin, the agonist of the best investigated heat receptor TRPV1. Using a gravity driven perfusion system together with a patch clamp amplifier we were able to do this kind of stimuli. For neuronal cell cultures a KCl stimulus is used to check the excitability and viability to make sure that the measured cells are neurons and they are viable. The cells from primary DRG culture were used 24h after plating. After loading with Fura-2 the cells were measured with an AxioObserver A1 from Zeiss (Figure 29).

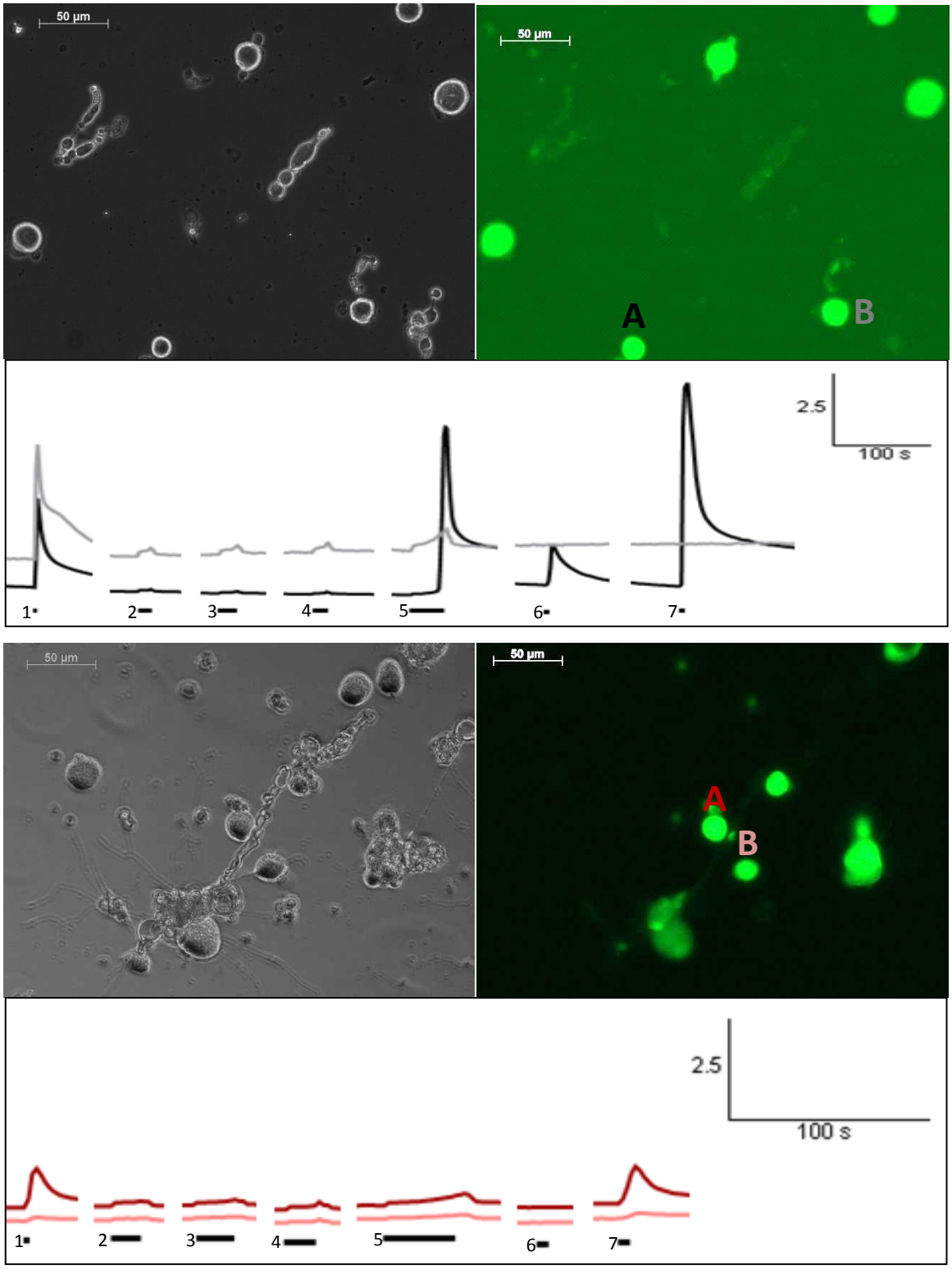

Figure 29: Example pictures and traces. Calcium imaging was performed in 24h primary culture of DRG neurons of mice with different genotype. Pictures show the cells immediately before measuring (upper: WT, lower: KO; left: brightfield; right: fluorescent picture after Fura-2 loading). Colored letters indicate the corresponding trace. Stimuli: 1: KCl (40mM); 2. fast 43°C; 3: slow 43°C; 4: fast 53°C; 5: slow 53°C; 6: capsaicin (100nM); 7: capsaicin (1µM).

The first parameter checked was the basal calcium level of the cells before any kind of stimulation. Therefore the ratio values 10 sec before the first stimulus (KCl) were recorded and analyzed.

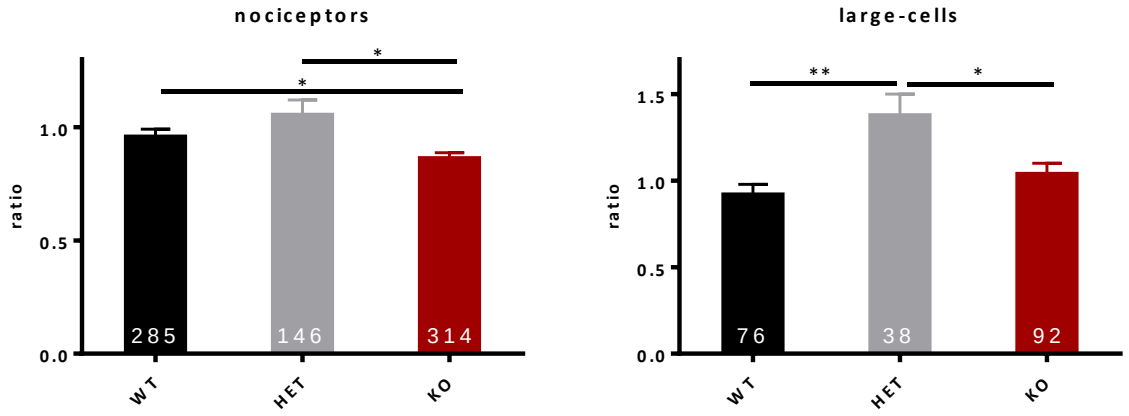

Figure 30: Baseline of DRG cells. The baseline intensity was recorded for 10s before the first stimulus (KCl). The cell-numbers are indicated in the bars. WT in black, HET in grey and KO in red. Error-bars indicate standard error (SEM). Statistics was done using t-test (* = $p < 0.05$; ** = $p < 0.01$). Animal numbers: WT = 13; KO = 11; HET = 6. For each animal, up to 4 cover slips have been measured.

For the small-cells (nociceptors) there is a significant difference between the WT and the KO as well as between HET and KO. For the big cells there are differences between WT and HET as well as HET and KO (Figure 30). For the further experiments we focus on the differences between WT and KO, the HET data are just shown to complete the data. The significant lower calcium level in KO mice was unexpected.

After the analysis of the baseline ratios we looked at the number of responding cells (Figure 31). Therefore only cells were analyzed that had a response to the KCl stimulus. This stimulus serves as a neuronal marker, because only neurons tend to depolarize upon a high KCl concentration, and this depolarization leads to a prominent calcium influx which is measured. The heat stimuli have two different final temperatures. 43°C is approximately the threshold when heat starts to get painful. And 53°C is for sure a painful heat stimulus. The different heating ramps/velocities are chosen because it was shown that different heating ramps activate different fiber types [60, 61]. As a chemical agonist for the TRPV1 heat receptor capsaicin in two concentrations was selected. The lower concentration serves for investigation of possible sensitization effects. The higher concentration is a very strong stimulus that should activate all cells that express TRPV1. The stimuli were given in the same order as indicated in Figure 29.

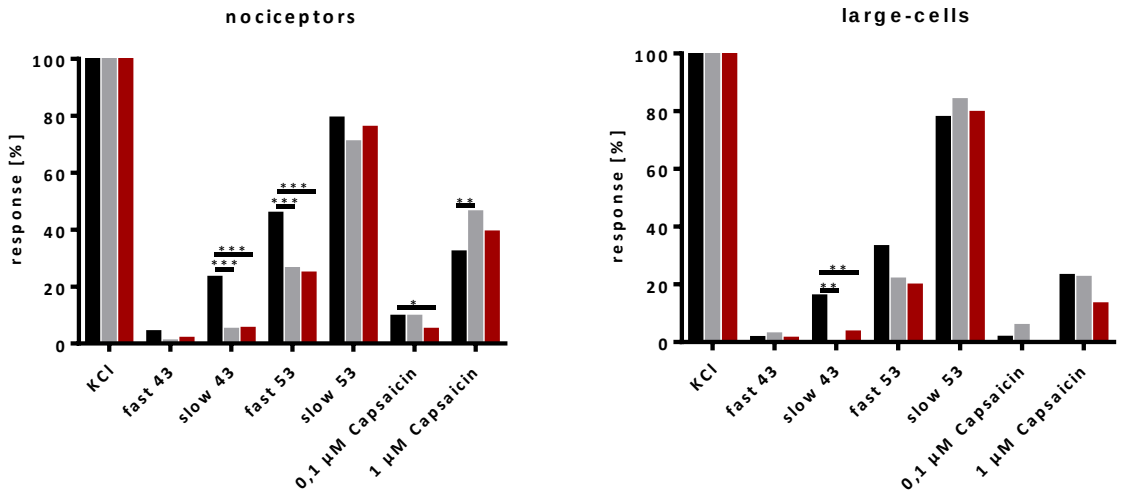

Figure 31: Responding DRG cells. Only KCl positive cells were used for analysis. The cell-numbers are indicated in Table 4 and Table 5. WT in black, HET in grey, KO in red. Statistics was done using Fisher's exact test (* = $p < 0.05$; ** = $p < 0.01$; *** = $p < 0.001$). Animal numbers: WT = 13; KO = 11; HET = 6. For each animal up to 4 cover slips have been measured.

The percentage of responding nociceptors is lower in the knockout mice, except for the 1µM capsaicin stimulus (Figure 31 left). Significances are found for the slow 43°C, the fast 53°C and the 0.1µM capsaicin stimulus. The 1 µM capsaicin stimulus shows for the heterozygous animals a significant increase in responding cells and the same tendency for the knockout. In case of the slow 43°C stimulus there is a significant reduction. Large cells are not expected to respond to temperature. Therefore the huge number of responding cells for the slow 53°C stimulus was unexpected. This might be regarded to the fact that high temperature stimuli anyway alter the membrane properties and therefore can lead to calcium influx.
The reduction in responding cells upon heat stimulation again fits with the observations in the hot-plate test where the animals are less sensitive. It also confirms the skin-nerve data, where a similar populational change for the Aδ-fibers occurred.

Next we analyzed the peak values in different ways to get more details about the alterations in calcium influx. Therefore we analyzed different peak values, the absolute peak, the peak subtracted by the baseline and the peak normalized to the baseline (Figure 32- Figure 34).

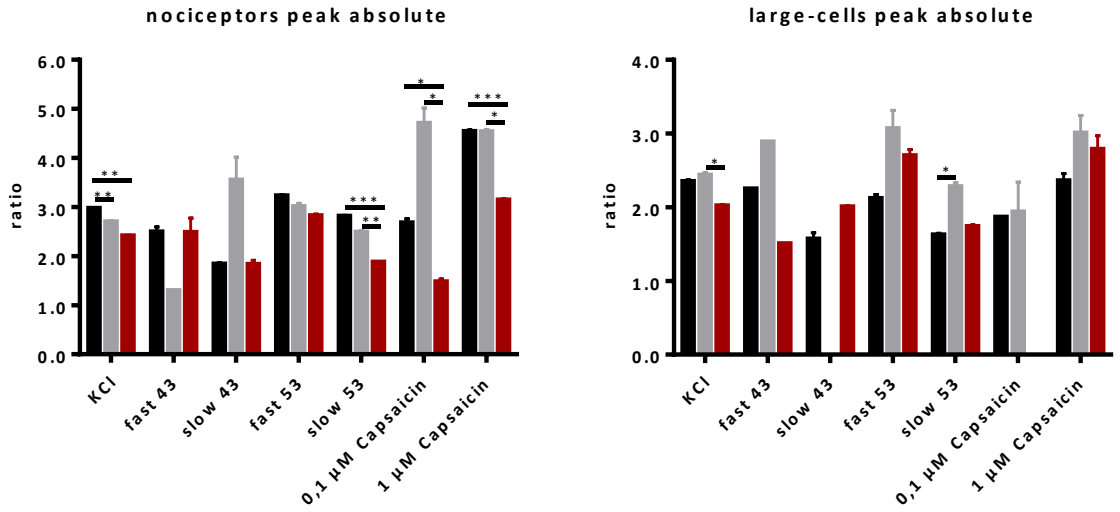

Figure 32: Absolute peak. The KCl stimulus served as the control stimulus. KCl positive cells were used for analysis. The cell-numbers are indicated in Table 4 and Table 5. WT in black, HET in grey, KO in red. Error-bars indicate standard error (SEM). Asterisks are indicating significances. Statistics was done using t-test (* = $p < 0.05$; ** = $p < 0.01$; *** = $p < 0.001$). Animal numbers: WT = 13; KO = 11; HET = 6. For each animal up to 4 cover slips have been measured.

Focusing on the differences between WT and KO animals all three peak values (absolute, subtracted and normalized) are showing the same tendencies in principle. Looking at the peaks of nociceptive cells (Figure 32 left) there is always a decrease in the knockout animals. For the KCl, slow 53°C and the both capsaicin stimuli the peaks differ significantly. For the large cells (Figure 32 right) there are no significant differences between the WT and the KO animals. These results are quite in line with the observed phenotype of the hot-plate test.

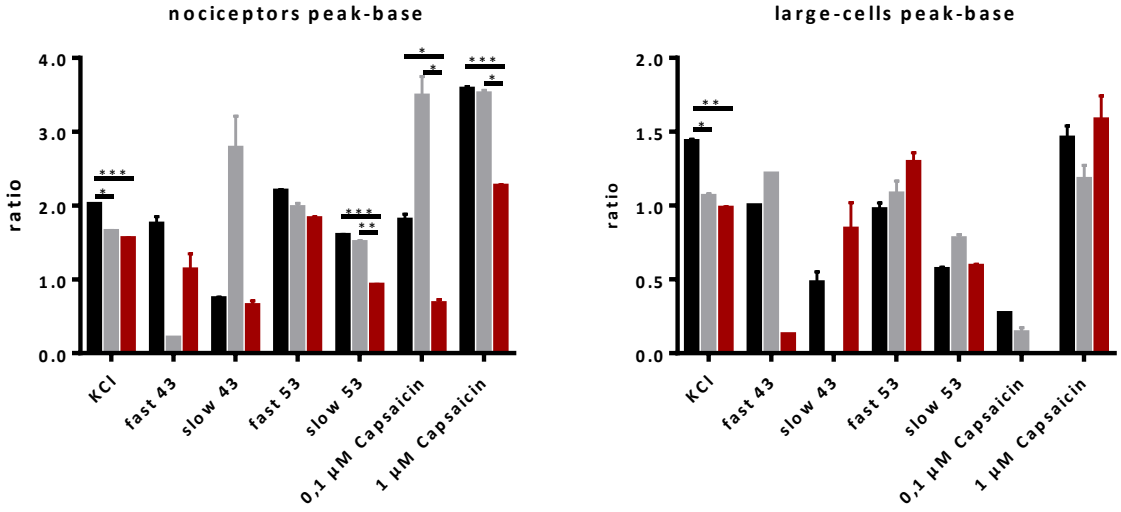

Figure 33: Peak minus baseline. KCl positive cells were used for analysis. The cell-numbers are indicated in Table 4 and Table 5. WT in black, HET in grey, KO in red. Error-bars indicate standard error (SEM). Asterisks are indicating significances. Statistics was done using t-test (* = p < 0.05; ** = p < 0.01; *** = p < 0.001). Animal numbers: WT = 13; KO = 11; HET = 6. For each animal up to 4 cover slips have been measured.

Because there are already differences in the baseline for the different phenotypes (Figure 30), we subtracted the baseline from the absolute peak values. After baseline subtraction the significances are still there, showing that the influences of the baseline differences are not so prominent. Now there appears even a significant difference for the KCl stimulus in large cells (Figure 33 right).

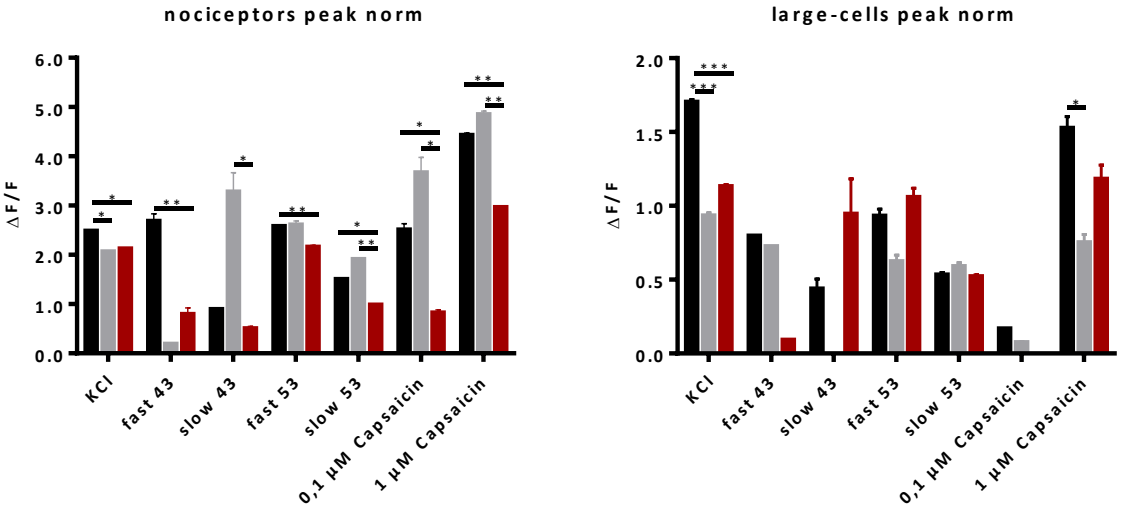

Figure 34: Peak normalized. KCl positive cells were used for analysis. The cell-numbers are indicated in Table 4 and Table 5. WT in black, HET in grey, KO in red. Error-bars indicate standard error (SEM). Asterisks are indicating significances. Statistics was done using t-test (* = p < 0.05; ** = p < 0.01; *** = p < 0.001). Animal numbers: WT = 13; KO = 11; HET = 6. For each animal up to 4 cover slips have been measured.

Because of the baseline difference the best way to analyze the peak data is to normalize it to the baseline (Figure 34). First it should be mentioned that in case of the KO animals both, nociceptors and large-cells show a significant decrease for the peak of the KCl stimulus, indicating a reduced excitability for the KO cells. This is again in line with the skin-nerve data showing a reduction in firing rate for the C-fibers.
For the nociceptors there are significant changes for every other stimulus (WT vs. KO) except the slow 43°C, showing a decrease in peak values, supporting the behavior data of the hot plate test.

As the last analyzing step we calculated the area under the curve (AUC). This value is representative for the amount of calcium that flows into the cells during the stimulation.

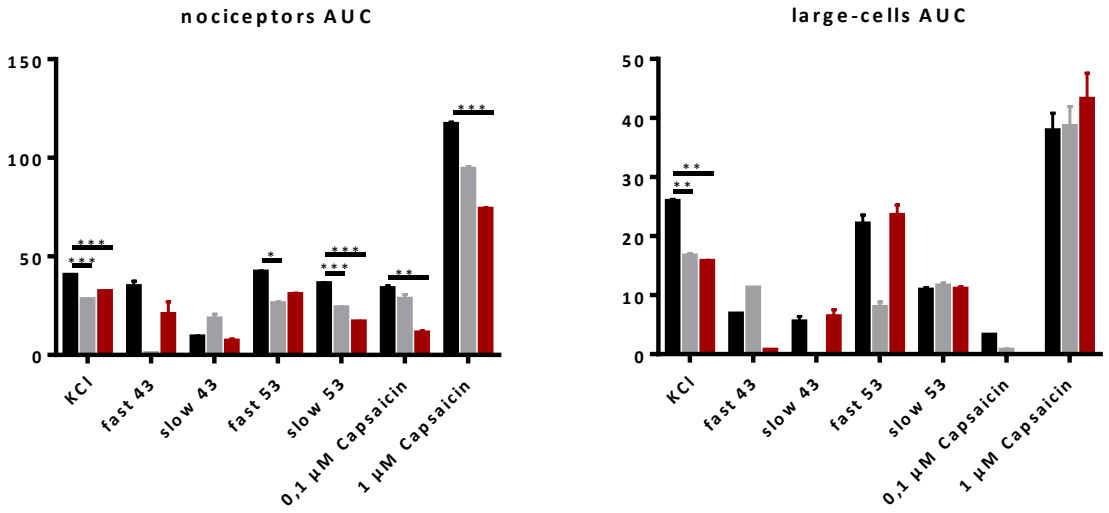

Figure 35: Area under the curve (AUC). The KCl stimulus served as the control stimulus. KCl positive cells were used for analysis. The cell-numbers are indicated in Table 4 and Table 5. WT in black, HET in grey, KO in red. Error-bars indicate standard error (SEM). Asterisks are indicating significances. Statistics was done using t-test (* = $p < 0.05$; ** = $p < 0.01$; *** = $p < 0.001$). Animal numbers: WT = 13; KO = 11; HET = 6. For each animal, up to 4 cover slips have been measured.

The AUC shows again a similar tendency. The value for the knockout is always lower in nociceptors (Figure 35, left). For the KCl, the slow 53°C and the both capsaicin stimuli the differences are significant. In large cells (Figure 35, right) the KCl stimulus shows a significant decrease in the knockout.
Overall these calcium imaging data show an overall tendency of decrease for the different stimuli in the α2δ-3 deficient mice. For the large-cell data it should be mentioned that the total cell numbers are not that high (Table 5) so that the interpretation of these data has to be done carefully.

Table 4: Cell-numbers of nociceptors, KCL positive. Animal numbers: WT = 13; KO = 11; HET = 6. For each animal up to 4 cover slips have been measured

Stimulus	Wiltype (+/+)	Heterozygous (+/-)	Knockout (-/-)
KCl	285	146	314
fast 43	11	1	5
slow 43	65	7	16
fast 53	128	35	77
slow 53	218	94	238
Capsaicin 0,1 µM	25	12	15
Capsaicin 1,0 µM	85	59	122

Table 5: Cell-numbers of large-cells, KCL positive. Animal numbers: WT = 13; KO = 11; HET = 6. For each animal up to 4 cover slips have been measured

Stimulus	Wiltype (+/+)	Heterozygous (+/-)	Knockout (-/-)
KCl	76	38	92
fast 43	1	1	1
slow 43	12	0	3
fast 53	25	8	18
slow 53	59	31	73
Capsaicin 0,1 µM	1	2	0
Capsaicin 1,0 µM	16	8	12

Another way to interpret the same data is to filter the cells not only according to the KCl response but further to the capsaicin (1 µM) response. In this case effects of the KO regarded to TRPV1 should become more evident. TRPV1 is a marker for a subgroup of nociceptive neurons. The analyzing steps are the same as before.

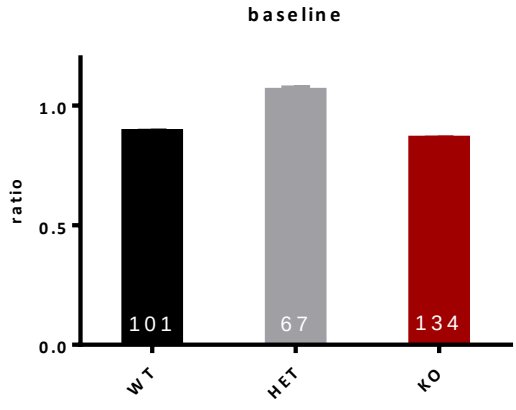

Figure 36: Baseline of the capsaicin positive cells. The baseline intensity was recorded for 10s before the first stimulus (KCl). The cell-numbers are indicated in the bars. WT in black, HET in grey and KO in red. Error-bars indicate standard error (SEM). Statistics was done using t-test (n.s.).

The baseline values of the different phenotypes (Figure 36) do not differ significantly if we look only at the capsaicin positive cells (WT vs. KO). But the tendencies are the same like in the analysis done before (Figure 30).

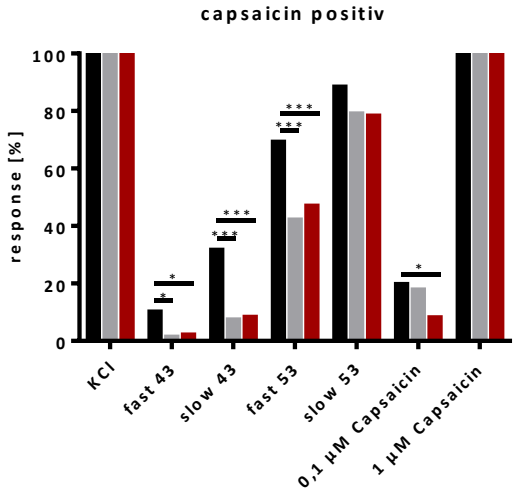

Figure 37: Responding, capsaicin positive cells. Only KCl positive and capsaicin positive (1 µM) cells were used for analysis. The cell-numbers are indicated in Table 6. WT in black, HET in grey, KO in red. Statistics was done using Fisher's exact test (* = $p < 0.05$; *** = $p < 0.001$).

Analyzing the responding cells (Figure 37) there is a significant decrease for all the stimuli except the slow 53°C. That fits very well to the data analyzed before, showing that the TRPV1 positive nociceptors are affected in the α2δ-3 deficient mice.

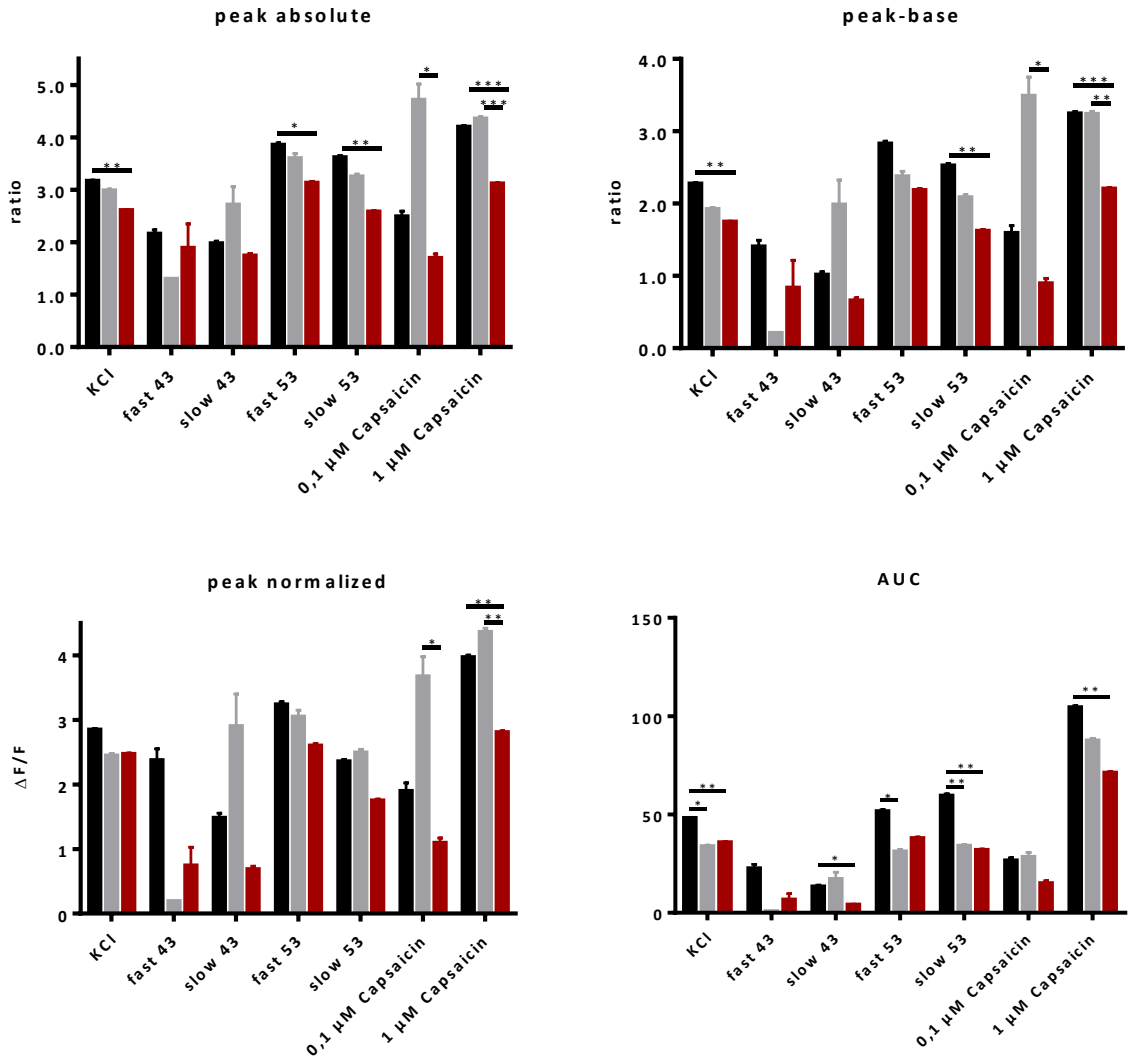

Figure 38: Peak analysis and AUC of capsaicin positive cells. The KCl stimulus served as the control stimulus. Only KCl positive cells were used for analysis. The cell-numbers are indicated in Table 6. WT in black, HET in grey, KO in red. Statistics was done using t-test (* = $p < 0.05$; *** = $p < 0.001$).

All this graphs (Figure 38) show more or less the same tendencies than the analysis before. In case of the normalized peak, there is only significance between WT and KO for the high concentration capsaicin stimulus, were the KO shows a decrease. The AUC shows more significance. Again for the KCl stimulus supporting the idea that the DRG-cells from KO are less excitable. For 3 out of 5 heat-stimuli there is a reduction as well, meaning less calcium is entering the KO cells after stimulation.

Table 6: Cell-numbers of **Capsaicin positive** cells.

Stimulus	Wiltype (+/+)	Heterozygous (+/-)	Knockout (-/-)
KCl	101	67	134
fast 43	10	1	3
slow 43	32	5	11
fast 53	70	27	63
slow 53	84	53	105
Capsaicin 0,1 µM	20	12	11
Capsaicin 1,0 µM	101	67	134

To sum the calcium imaging data up: there seem to be a deficiency in calcium influx upon stimuli like heat and capsaicin, acting on TRPV1. Furthermore there seems to be a reduced excitability in the neurons of the α2δ-3 deficient mice, shown by the reduced responses to KCl-stimuli.

3.2.3. Basic electrophysiological properties are altered. (Experiments done by Dr. Jing Hu)

To investigate the calcium channel function and the basic electrophysiological properties we used whole cell patch clamp recording. This is a standard method to investigate the electrical properties of cells. Therefore we used primary cell-culture of DRG neurons. The cells were challenged with the same kind of stimuli as used in calcium imaging and in ex-vivo-skin-nerve recording. Because the α2δ-3 subunit is regarded as a calcium channel subunit we first investigated the calcium currents (Figure 39).

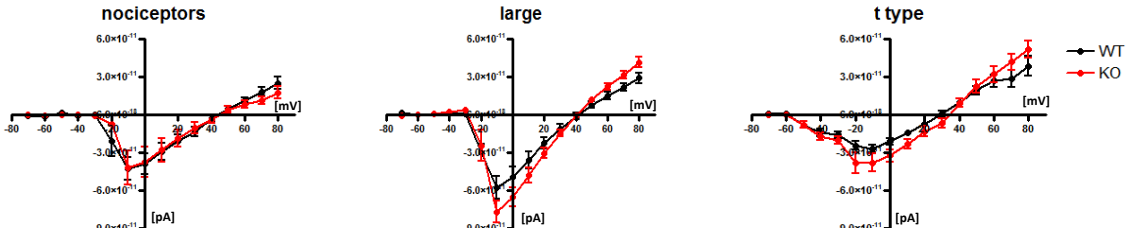

Figure 39: Calcium channel recording. Sodium and potassium channels have been blocked. There was no significant difference neither in nociceptors (cells < 25 µm) nor in large cells (> 25 µm). The I-V curve was acquired using voltage steps of 10 mV from -70 to 80 mV. For statistical analysis two-way-ANOVA was performed (n.s.). The graphs were kindly provided by Dr. Jing Hu. (Cell numbers: nociceptors: WT = 11, KO = 12; large: WT = 33, KO = 28; t-type: WT = 11, KO = 7)

There was no significant difference found in the calcium currents recorded. Also a look on T-Type calcium channels did not reveal any significant difference. Therefore we went

on to investigate the general electrical properties of the currents by giving increasing voltage steps (from -70 to 60 mV in 5 mV steps). that are mainly consist of sodium- (inward) and potassium-currents (outward).

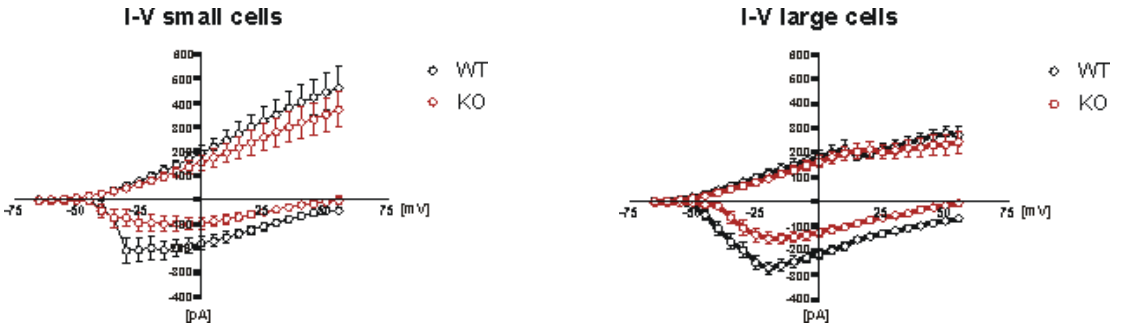

Figure 40: I-V curves of small (nociceptors) and large cells. The outward current (upper curves) doesn't differ in the different genotypes. But the inward current (lower curves) shows a reduction in the α2δ-3 deficient mice. The I-V curve was acquired using voltage steps of 5 mV from -65 to 55 mV. The graphs were kindly provided by Dr. Jing Hu. Statistics was done using two-way-ANOVA (small cells: p = 0.0522; large cells: *** = p < 0.001). (Cell numbers: KO, small = 21, large = 35; WT, small = 25, large = 39)

Interestingly the inward current seems to be reduced in the α2δ-3 deficient mice (Figure 40). This inward current is mostly sodium current, raising the question about the influence of α2δ-3 subunit on sodium channels. As α2δ-3 was first described as an auxiliary subunit of voltage gated calcium channels, this result was quite unexpected.

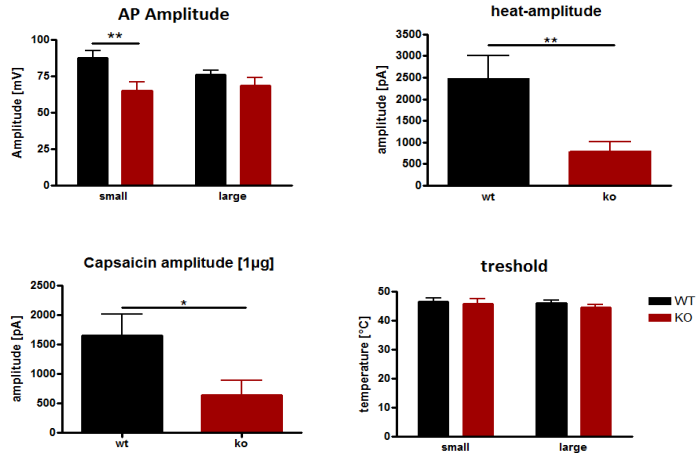

Figure 41: Properties of DRG after heat or capsaicin (1µM) stimulation. AP amplitude is significantly reduced in the deficient mouse (upper left). Also the amplitude for the heat induced response (upper right). The capsaicin induced response is significantly reduced in deficient mice (lower left). The heat-threshold for AP generation is not changed (lower right). For statistics t-test was used. Asterisks indicating significant difference (* = p < 0.05 ** = p < 0.01). The graph was kindly provided by Dr. Jing Hu. Cell numbers are indicated in Figure 40.

The AP amplitude is decreased in the small cells (nociceptors) of DRG neurons. This is in line with the observation of the reduced inward current. The reduced heat induced amplitude in the α2δ-3 deficient mice fits very well with the results from the skin-nerve

experiments and calcium imaging data. The capsaicin induced amplitudes are significantly reduced too and the threshold for AP generation didn't seem to be changed (Figure 41).

To sum the electrophysiological data up, there is a reduced input from the periphery to the spinal cord which can be a reason for the observed behavioral deficits in the hot-plate-test. But calcium channels don't seem to be involved; therefore sodium channels might be affected.

3.2.4. Innervation patterns in KO mice are not altered

Because of lack of a functioning α2δ-3 antibody we looked for differences in the organization of structures that are known to be involved in pain perception in the skin and the SC.

The first antibody we used was PGP9.5 (protein gene product 9.5), a common marker for all neurons [62]. With this marker we stained skin sections of WT and KO animals to look for alterations in the free nerve endings.

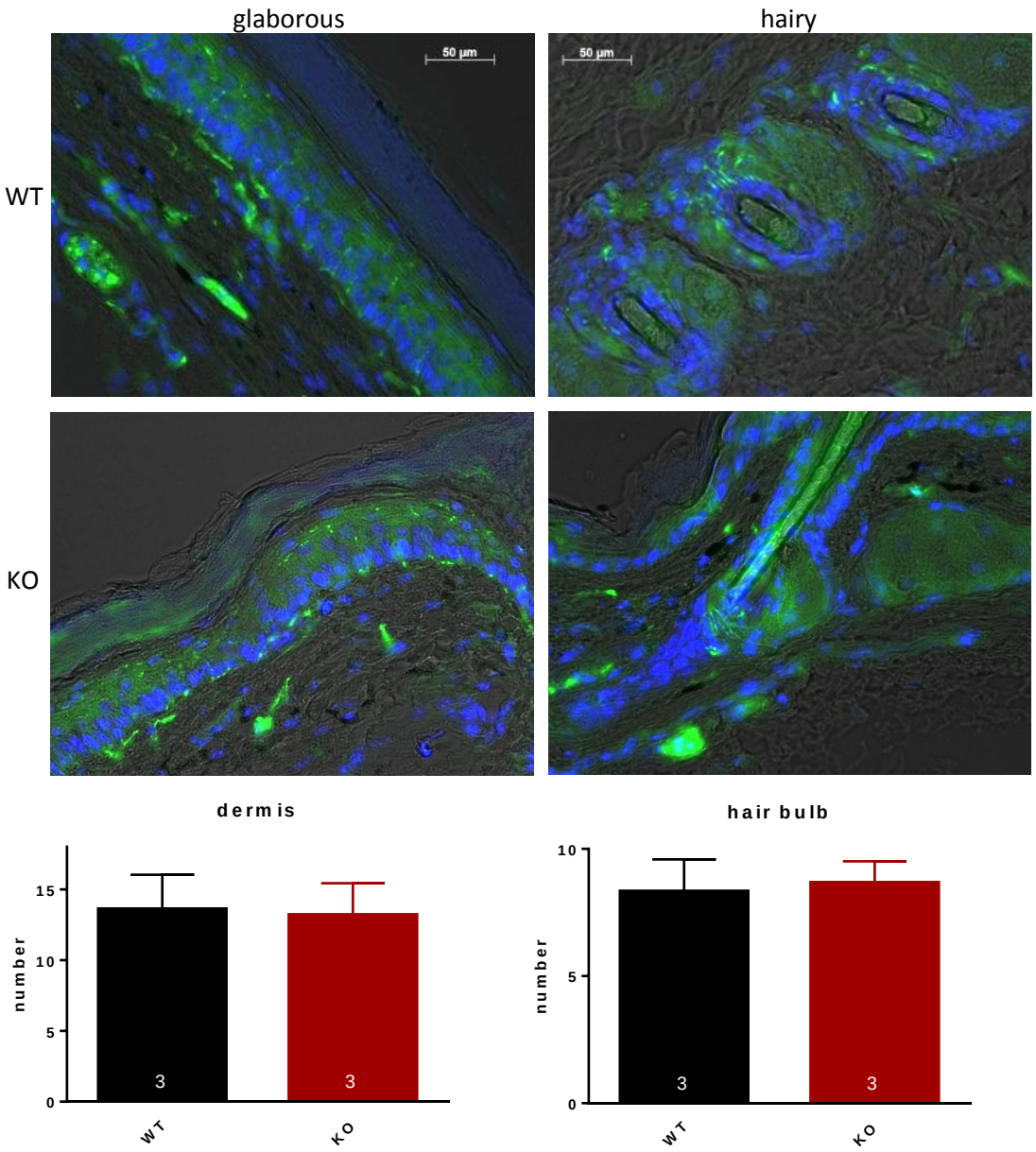

Figure 42: PGP 9.5 staining of skin sections. PGP 9.5 (green) is a pan-neuronal marker, staining the free nerve endings in the skin. Hoechst (blue) was used for nuclear staining. The tissue was fixed as described (2.3.1). The innervation pattern in the glabrous skin (left) doesn't differ between WT and KO. The innervation of the hair bulbs (right) has a very special and prominent pattern but doesn't show a difference as well. Stained fibers were counted. Animal numbers are indicated in the bars. Error bars indicate standard error (SEM). For each animal 3-4 sections (6 cuttings) have been counted. For statistics, t-test was used (n.s.).

The pan-neuronal staining with PGP 9.5 didn't show a difference between WT and KO animals (Figure 42), suggesting that there is no obvious alteration in the innervation pattern or the structural organization of the free nerve endings in the dermis.

The next stainings were done in the SC. In the dorsal horn of the SC where the fibers of the primary afferents project to, a laminar organization is set (Figure 2). Nociceptors project more to the superficial layers I and II and the Aβ-fibers project to the deeper layers. Given the heat phenotype in the behavior we focused on the superficial layers. Within the laminas different types of neurons are located, like inhibitory/excitatory interneurons (lamina II) or projection neurons (lamina I). The pre-synapses formed by the primary afferents are mostly glutamatergic [63]. Therefore we checked the vesicular glutamate transporter 1 (VGlut1) in spinal cord sections. The vesicular glutamate receptors are common markers for excitatory synaptic terminals [64] and VGlut1 stains most of the primary afferent terminals in Lamina II [65]. Beside the excitatory synapses, the primary afferents form in the spinal cord, the inhibitory interneurons, were some of this glutamatergic synapses project to, are of our interest. The glutamate decarboxylase (GAD67 is one of two isoforms), an enzyme that produces GABA is an accepted marker for inhibitory interneurons [66]. So we tried to look for alterations doing a double staining with VGlut1 and GAD67. Alterations in the staining here could be an explanation for the behavioral phenotype, for example if in the KO the excitatory terminal project to areas where they do not in the WT.

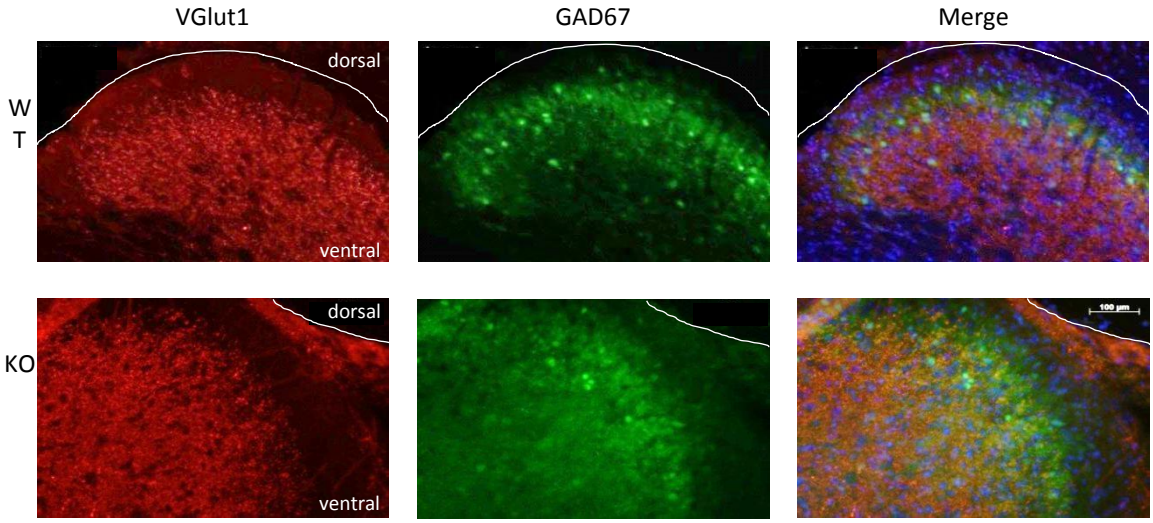

Figure 43: Co-staining of VGlut1 (red), GAD67 (green) and Hoechst (blue). The antibodies were used in dilution: VGlut1 (1:500), GAD67 (1:500). For nuclear staining Hoechst (blue; 1:1000) was used. The tissue was fixed as described (2.3.1). The tissue was cryo-sectioned at 12 µm. The white line shows the edge of the spinal cord tissue on the dorsal horn. The staining was repeated 3 times.

The co staining of the VGlut1 and GAD67 (Figure 43) didn't show any differences, suggesting the innervation pattern of the excitatory synaptic terminals (VGlut1, red) and the inhibitory interneurons (GAD67, green) is same in WT and KO. The stainings show very nicely the anatomy of the spinal cord, the non-stained area (neither green nor red)

is the lamina I and the layer were the green staining is most prominent is the lamina II spreading to some extend into lamina II. So in both, WT and KO the VGlut1 expressing terminals reach the lamina III and II.

Immuno-stainings are often problematic. Therefore we crossed our α2δ-3 deficient mice with an EGFP (enhanced green fluorescent protein) expressing reporter mouse. This EGFP is under control of the promoter from the GAD67 gene (*Gad1*). In this case no additional staining has to be done to look for the pattern of GAD67 expression.

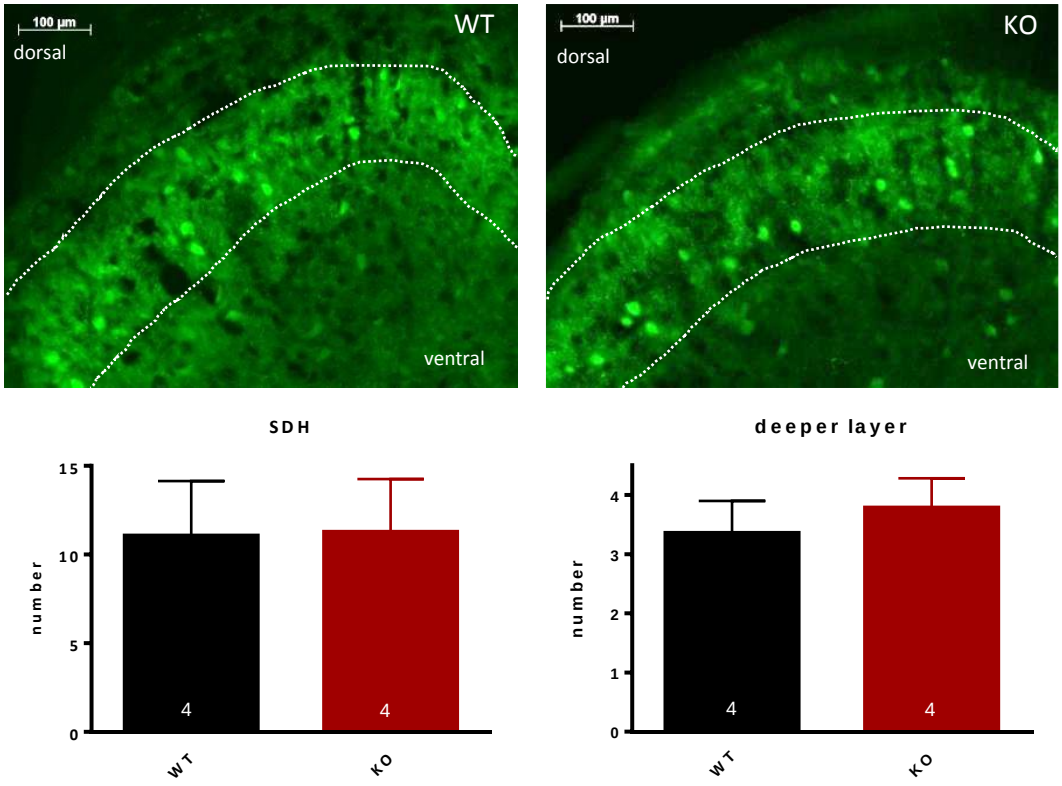

Figure 44: EGFP expression in GAD67 positive cells. The tissue was fixed as described (2.3.1). No obvious differences could be recognized. Dashed lines show approximately the borders of laminae. The tissue was cryo-sectioned at 12 µm. Animal numbers are indicated in the bars. Error bars indicate standard error (SEM). For each animal 3-4 sections (6 cuttings) have been counted. For statistics, t-test was used (n.s.).

The expression pattern of the EGFP (Figure 44) didn't show any difference, same as for the antibody staining (Figure 43). The expression pattern looks quite similar to the antibody staining, although in case of expression, the green fluorescence is much stronger, what the pictures shown here might not capture totally.

3.2.5. The activation pattern of neurons in the spinal cord does not differ

With the previous immuno stainings we weren't able to see any difference. Therefore we wanted to investigate whether the activation of SC neurons is altered in WT and KO mice. C-fos is a transcription factor that is commonly used to stain for activity in neurons after noxious stimulation [67]. So we are able to look for differences in the number or location of activated neurons. The hind paw of wild-type and deficient mice was immersed into 50°C hot water 3 times for 10 seconds with 30 seconds delay in-between. 2h later the animal was sacrificed and spinal cord tissue was fixed. The c-fos (1:200) staining was quantified via counting of positive cells in the spinal cord at levels L3, were a big portion of the sciatic nerve, the one activated by the heat stimulation, invades the SC.

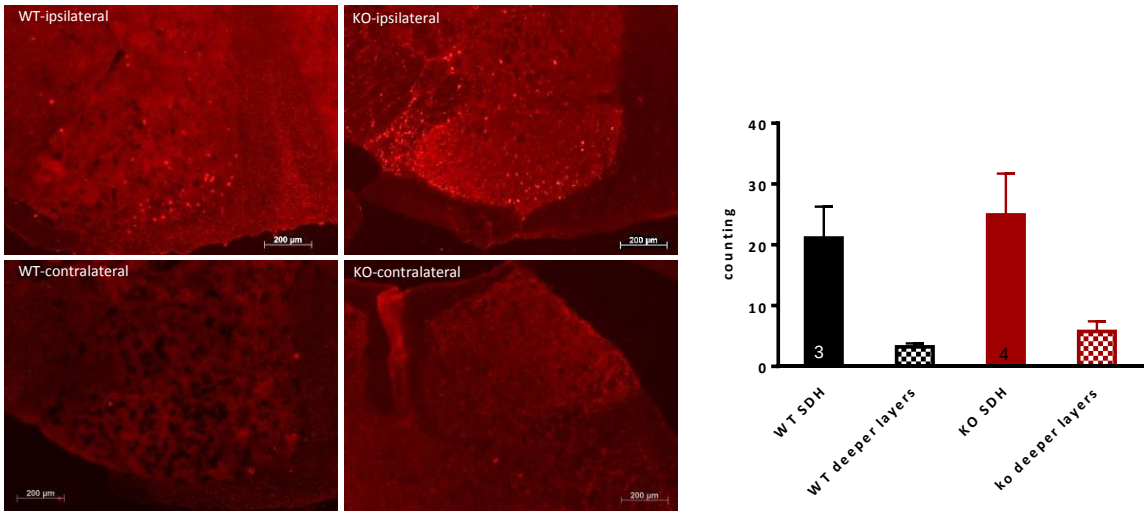

Figure 45: C-fos positive cells after thermal stimulation. Pictures show c-fos staining (red) in spinal cord. The animals were stimulated at one hind paw 3 times for 10s in 50°C hot water with 30s delay in-between. Slices from lumbar level 3 were analyzed. Superficial (SDH) and deeper dorsal horn were separately analyzed. Contralateral images served as control (lower images). Animal numbers are indicated in the bars. Error-bars indicate standard error (SEM). For statistics t-test was used (n.s.).

We were not able to observe any difference in the staining on the lumbar level 3 (Figure 45), neither in the superficial layers nor in deeper layers. These data suggests that the already mentioned difference in behavior and electrophysiological properties are not due to different activation patterns in the SC.

3.2.6. TRPV1 as potential interaction partner

Because the mutant mice show a heat phenotype and we saw some alterations in the capsaicin induced calcium influx we wanted to investigate if there is a connection between α2δ-3 and TRPV1. At first we tried to co-localize the two proteins. In lack of an α2δ-3 antibody we used a β-gal antibody and primary cell-culture of DRG-neurons from heterozygous mice.

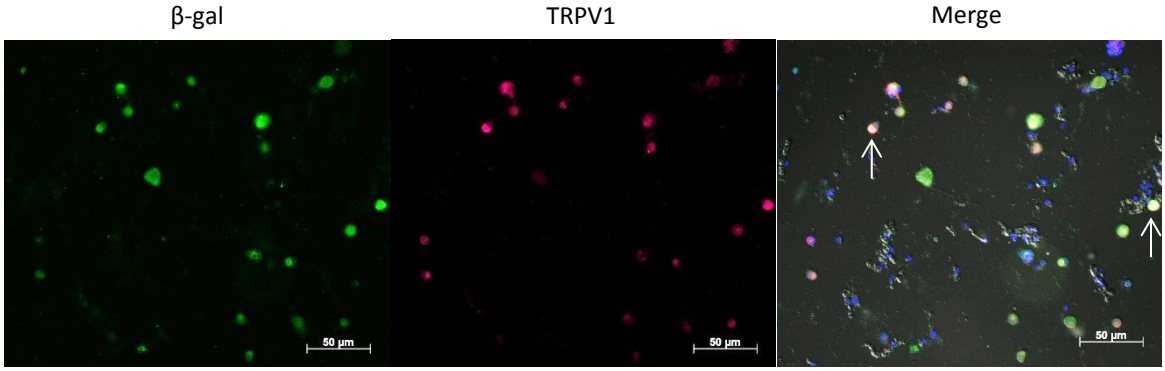

$$\frac{TRPV1}{\beta - gal} = 46.2\,\%$$

$$\frac{\beta - gal}{TRPV1} = 39.3\%$$

Figure 46: Immuno staining of DRG primary culture. TRPV1 (red) and β-gal (green) are co-expressed in some cells (white arrows). Dilution of antibodies: TRPV1, 1:1000; β-gal, 1:500. Hoechst was used for nuclear staining. 46.2% of β-gal positive neurons are TRPV1 positive and 39.3% of TRPV1 positive cells are β-gal positive. 186 cells from two animals have been counted (10 Experiments). TRPV1 positive = 57.5% (107/186); β-gal positive = 48.9% (91/186).

The Immuno-staining (Figure 46) shows that there are cells that show staining for TRPV1 and the β-galactosidase that indicates the expression of α2δ-3 subunit. 46.2% of the β-galactosidase positive cells are positive for TRPV1 and 39.3% of TRPV1 positive cells are positive for β-galactosidase. This supports a possible interaction between α2δ-3 and TRPV1.

A standard method for checking direct protein-protein interactions is the co-immuno-precipitation (CoIP). Because the lack of good antibodies we used the expression of tagged-constructs in HEK-cells. The α2δ-3 construct was tagged with an HA-Tag and the TRPV1 construct was tagged with YFP. As a first experiment we had to proof that the HA-Tag antibody and the one for YFP, which is against GFP and can also detect YFP, work properly.

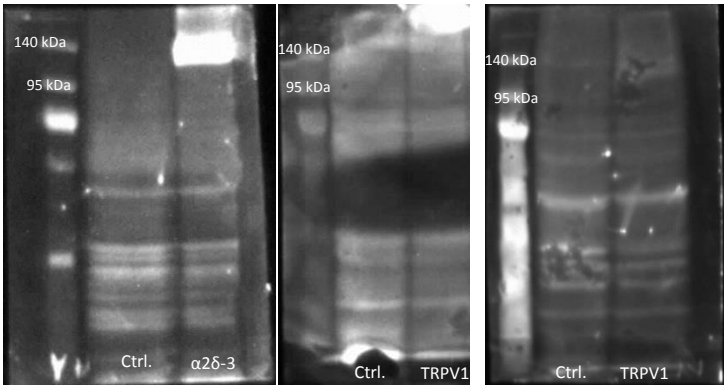

Figure 47: Western blot of transfected HEK cells. Left: α2δ-3-HA Tag (131 kDa) was transfected in HEK cells. Middle: TRPV1-YFP construct (122 kDa), detected with a GFP antibody. Right: TRPV1-YFP construct detected with a TRPV1 antibody. For α2δ-3-HA construct (left) there is a band, showing HA antibody is working. For TRPV1-YFP construct (mid) there is no difference between ctrl. and transf. cells, so the antibody didn't work. For the detection with TRPV1 antibody (right) there is a light band below 140 kDa that could be the expected one.

The Antibody against the HA-Tag shows a clear Band (Figure 47 left) a bit below the 140 kDa marker, which actually fits well with the expected size of 131 kDa. Further, the band only apperas in the transfected cells, not in the non transfected control cells. For the TRPV1-YFP construct (Figure 47 middle) there was no difference between control and transfected cells showing that the antibody doesn't work properly. Therefore we tried a TRPV1 antibody and we saw a very weak band at the expexted size.

For the Co-IP we co transfected the two proteins and did the extraction. Than we immobilized first the TRPV1 antibody as well as the EGFP one, to compare these two. After the Co-IP and the westernblott the protein was detected with the HA antibody.

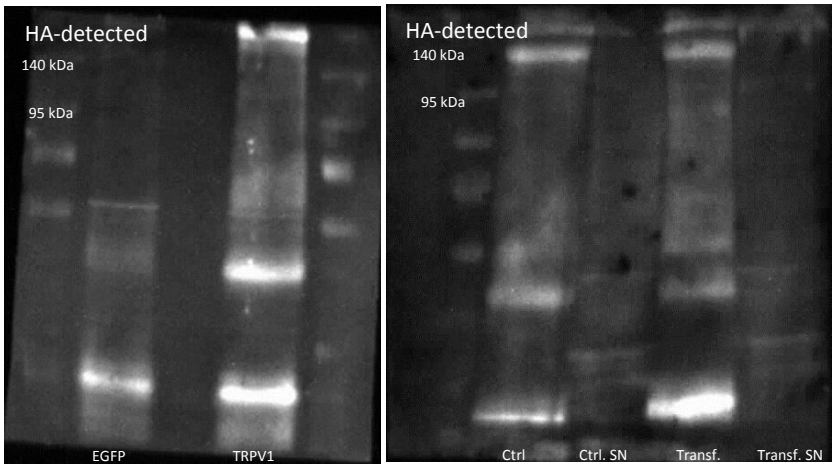

Figure 48: CoIP of co-transfected HEK cells. Left: comparison of immobilization of GFP and TRPV1 antibody. Right: comparison of the un-transfected control and its supernatant with the TRPV1 antibody captured fraction and its supernatant.

The comparison of the GFP and TRPV1 antibody for capturing the protein leads to a quite similar picture (Figure 48 left). It seems like the TRPV1 antibody is a bit better in detection, shown by stronger bands, although the band sizes are all not expected. We repeated the experiment with the TRPV1 antibody and the proper controls (Figure 48

right). The supernatant of both, control and TRPV1 transfected cells show almost no staining, showing the Co-IP itself worked. If the α2δ-3-HA construct and the TRPV1-YFP have a direct protein-protein interaction we would expect to see a band in the TRPV1 fraction with a size of 131 kDa which we actually not see. Therefore at this point we cannot really tell if there is a direct interaction between α2δ-3 and TRPV1.

One of our hypothesis is that α2δ-3 might interact with TRPV1 in a way, serving as a transport or sorting protein that can bring TRPV1 into lipid rafts or out of them. Lipid rafts are micro-domains in membranes with higher amounts of cholesterol. It was already shown, that TRPV1 locates in lipid rafts and shows higher activity in there [68]. Treatment of cells with mβCD (methyl-β-cyclo-dextrine) depletes the cholesterol in lipid rafts, so that these lipid micro domains are disappearing [69].

As a further experiment we again performed calcium imaging. But now with HEK 293 cells that have been transfected with a TRPV1-YFP construct and a α2δ-3 construct with a T7 tag. We tested three different transfection conditions: vehicle transfected, TRPV1 transfected and TRPV1 + α2δ-3 co-transfected (ratio 1:8). Because the TRPV1 construct contains YFP we only measured cells that showed an YFP signal. Because of the transfection ratio of 1:8 it is very likely that in these cells α2δ-3 was transfected as well. HEK 239 cells do intrinsically express α2δ-3 to lower amounts [58]. With the co-transfection we created a system that over-expresses TRPV1 and α2δ-3 to look for possible interactions. In fact those HEK-293 cells are not neurons they do not respond to the KCl stimulus. So we used only cells for analysis that respond to the 1 µM capsaicin stimulus to make sure that TRPV1 was transfected (Figure 49). Data was acquired with the help of Susanne Tulke, who did an internship in our lab.

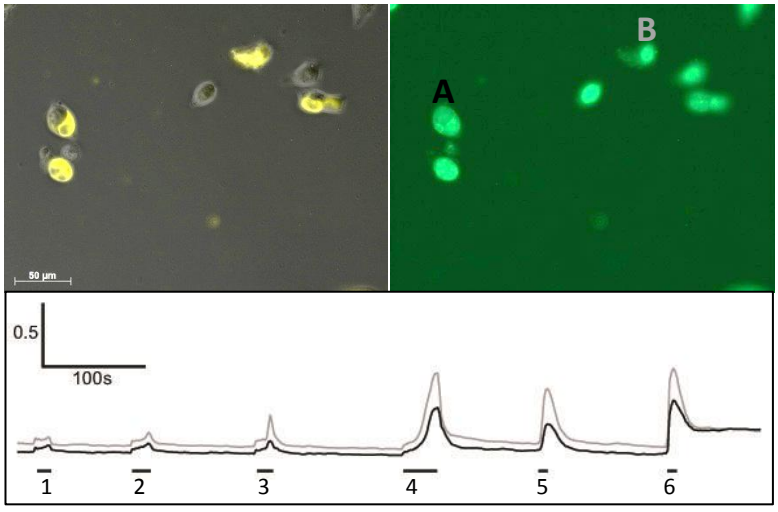

Figure 49 Example traces of calcium imaging in HEK 293 cells. Calcium imaging was performed 20h after transfection. TRPV1-YFP and α2δ-3-T7 (1:8). Pictures show the cells immediately before measuring (left: bright-field with YFP; right: fluorescent picture after Fura-2 loading). Colored letters indicate the corresponding trace. Stimuli: 1. fast 43°C; 2: slow 43°C; 3: fast 53°C; 4: slow 53°C; 5: capsaicin (100nM); 6: capsaicin (1µM).

For this experiments the same stimuli and settings as for the previous calcium imaging with DRG neurons was used. Except the KCl was not used, because they are not neuronal cells.

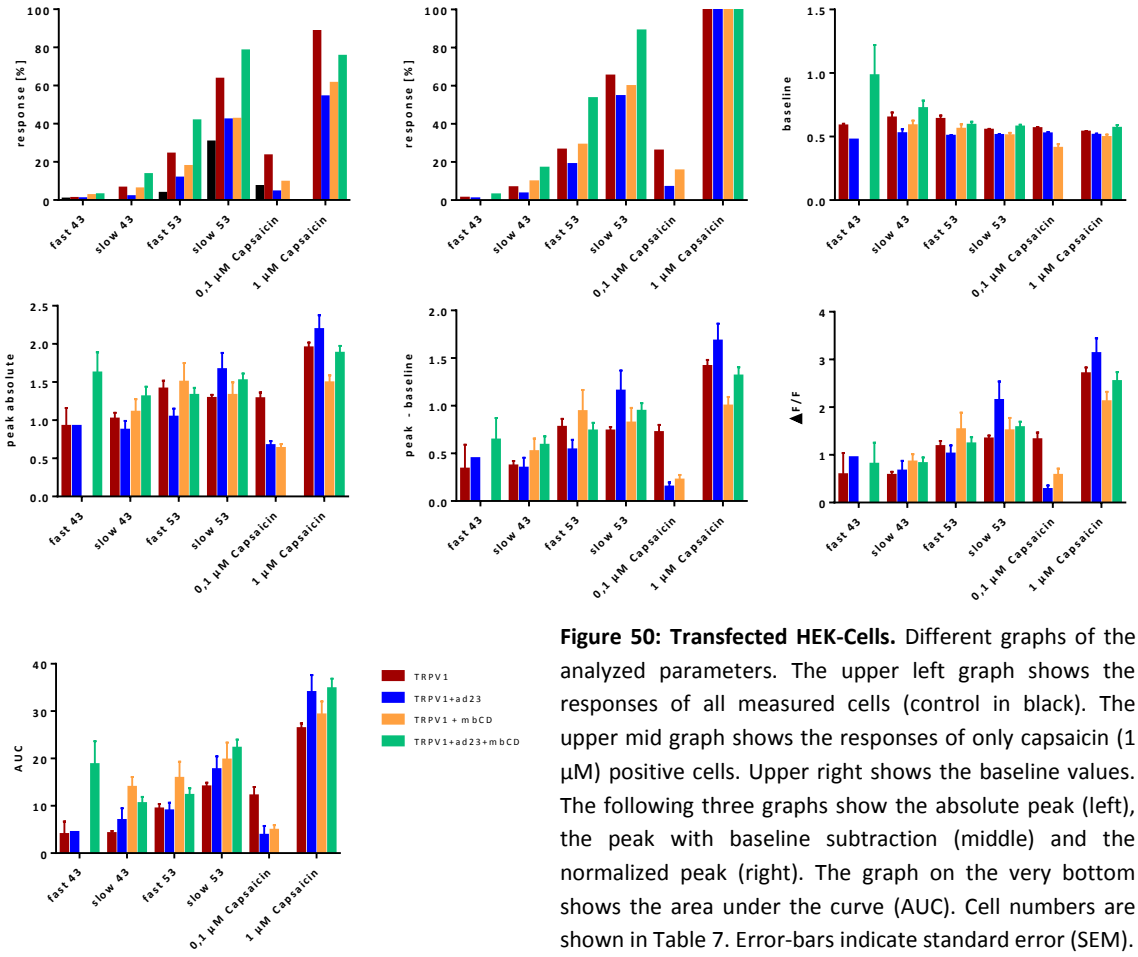

Figure 50: Transfected HEK-Cells. Different graphs of the analyzed parameters. The upper left graph shows the responses of all measured cells (control in black). The upper mid graph shows the responses of only capsaicin (1 µM) positive cells. Upper right shows the baseline values. The following three graphs show the absolute peak (left), the peak with baseline subtraction (middle) and the normalized peak (right). The graph on the very bottom shows the area under the curve (AUC). Cell numbers are shown in Table 7. Error-bars indicate standard error (SEM).

The different graphs in Figure 50 show the different parameters that have been analyzed. For better understanding the significances are shown in additional graphs, were further separation of the different experimental groups allows to show the significances. Because of the fact that there are already changes in the baseline of the separate groups we used the normalized peak and the area under the curve for interpretation. The tendencies are in all peak related graphs the same. Co-expression of α2δ-3 leads to a reduction in response and peak amplitude to the 100nM capsaicin stimulus.

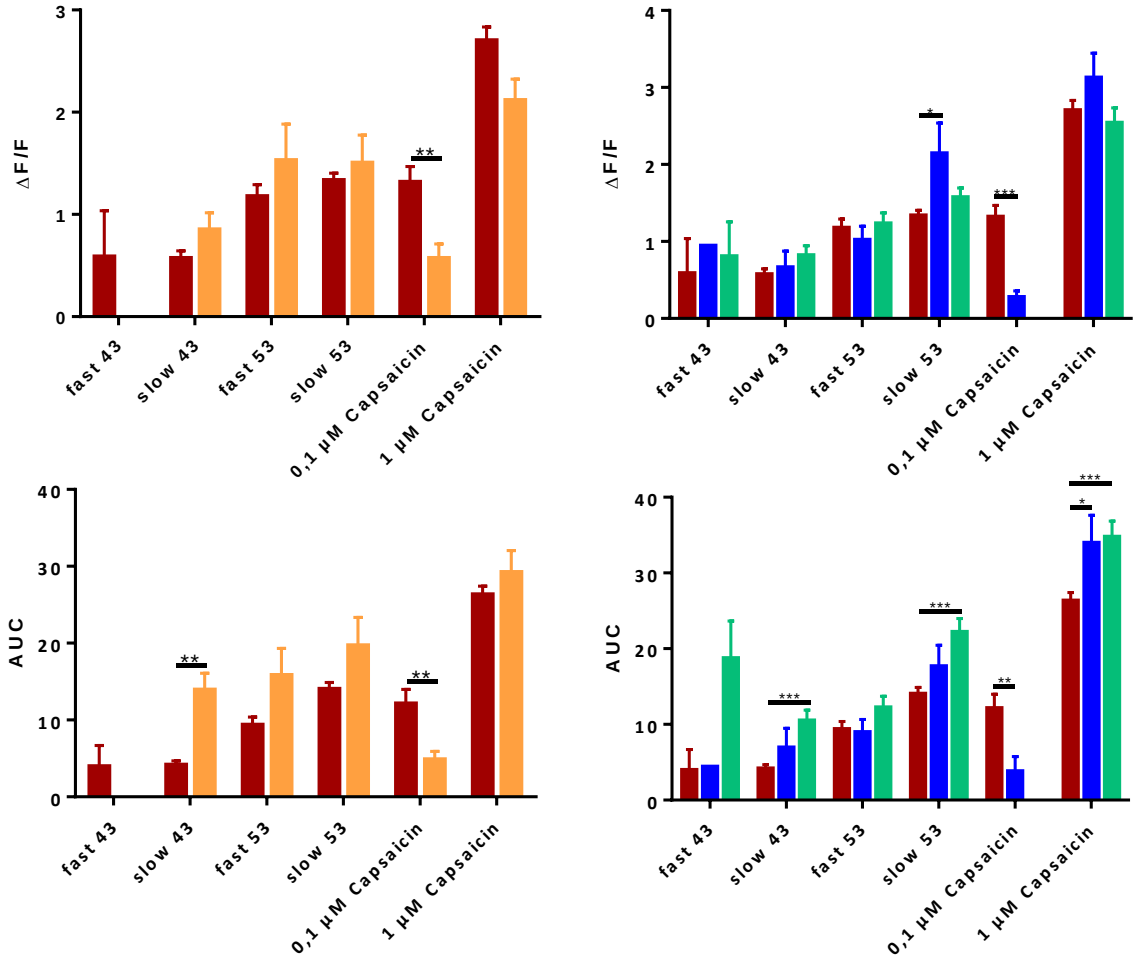

Figure 51: Transfected HEK-cells additional graphs. Here the same graphs as in Figure 48 are shown in a different way for better understanding. The color code is same too. There are significant differences in the normalized peak amplitudes (upper graphs). The same accounts for the area under the curve (AUC). There are significant differences in all 4 graphs for the 100 nM capsaicin response that is reduced after mβCD treatment and after co-transfection of TRPV1 and α2δ-3. Cell numbers are shown in Table 7. Error-bars indicate standard error (SEM). Asterisks are indicating significances Statistics was done using t-test (* = $p < 0.05$; ** = $p < 0.01$; *** = $p < 0.001$).

The graphs in Figure 51 show significant differences after mβCD treatment and co-transfection with α2δ-3. The peak amplitude and the AUC show a significant decrease for the lower capsaicin concentration. Surprisingly for the AUC in case of the higher capsaicin concentration there is a significant increase after α2δ-3 co-transfection. The fact that on one hand there is a reduction in responses and on the other hand an increase depending of capsaicin concentration could be a hint to a concentration dependent mechanism.

Table 7: Cell numbers of capsaicin (1µM) positive cells

Stimulus	TRPV1	TRPV1 + α2δ-3	TRPV1 + mβCD	TRPV1 + α2δ-3 + mβCD
fast 43	2	1	0	3
slow 43	13	5	5	18
fast 53	52	28	15	57
slow 53	129	81	31	95
Capsaicin 0.1 µM	51	10	8	0
Capsaicin 1.0 µM	198	150	52	107

To further investigate the interaction of α2δ-3 and TRPV1 we performed the capsaicin-test on WT and KO animals. In this test the agonist of TRPV1, capsaicin (3 µg) is injected into one hind paw of the animal. Immediately after injection the time spent for licking and the number of shaking is counted for 10 min.

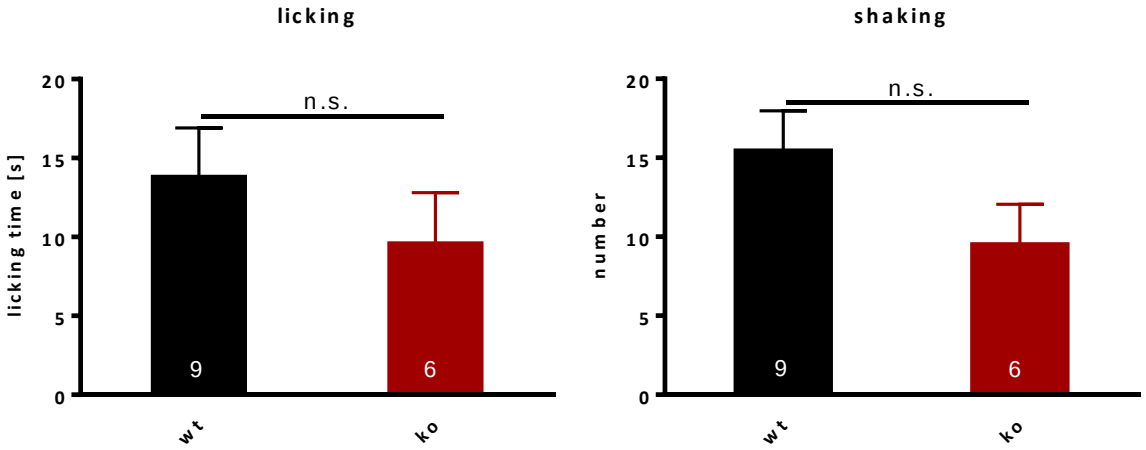

Figure 52: Capsaicin test. Animals were observed for 10 min. Time spent for licking was summed up and the shaking was counted. The WT is shown in black and the KO in red. The Error bars indicate the standard error (SEM). Statistics was done using t-test.

As Figure 52 shows, there is no significant difference in the capsaicin test between WT and KO animals. Although there is a tendency showing the KO might be a bit less sensitive to capsaicin, but not significantly.

3.2.7. The deficient mice show increased sensitivity in spinal reflexes.

Another way to look for mechanical induced pain in a more detailed way is the manual von Frey test. The already described automatic von Frey test gives just a threshold and therefore only poor information. In the manual von Frey test single filaments with different strength (in g) are pushed against the hind paw of the animals. After 5 times repetition a 3 times pain response would be regarded as positive. We used in total 10 different filaments (in g: 0.008; 0.02; 0.04; 0.07; 0.16; 0.4; 0.6; 1.0; 1.4; 2.0).

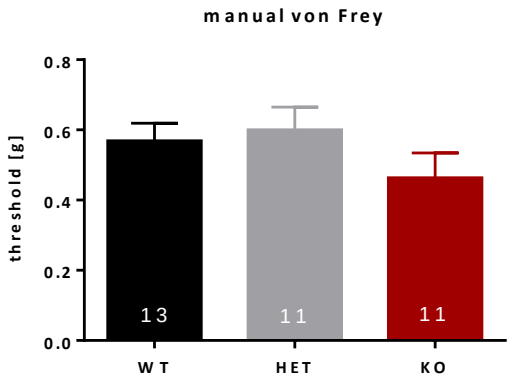

Figure 53: **Mechanical threshold of different Genotypes.** 10 different filaments have been used. If the animal responded three times out of five stimulations with a pain behavior, the stimulus was regarded as positive. Black for WT (0.57), grey for HET (0.6) and red for KO (0.46). Animal numbers are indicated within the bars. Error-bars indicate standard error (SEM). Statistics was done using one way ANOVA with Dunn's multiple comparison test (WT vs. KO,n.s.).

We didn't find a significant difference between the different genotypes in the manual von Frey (Figure 53), although there is a tendency for the KO to be more sensitive according to the stimuli. This tendency was not so obvious in the previous von Frey test.

To further look more detailed at this tendency we plotted the data in another way. The responses were plotted over the different filament strengths.

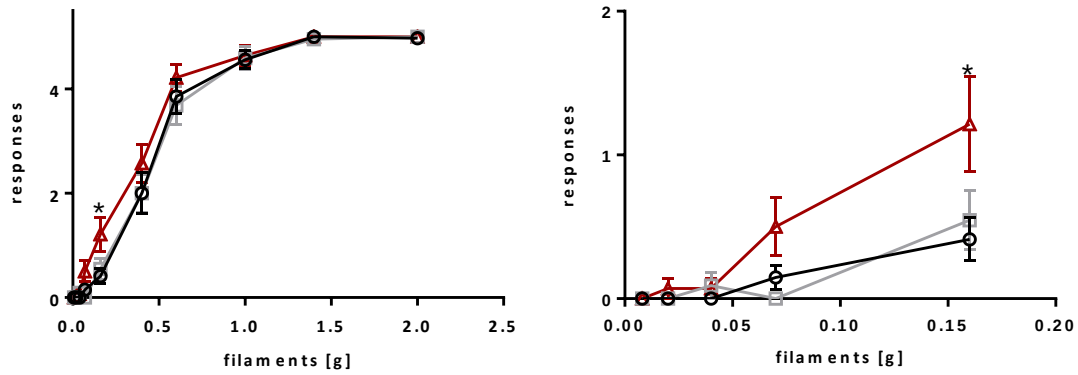

Figure 54: Mechanical threshold of single filaments. The responses are plotted over the different filament strength. Animal numbers are same as in Figure 53. On the right is an enlargement of the lower filaments of the left graph. Error bars indicate standard error. Statistics was done using two way ANOVA (WT vs. KO n.s.) with post hoc Bonferroni test (WT vs. KO; * = $p < 0.05$).

In this additional presentation of data we were able to detect a significant difference for one filament, 0.16 g (Figure 54). This significance appears below the threshold of 3 responses which would be regarded as positive. But it supports the tendency in the automatic von Frey test, because here the KO animals are as well more sensitive to this particular filament. This result is opposite of what we found for the hot-plate test in which the animals are less sensitive. But this result is in line with the increased tactile startle response, reported by Pirone et al. [52] because the deficient animals are more sensitive.

The Hargreaves- or Plantar-test is another acute thermal pain test. Different from the Hot-Plate test, it is supposed to be a spinal reflex, same as the von Frey test for mechanical pain [59]. Animals are put on a glass plate and an infrared device is put underneath the hind-paw. The device heats up the skin of the paw with different intensities (here 80 and 20). As soon as the animal feels pain it removes the paw from the heating spot and the latency-time is measured. The different intensities are chosen, because it was already shown that different heating rates activate different fiber types of nociceptors [60, 61].

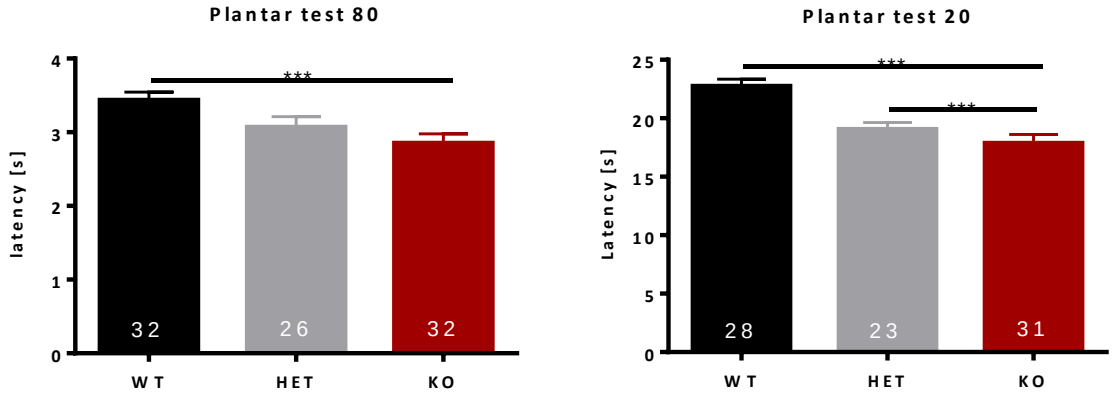

Figure 55: Plantar Test with different intensities. The intensity 80 (left) should activate C-fibers and the intensity 20 (right) is supposed to activate more Aδ-fibers. Animal numbers are indicated within the bars. Error-bars indicate standard error (SEM). Statistics was done using one way ANOVA with Dunn's multiple comparison test (*** = $p < 0.001$).

Surprisingly in the plantar test the KO animals are more sensitive than the WT animals (Figure 55). This observation is opposite to what we found for the hot plate test. Different from the "pure" spinal reflex as it's supposed to happen in the plantar test; in the hot plate test supra spinal areas (brain) are involved. On the other hand, this result is quite in line with the observed difference in the manual von Frey test were an increased sensitivity was observed too. Therefore this results supports even the tactile startle phenotype, which was increased in the mutants. Neely et al. did not do the Hargreaves test but a tail immersion and tail flick test, which are quite different according to the stimulation site.

3.3. Chronic pain

3.3.1. The KO mice show delayed recovery after induction of neuropathic pain

As a standard model for the induction of neuropathic pain we used the chronic constriction injury (CCI) [56]. This model is a reliable mouse model that results in robust and reproducible data. In this model the sciatic nerve is ligated with a surgical thread. 4 ligatures are made surrounding the nerve. The strength of the ligature influences the progress of the pain phenotype. We chose here a rather light ligature that responds in a pain phenotype, that shows a recovery like behavior after 7 days. Therefore we were able to discover not only the establishment and maintenance but also the recovery. In this model we would call the phase from baseline until day 2-3 establishment of neuropathic pain. From day 3-7 we would assume the maintenance processes and starting from 7 or 14 days after injury the recovery phase. The mice were habituated to the behavioral setups and a baseline was measured. Pain tests were done 1, 2, 3, 5, 7, 14, 21 and 28 days after CCI.

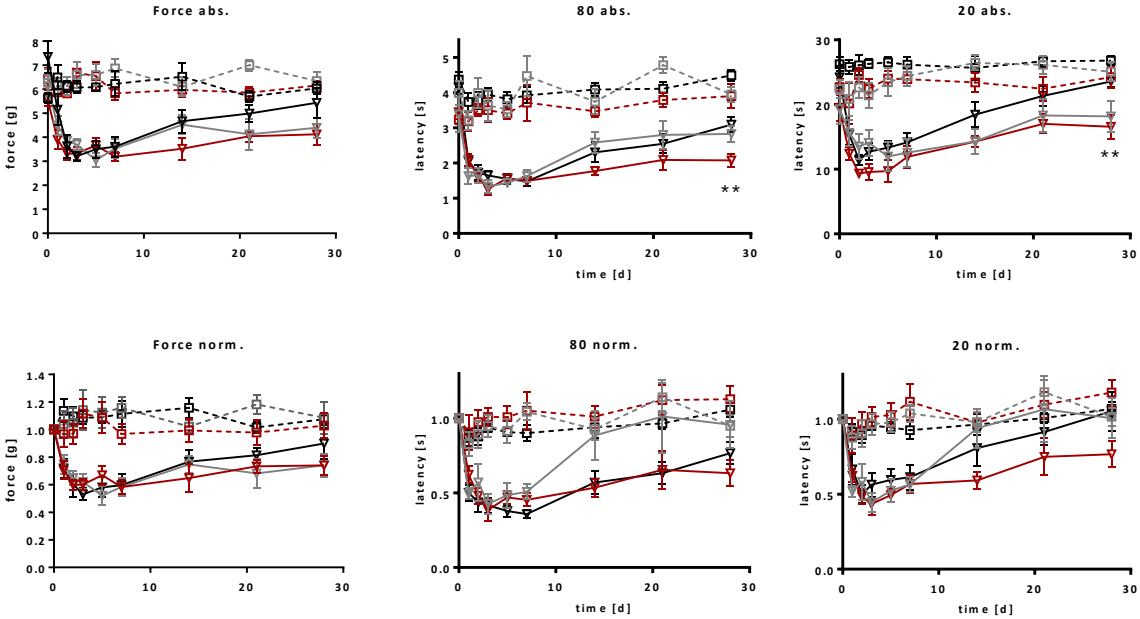

Figure 56: Behavior experiment for neuropathic pain, absolute and normalized values. WT in black, KO red and the HET in grey. The injured paws are shown with triangles and the sham paws with rectangles and dashed lines. Animal numbers: right: WT = 5 injury and 6 sham, HET = 6 injury and 5 sham, KO = 6 injury and 5 sham; mid and left: WT = 11 injury and 11 sham, HET = 7 injury and 6 sham, KO = 10 injury and 8 sham. Error bars indicate standard error (SEM). Statistics was done using two-way-ANOVA (injury vs. sham, Force abs. WT=**; KO=***; 80 and 20abs. WT and KO=***; WT injury vs. KO injury, force abs.=**; 80 and 20abs.=**; force, 80 and 20norm. n.s.) with post hoc Bonferroni test (WT injury vs. KO injury;** = p <0.01; *** = p <0.001).

We didn't detect any significant differences for the absolute values in the automatic von Frey test. 28 days after CCI treatment the high and low intensity Hargreaves-test shows a significant difference. For the normalized data we do not see any significant differences although the tendency is still there. The KO animals seem to be a bit more sensitive after CCI.

Additional to the automatic von Frey there is also a manual von Frey test available. In this test the experimenter uses von Frey filaments with different strength (in gram) to push it against the hind paw of the animals. Each filament is pushed 5 times against the hind paw. For a positive response the animal has to show at least in 3 of the 5 repetitions a pain behavior. With this method it is possible to have a closer look of the behavior with the different filaments and so we are able to detect allodynia if present.

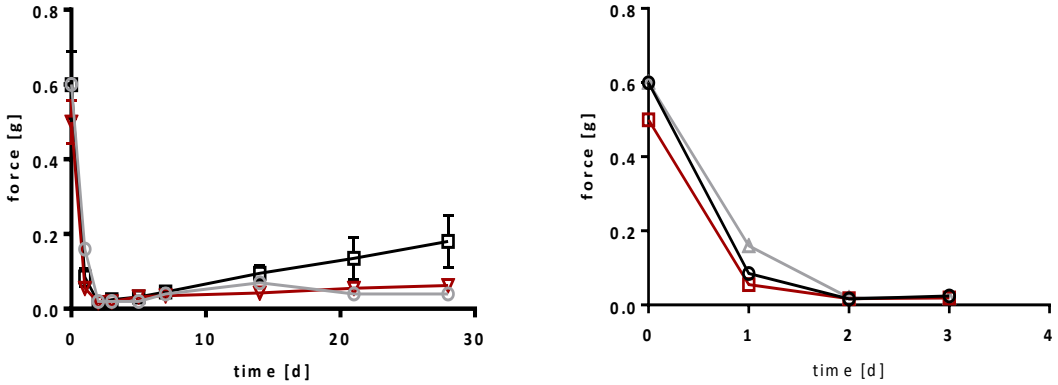

Figure 57: Mechanical thresholds after CCI. For a positive event, the animal had to respond at least 3 out of 5 stimulations with the individual filament. The lowest filament evoking 3 out of 5 responses was regarded as the threshold. WT in black, KO red and the HET in grey. Error bars indicate standard error (SEM). Animal numbers: WT = 6; HET = 1; KO = 4. Statistics was done using two-way-ANOVA (WT vs. KO n.s.) with post hoc Bonferroni test (WT vs. KO n.s.).

We didn't observe any significant difference in the mechanical threshold after CCI (Figure 57). Therefore it is unlikely that the mutated animals have any deficits in the mechanical sensation in this neuropathic pain model. But there is a tendency after 21 days of injury, showing that the WT animals show a faster recovery in this model, although it's not significant.

The data can also be analyzed by taking each filament and plot the responses over time. Here we preferentially show filaments from the normal threshold and below starting with the softest one.

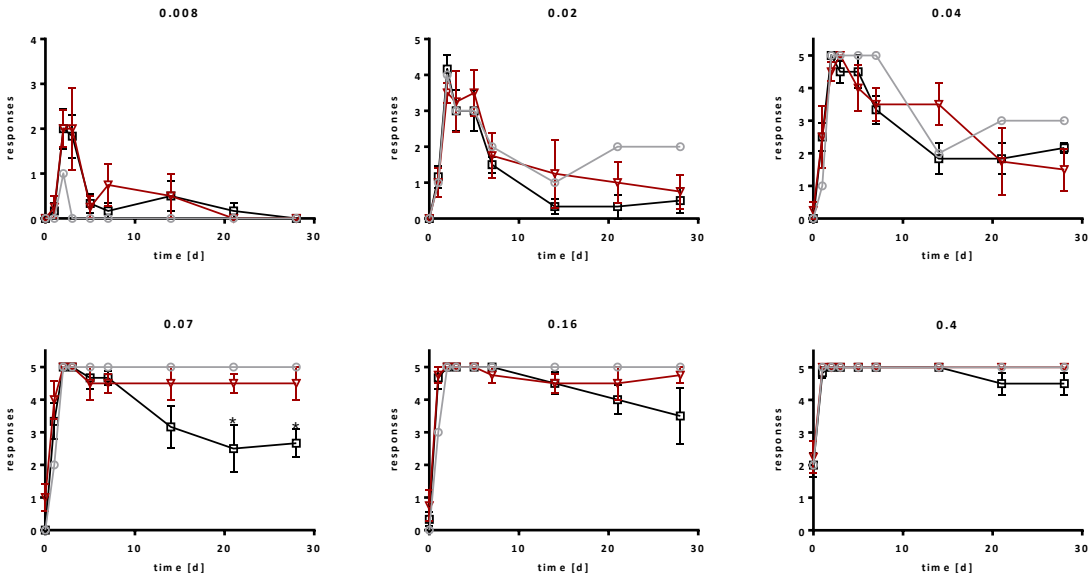

Figure 58: Single filament responses. Responses of injured paws to the 6 lowest single filaments. For a positive event, the animal hat to respond at least 3 out of 5 stimulations with the individual filament. WT in black, KO red and the HET in grey. Statistics was done using two-way-ANOVA (WT vs. KO, 0.07=*) with post hoc Bonferroni test (WT injury vs. KO injury * = $p < 0.05$). Error bars indicate standard error (SEM). Animal numbers: WT = 6; HET = 1; KO = 4.

For the single filament responses we detected a significant difference for the 0.07 g filament. The significance shows up 21 days (0.07g) after CCI. Therefore the difference between wilt-type and knock-out manifests more in the recovery phase of the CCI model.

An additional way to analyze the data is to plot the responses according to the different time-points.

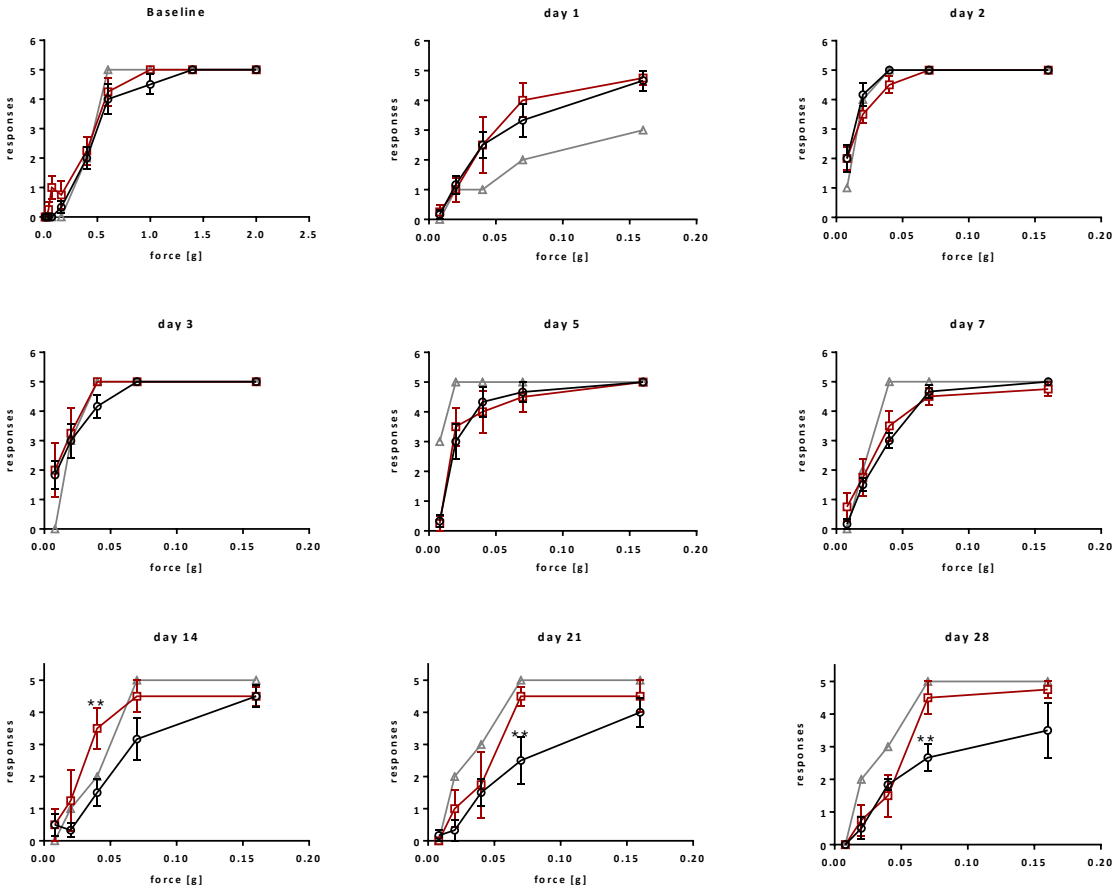

Figure 59: Single filament responses plotted by time-points. For the baseline, responses to all the filaments are plotted. Other graphs only show responses until filament 0.16g are plotted. WT in black, KO red and HET in grey. Error bars indicate standard error (SEM). Statistics was done using two-way-ANOVA (WT vs. KO; n.s.) with post hoc Bonferroni test (WT injury vs. KO injury; ** = $p < 0.01$). Animal numbers: WT = 6; HET = 1; KO = 4.

In this alternative way of plotting the results (Figure 59), we detected a significant difference starting from day 14, showing again that there is a difference in the recovery phase between WT and KO. Here the KO is more sensitive as the WT.

Having the possibility to check all the important calcium channels and subunits via qRT-PCR, we were very much interested to have a look on the RNA expression after CCI. With the knowledge from the first expression profile in naïve animals (Figure 19) we decided to only look for channels and subunits that are robustly expressed.

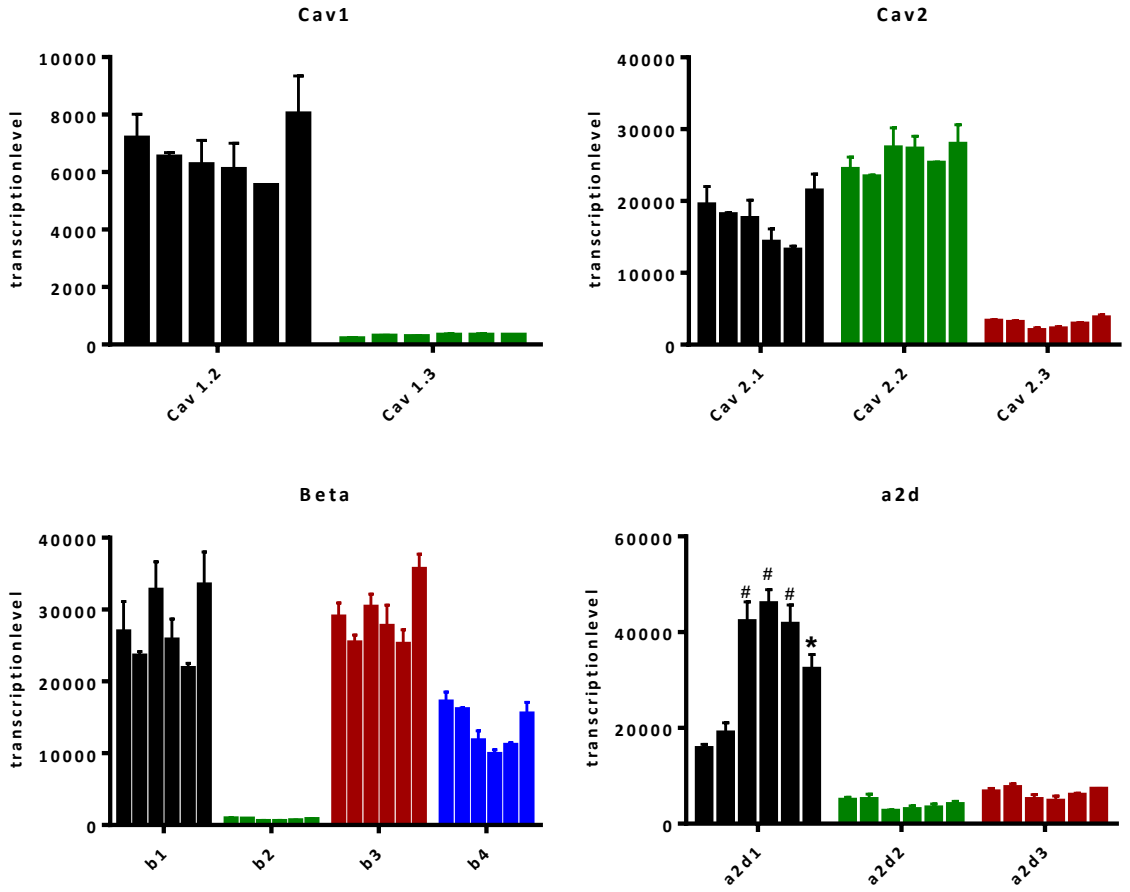

Figure 60: qRT-PCR after CCI. The different bars are time points after injury (from left to right: baseline, 2h, 2d, 7d, 14d and 28d). The Ca_V1 channels (upper left) are also called L-Type channels. The Ca_V2 channels (upper right) are also called PQ-Type (Ca_V 2.1), N-Type (Ca_V 2.2) and R-Type (Ca_V 2.3) channels. The β- (lower left) and the α2δ-subunits (lower right) are supposed to be auxiliary subunits of the pore forming Ca_V proteins. Error bars indicate standard error (SEM). For Statistics one-way-ANOVA was used (α2δ-1 = $p < 0.001$; Ca_V 1.3 and 2.3, β2 and 4 = $p < 0.01$), significances vs. baseline are indicated (* = $p < 0.05$; # = $p < 0.001$).Tissue from 3 times 3 animals was used, each measurement was 3 times replicated.

The transcription levels of the different calcium channel subunits show very different results (Figure 60) $Ca_V1.2$ channel seem to be slightly down regulated after injury but after 28 days it is back to baseline. Transcription level of $Ca_V2.1$ channel looks very much the same. $Ca_V1.3$ is only expressed in very low amounts, same as β-2 subunit. For $Ca_V2.2$, β-1 and β-2 subunit there are no real changes, the fluctuations are quite big. Interesting is the fact that $Ca_V2.3$, β-4 and α2δ-2 and -3 show the same time course of transcript expression. There is a down regulation that peaks 2-7 days after injury. The α2δ-1 subunit is the only subunit that is tremendously up-regulated after injury.

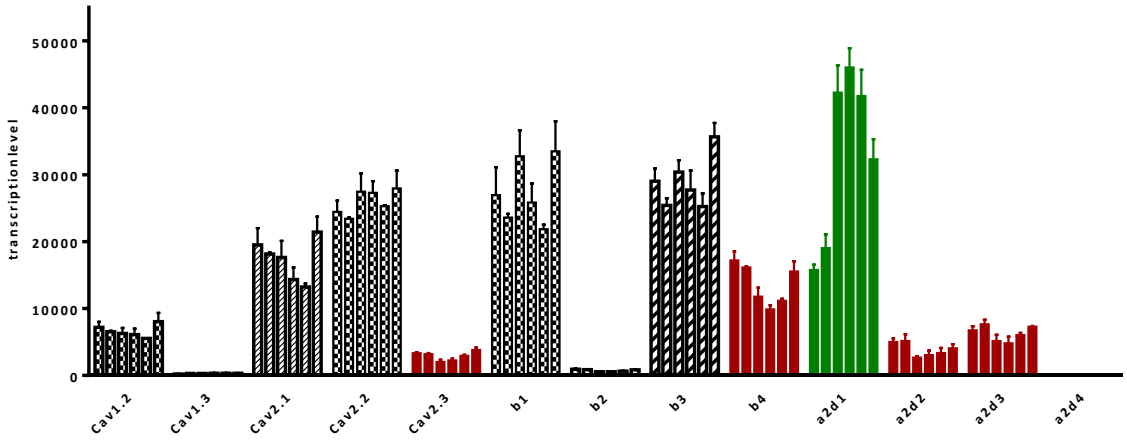

Figure 61: Overview of all transcripts checked. The colors indicated proteins that share similar expression profiles. The different bars are time points after injury (from left to right: Baseline, 2h, 2d, 7d, 14d and 28d). In red are subunits that show the same tendencies. In green the only transcript is shown, that is up-regulated. Error bars indicate standard error (SEM).Tissue from 3 times 3 animals was used; each measurement was 3 times replicated.

In the overview of all transcript levels, the already mentioned facts are even more obvious (Figure 61). The shared expression time course of the red labeled channel and subunits again might be a hint for common regulation during neuropathic pain.

3.3.2. The deficient mice show differences in initiation and maintenance phase after chronic inflammation

As a further study we wanted to know to what extent the α2δ-3 subunit is involved in inflammatory pain. Therefore we used a common standard model for this kind of pain, the CFA-model [57]. CFA stands for complete Freund's adjuvant. This substance contains heat inactivated myco-bacteria in non-metabolizable oils (paraffin and mannide monooleate), which serve as adjuvant. This substance when injected to the paw induces a strong, local and sustained inflammation. A big advantage is the good reproducibility that can be achieved with this model. After induction of inflammation the animals can be tested with the Hargreaves- and the von Frey tests same as for the phenotyping. The mice were habituated to the behavioral setups and a baseline was measured. 4h after the Injection of CFA the first time-point was recorded followed by time-points at 1, 2, 3, 5, 7, 14, 21 and 28 days after the injection. The Phases (establishment, maintenance and recovery) are quite similar as in the neuropathic pain model.

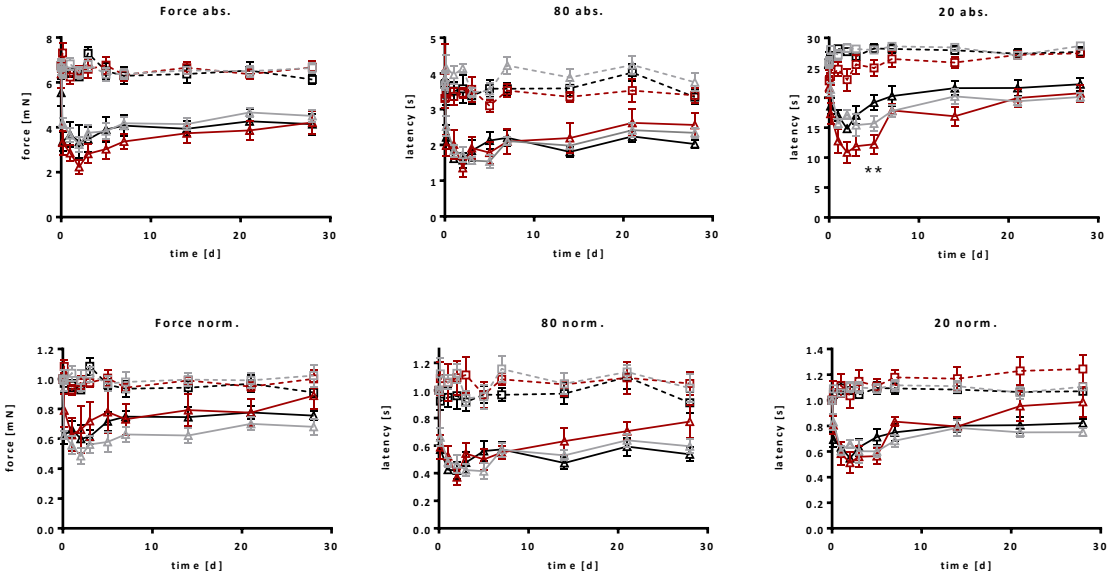

Figure 62: Behavior experiment for inflammatory pain, absolute and normalized values. WT in black, KO red and the HET in grey. Injured paws are shown with triangles and control paws with rectangles and dashed lines. Upper graphs show absolute, lower ones normalized values. Statistics was done using two-way-ANOVA (injury vs. control, WT: force, 80 and 20, abs. and norm. =***; KO: force and 20abs., and 80norm =***; 80abs. and 20norm. =**; WT injury vs. KO injury 20abs.=**) with post hoc Bonferroni test (WT injury vs. KO injury ** = $p < 0.01$; *** = $p < 0.001$). Error bars indicate standard error (SEM). Animal numbers: WT = 6, HET = 9, KO = 6.

The only difference observed in these test was again in the low intensity thermal (Hargreaves) test. But different from the neuropathic pain model here the difference occurs in the maintenance phase (day 5). After normalization of the data this significance is gone. This shows that if the already mentioned baseline difference is taken into account there will be no difference anymore (Figure 62).

For this inflammatory pain model we did additional the manual von Frey as we did for the neuropathic pain. This enables us to compare the two different chronic pain models directly in regard to allodynia and hyperalgesia.

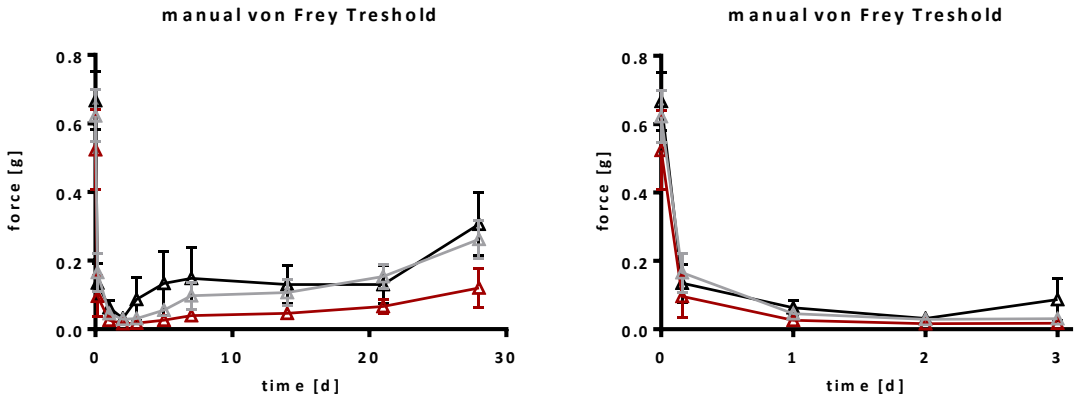

Figure 63: Mechanical thresholds after CFA. WT in black, heterozygous in grey and knockout in red. Only injured paws are plotted. WT in black, KO red and the HET in grey. The right graph is an enlargement of the first 3 days in the left graph. Error bars indicate standard error (SEM). For statistics two way ANOVA was performed (WT vs. KO n.s.) with post hoc Bonferroni test (n.s.). Animal numbers: WT = 6, HET = 9, KO = 6.

We observed no significant difference in the mechanical threshold after CFA (Figure 63) The KO mice tend to be more sensitive than the WT which is in line with the observations in the Hargreaves test.

Here again the data is plot according to the single filaments, responses over time.

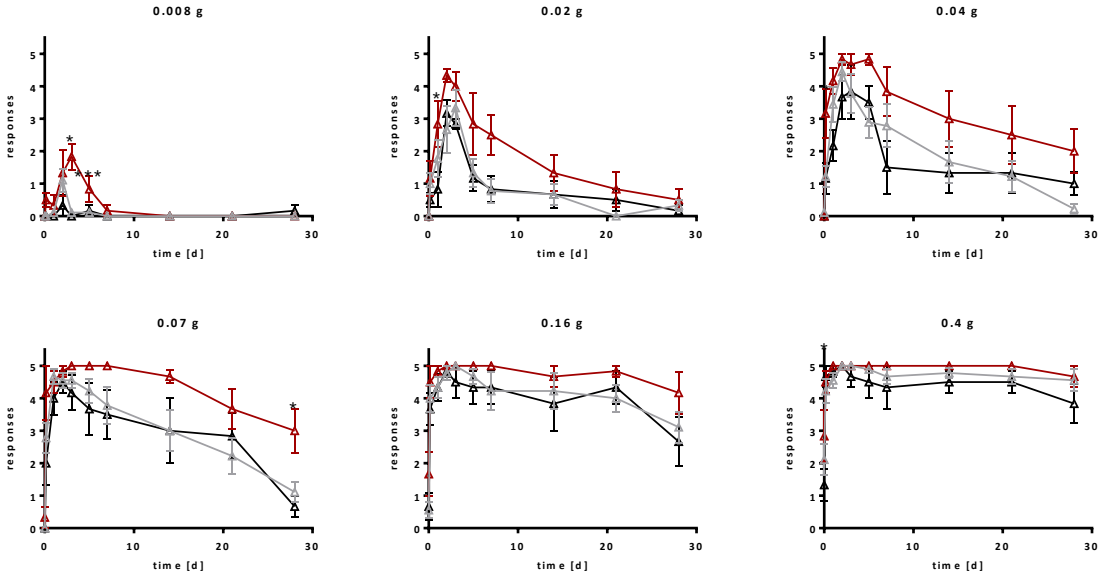

Figure 64: Single filament responses after CFA. Responses to the 6 lowest single filaments of injured paws are plotted. For a positive event, the animal hat to respond at least 3 out of 5 stimulations with the individual filament. WT in black, KO red and the HET in grey. Error bars indicate standard error (SEM). Statistics was done using two-way-ANOVA (WT vs. KO, 0.008, 0.02 and 0.04=*) with post hoc Bonferroni test (WT vs. KO * = $p < 0.05$; *** = $p < 0.001$). Animal numbers: WT = 6, HET = 9, KO = 6.

In this chronic pain model we detected differences at 0.008g (day 3 and 5), at 0.02g (day 1), at 0.07g (day 28) and 0.4g (baseline).This data shows that the mutated animals are more sensitive after CFA treatment than the WT. Again, the differences show up in the maintenance phase but also in the establishment phase. For one filament even the recovery phase seems to be affected.

Same as for the neuropathic pain model, we display the data in the alternative way, according to the different time-points.

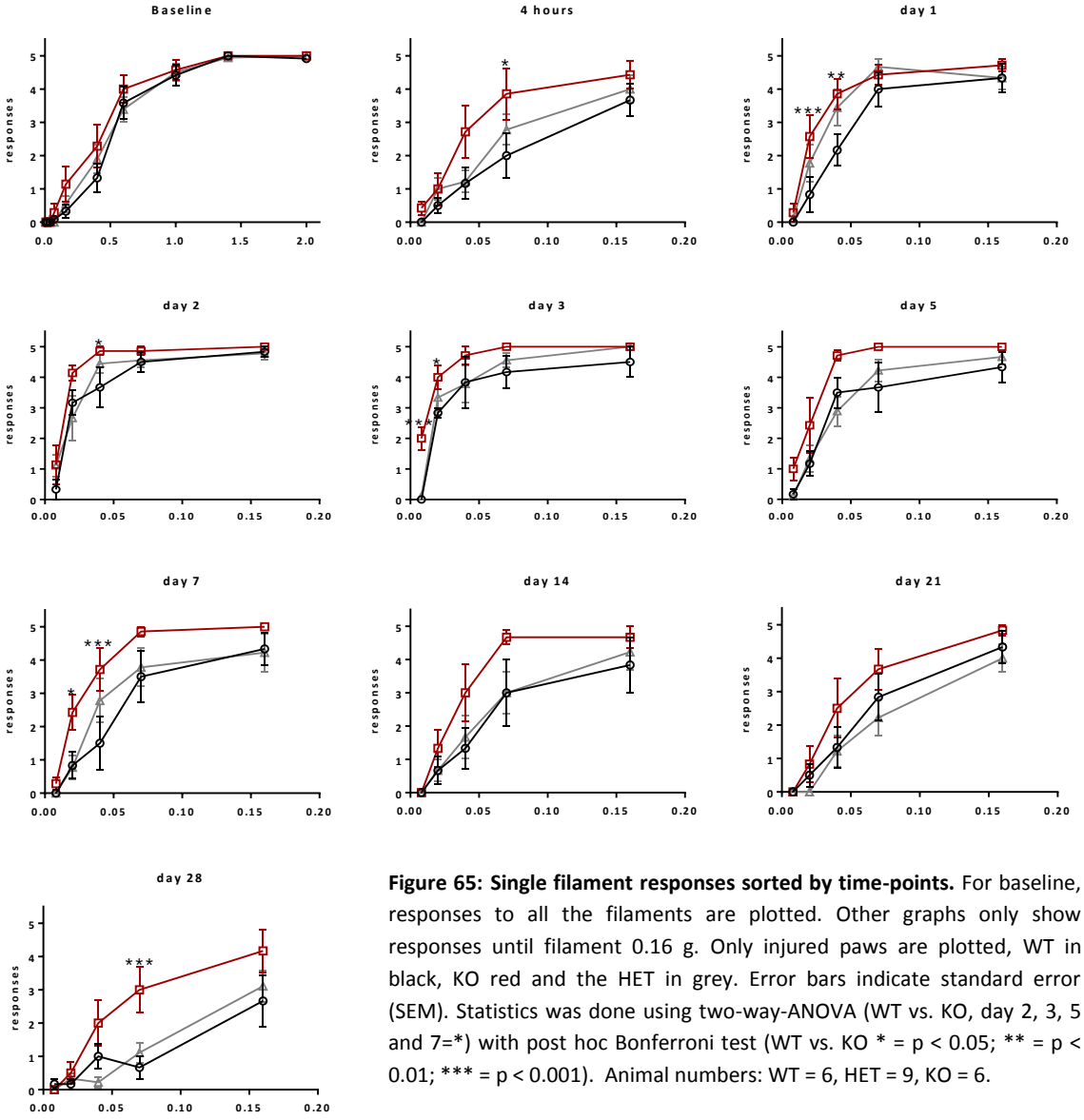

Figure 65: Single filament responses sorted by time-points. For baseline, responses to all the filaments are plotted. Other graphs only show responses until filament 0.16 g. Only injured paws are plotted, WT in black, KO red and the HET in grey. Error bars indicate standard error (SEM). Statistics was done using two-way-ANOVA (WT vs. KO, day 2, 3, 5 and 7=*) with post hoc Bonferroni test (WT vs. KO * = $p < 0.05$; ** = $p < 0.01$; *** = $p < 0.001$). Animal numbers: WT = 6, HET = 9, KO = 6.

In this way of plotting we saw no differences in baseline and at days 5, 14 and 21. For all other time-points we saw differences always showing the KO more sensitive than the WT. These results are quite in line with the results from the neuropathic pain model, the animals are more sensitive. But in case of inflammatory pain the differences occur much earlier, already after 4 hours. The differences occur quite specific for the 0.02, 0.04, and 0.07 filaments. In this range of filaments it's supposed to be allodynia, because it's below the normal threshold.

Taken together this pain behavior data shows that there is an influence of the α2δ-3 subunit. In both models the animals tend to be more sensitive for mechanical pain. In neuropathic pain the influence of the subunit seem to be more restricted to the recovery phase. In the inflammatory model the effect seems to be more evident in the initiation and maintenance phase.

4. Discussion

The somatosensory system is of quite some complexity. The idea to investigate the role of the α2δ-3 subunit in this system we got from an interesting talk mentioning the different startle phenotypes the α2δ-3 KO animals showed. This was reduced for acoustic and enhanced for tactile stimulation [52]. Given the fact that both startle pathways share most of the central nuclei and pathways this result shows that the cause for this difference should locate in the periphery. A further study showed α2δ-3 involved in heat pain in drosophila, mouse and human. But this study didn't suggest any mechanism for peripheral contribution of the α2δ-3 subunit [1]. Therefore we wanted to investigate it.

4.1. Alterations in periphery cause the hot-plate phenotype

The phenotype discovered in the hot-plate test clearly shows that the loss of α2δ-3 leads to alterations in heat perception. We saw a significant change at 50°C, for 53°C we saw the same tendency but no significance. In the study from Neely et al. [1] a significant difference at various temperatures was reported. This discrepancy might account for the fact that they used male and female mice. For our study we used exclusively male mice, to avoid the hormonal changes caused by the ovarian cycle, which could severely influence the results.

The focus in the mentioned study was on the brain, because they were not able to detect the protein in the periphery. Therefore one aim was to confirm that there is expression of α2δ-3 in the periphery. In Lack of reliable antibodies for α2δ-3 we used the advantage of the genetically modified knockout mouse. Instead of α2δ-3, the deficient mouse expresses β-galactosidase an enzyme whose activity can be monitored with a special substrate called X-gal. The active enzyme synthesizes a blue colored precipitate out of the substrate, which can easily be detected under the microscope. The β-galactosidase enzyme is driven by the promotor of α2δ-3 meaning the enzyme expression is very likely to reflect the expression pattern of the real protein of interest. Although it is just an indirect method, for us it was the only way to go.

We were able to detect prominent staining in the DRG other than the aforementioned study. This result was quite striking and after a size distribution analysis in DRG we saw that mainly big cells (>25 µm, Aβ-fibers) but also a smaller proportion of small cells (Aδ- and C-fibers) express α2δ-3. This matches perfectly with the transcriptional profiling study mentioned [47], increasing evidence that there is expression in DRG and SC. One reason, why Neely et al. could not detect expression in the periphery could be a fixation problem. Although the β-galactosidase is quite robust for fixation some care has to be

taken for the concentration of fixative as well as temperature and duration. Especially for DRG, which are quite small in size, the fixation happens rather fast so a mild fixation protocol should be chosen. Another important point is the pH of the fixation-solution which should be adjusted to pH 8 [70].

Having the expression of α2δ-3 monitored via X-gal we wanted to further proof this result. We checked several conditions (first antibody and afterwards X-gal staining and vice versa) but co-staining with antibodies and X-gal was not durable. The only antibody that worked in combination with the X-gal was the one for neurofilament (NF-200), the marker for myelinated fibers. The fact that most of the X-gal positive neurons are positive for NF-200 fits nicely with the size distribution pattern, showing that most of the big cells, which are myelinated and therefore positive for NF-200, express α2δ-3. An explanation for the failure with all other antibodies tested could be the redox reaction that has to happen for the X-gal staining. Therefore the staining-solutions are rather harsh to the tissue and alter either the binding sites for antibodies or directly kill the fluorescence very fast by the reactive environment.

For further confirmation the PCR and qRT-PCR can be counted, showing that the α2δ-3 mRNA is present in the DRG. Meanwhile other studies showed similar results with different techniques. The most interesting one was already mentioned and is from Chiu et al. [47]. In this study a genetic approach was used, to classify different subpopulations of DRG neurons for transcriptional profiling. At first separation was done according to $Na_V1.8$ (SNS) positive cells which are generally accepted as nociceptors [71] and Parv-albumin (P_{arv}) positive ones labeling most of non-nociceptive cells [72]. A further separation for the $Na_V1.8$ positive cells was done with IB4, a common marker for non-peptidergic nociceptive neurons. These three groups have been investigated with gene chip array. The results are quite impressive. In the P_{arv} positive cells there is a prominent expression of α2δ-3, which is in line with the X-gal and NF-200 stainings (both markers for big cells) we did. $Na_V1.8$ positive and IB4 negative cells show expression too but much less compared to the P_{arv} positive cell type. In $Na_V1.8$ and IB4 positive cells no α2δ-3 RNA was detected. This study shows that there is RNA in the non-nociceptive cells, meaning Aβ fibers and one special subpopulation of nociceptors, namely the IB4 negative ones. This subgroup of nociceptors also expresses the TRPV1 receptor [47].

Another interesting point for us was the expression level of α2δ-3 during development. In collaboration with a laboratory in Innsbruck we got the possibility to investigate the most relevant subunits of voltage gated calcium channels. Interestingly α2δ-3 is not down regulated during development like most other proteins of calcium channel complexes, it is up-regulated. Given the fact that a down regulation on mRNA level does not necessarily mean less protein is translated, because during development the efficiency of the whole machinery can increase, so that in adults the less mRNA can lead

to same amount of protein [73], our finding is even more interesting. There was only one further protein, the β-4 subunit, which was up-regulated too. This could be a hint to common functions for these two proteins. And more important, this is a further hint for acting apart from calcium channels, because all the pore forming subunits are down regulated. In the transcriptional profiling study the β-4 subunit is not present in the P_{arv} positive cells this is where the α2δ-3 is expressed mostly. But the β-4 is in both subpopulations of nociceptors. So both proteins are expressed in the peptidergic (IB4 negative) nociceptors [47].
In the calcium channel field there is an ongoing debate if certain subunits preferentially interact with each other. This expression profiles can give some hints about such possible interactions. For example the profiles of $Ca_V2.2$, β-1 and α2δ-2 look quite similar. This similarity supports the idea of preference for subunits to interact with each other. But having just the mRNA detected does not necessarily mean that there is protein expression.

With immuno histo chemistry we checked the free nerve endings in the skin. A pan-neuronal marker (PGP9.5, [62]) was used to stain all the nerve fibers in glabrous and hairy skin but no difference was found. This shows that the behavioral phenotype is not due to a loss of nerve fibers in the skin.

For a more mechanistic view we did electrophysiological and calcium imaging experiments. With the ex-vivo-skin nerve recording the most peripheral part of the somatosensory system can be studied. All ex-vivo-skin nerve recordings have been done by Dr. Jing Hu. The free nerve endings in skin can directly be stimulated with heat or capsaicin. In these experiments Dr. Hu was able to observe a reduction in the firing frequency in C-fibers in the deficient mice. This reduction was accompanied with an increase in the heat threshold. Both results show that a α2δ-3 deficiency already affects the most peripheral part of the somatosensory system, leading to a reduced information flow to the soma of DRG and SC. Further Dr. Hu showed that in Aδ-fibers, the second important class of nociceptive fibers, a populational change happens. In the α2δ-3 deficient mice the population of heat responding Aδ-fibers is significantly reduced. Same like for C-fibers, in Aδ-fibers less heat-information is transmitted to the SC. Because of the prominent heat phenotype in the hot-plate test Dr. Hu focused on the investigation of C- and Aδ-fibers.
These results can give a first explanation for the observed reduction in sensitivity in the hot plate test. The deficit in transmission of heat-pain information would as easiest consequence lead to an increase in the latency in the hot-plate test.

In the calcium imaging we concentrated on the thermal stimulation and the direct activation of one particular heat-receptor, namely TRPV1, according to the results we acquired so far. The decision to look for the TRPV1 heat receptor was based on the huge knowledge that has been acquired for it so far. The data from heterozygous animals in these experiments are not mentioned here, because the n-number is much lower as for WT and KO. The difference in the baseline values for the smaller nociceptors was not expected; therefore it is likely that the subunit has even some role in calcium homeostasis which has not been described so far. In the big cells (non-nociceptive) that are almost in total α2δ-3 positive there was no such difference found. Because of this difference in the baseline of nociceptors, here only the data from the normalized peak values are discussed as well as the once for the area under the curve (AUC). The direct populational comparison of nociceptors from WT and KO revealed that except for the higher concentrated capsaicin stimulus, there is always a reduction of responding cells. That is in line with the aforementioned results from the skin-nerve recordings, showing a reduction as well. For the normalized peak values in nociceptors there is always a reduction in peak size found, even for the KCl stimulus, showing that cells from deficient mice are less excitable than WT cells. This decrease in excitability could be an explanation for the observed deficiency in heat perception in the KO mice. Looking at the AUC the same phenomenon shows up. There is always a reduction, which here means the amount of calcium entering the cell is reduced.
Just looking at the cells that respond to capsaicin, the difference in baseline (WT vs. KO) was gone. That means that the calcium homeostasis at least in the TRPV1 positive nociceptors is not affected. But according to heat and capsaicin stimulation the same phenomenon occurs in this subpopulation of nociceptors. The numbers of responding cells are reduced and the normalized peak elicited by 1 µM capsaicin is reduced as well as the AUC for all stimuli.
Reduced excitability and less calcium influx in DRG neurons of α2δ-3 deficient mice clearly show that there are deficits at the soma of the neurons. Together with the skin-nerve data it further explains and confirms the reduced sensitivity observed in the hot-plate test.

For checking the electrophysiological properties of the DRG neurons Dr. Hu performed whole cell patch clamp. It has already been shown that in the deficient mice the voltage gated calcium currents are not altered [1]. But in this study only the small cells, namely the nociceptors have been investigated. We also looked for the large cells, where the subunit is prominently expressed. In Dr. Hu's patch-experiments we were not able to detect a difference in the voltage gated calcium currents. Dr. Hu even checked the T-type channels (low voltage activated calcium channels) but there was no difference too. This observation is quite different from experiments done with the other isoforms (α2δ-

1 and α2δ-2) which show clear effects on voltage gated calcium currents [74]. That might support the hypothesis that the function of α2δ-3 in these cells might be independent from the calcium channels. Looking at the IV-curve, Dr. Hu observed something unexpected. There was a reduction in the inward current, which is mainly caused by sodium channels. To our knowledge nobody ever before reported such phenomenon according to α2δ subunits. A more detailed analysis revealed other striking results so the electrically stimulated AP amplitudes in small cells are significantly reduced, which fits quite well with the calcium imaging data for the KCl stimulus. The reduced calcium influx could be due to reduced AP amplitudes. For heat or capsaicin induced APs the same holds true, still in line with the calcium imaging. The temperature threshold does not seem to be changed. That differs from the findings in the skin-nerve-recordings, were the threshold for C-fiber activation was increased. This difference might be due to the fact that in patch clamp recordings again like in calcium imaging, the recording happens at the soma. In case of the skin-nerve-recording it is the “cable” properties of the primary afferent processes that are measured. Therefore the different outcome can be explained, meaning that the soma of C-fiber neurons does not further influence the threshold-shift.
The overall message from the electrophysiological and calcium imaging data could be reduced to a quite simple statement: there is less input from the periphery reaching the SC. In last consequence this could be the reason for the delayed response in the hot plate test.

To look for further details we asked the question if there is a direct connection between α2δ-3 and the best studied heat receptor TRPV1. Using capsaicin, the agonist of TRPV1 we already saw that there are changes in the deficient mice. From the co-immuno staining for β-gal and TRPV1 we know that there are cells where both proteins (α2δ-3 and TRPV1) are expressed. In the already mentioned study for gene transcription profiling the TRPV1 transcripts were found in one subpopulation that was also positive for α2δ-3 (IB4 negative nociceptors) [47]. Unluckily we were not able to answer the question of direct interaction, because the co-IP did not work out in lack of reliable antibodies. But therefore it is still possible that there is a direct interaction between α2δ-3 and TRPV1. Both proteins have several binding sites for protein-protein interactions [41, 75, 76]. For TRPV1 it was already shown that there are several binding partners, for example cytoskeletal proteins like tubulin [77] or even ion channel subunits like the β-2 subunit of voltage gated potassium channels [31].
A possible indirect interaction between the two proteins of interest could be through cholesterol rich micro domains (lipid rafts). For the α2δ subunit it’s known that they localize in lipid rafts [40] and TRPV1 was shown to depend on cholesterol levels for

proper function [68]. In our calcium imaging experiments we checked the effect of a cholesterol depleting agent (mβCD) on the heat or capsaicin induced currents. The capsaicin induced amplitude was reduced, as expected from literature [68]. Co-expression of α2δ-3 and TRPV1 lead to the same phenomenon, a reduction in capsaicin induced calcium influx. This result is not according to the hot plate phenotype, where we saw less sensitivity in the deficient mice, therefore a co-expression of both proteins should lead to an increase in response. But for the Hargreaves test this result would fit, showing more sensitivity after depletion of α2δ-3.
On the other hand for heat stimuli we saw increased AUC values after mβCD treatment or co-expression of α2δ-3 and TRPV1, showing that the amount of calcium that enters the cells is increased for heat stimuli but not for capsaicin. Treating the co-expressed cells with mβCD seems to add up both effects and further reduce the capsaicin induced effects and further increase the AUC values. For further interpreting this data more detailed experiments would be needed. But at least there are both opposing behavioral phenotypes represented in this calcium imaging data.
In the capsaicin test we did not detect a significant difference, but at least a tendency shows that in the deficient mice the pain behavior is reduced, which fits nicely with the hot-plate phenotype.
We weren't able to answer the question of interaction in a satisfactory way, but from our data we would assume that there should be a direct or indirect interaction. Therefore further investigation is needed.

All the experiments mentioned in this paragraph support the observed hot-plate result. Therefore the mechanism turns out to be rather simple. The loss of α2δ-3 leads to alterations in the primary afferent fibers and the DRG soma that would lead to a reduced information flow to the CNS. This reduced flow causes the reduced sensitivity for heat pain.

4.2. Changes in spinal cord could explain the Hargreaves result

Until here all the discussed experiments show clear evidence to explain the measurements in the hot-plate test. But the other thermal pain test performed, showed the opposite result. In the Hargreaves test the animals are more sensitive according to WT littermates. The difference between hot-plate and Hargreaves test regards to the circuit in the SC. A pure spinal reflex, like activated in the Hargreaves test, does not involve higher brain areas. Incoming pain fibers are supposed to be directly linked to motor-neurons. For the hot-plate test, higher brain areas are involved. This difference

led us to the hypothesis that it might be the inhibitory interneurons that are a key element for explaining the Hargreaves result. According to Melzack and Wall's "gate control theory" [78], the non-nociceptive Aβ-fibers project to inhibitory interneurons which can release pain via suppression of the signals from nociceptors. This can be even done via presynaptic inhibition, recently shown by our group to play a big role in spinal signal processing [79]. Because of the higher grade of myelination, Aβ-fibers are much faster. If the α2δ-3 subunit is needed for proper function of this inhibitory circuit, a loss of it could lead to a stronger output, respectively a faster reaction of the motor system.
Beside the Hargreaves test data, the data from the manual von Frey experiments support this hypothesis. There, an increased sensitivity is shown as well. We found a sub-threshold difference for one filament (0.16g), showing the deficient mice are slightly more sensitive for mechanical stimuli. The mechanical thresholds were not changed but the tendency shows a reduction for the deficient mice.

Same as for the DRG we detected a strong X-gal staining in the SC, showing that it is widely expressed there. Because of the prominent α2δ-3 expression in the motor neurons in the ventral horn of SC we did a motor function test that did not show any alterations. This can be due to compensatory effects, meaning that the lack of α2δ-3 from the very beginning can be compensated by the system. The motor function does not seem to be affected, therefore the measured effects should regard to alterations in the circuits in the dorsal horn of the spinal cord.

Unluckily on the SC level we did not observe any changes in the morphological pattern or number of activated cells in the corresponding layers. From the literature it is known that in other species the subunit is involved in synaptogenesis [46] therefore we tried to look for morphological changes in the spinal cord. The used markers were chosen to mark excitatory synapses (VGlut1, [64]) and inhibitory interneurons (Gad67, [66]), two key elements in our hypothesis. But no obvious differences for the expression of VGlut1 and Gad67 were observed. Especially the laminar distribution was not changed. But the number of known markers in the SC is rather big and therefore an ongoing project to look for further cell types. For example VGlut3 [80] and Gad65 [81] are other markers for excitatory synapses and inhibitory interneurons.

With the c-Fos staining, activation of neurons can be monitored. After a prominent thermal stimulus there was no change compared to WT animals. This shows that the less input form the periphery not necessarily leads to less activation of downstream neurons like interneurons or projection neurons in the SC. Because the pattern of activation looks quite similar, we hypothesize that it is still the same cell-type that is activated, which according to the layer are mostly interneurons [63]. This result gives a

lot of space for interpretation. We think that it is not a change in cell type (morphological change) that in the end leads to the behavioral phenotype. We think it might be a more integrative mechanism in which the less input from the periphery is still able to activate the same amount of cells but these cells might not able to activate their follow up cells, or maybe even more important, might not be able to inhibit them. On the other hand if we think again of the distribution of the α2δ-3 subunit, it is mostly the Aβ-fibers that express it. This fiber type is normally not supposed to conduct heat induced signals. Therefore, to make the difference in the c-Fos staining visible a proper stimulus, like a mechanical should have been chosen (Figure 66).

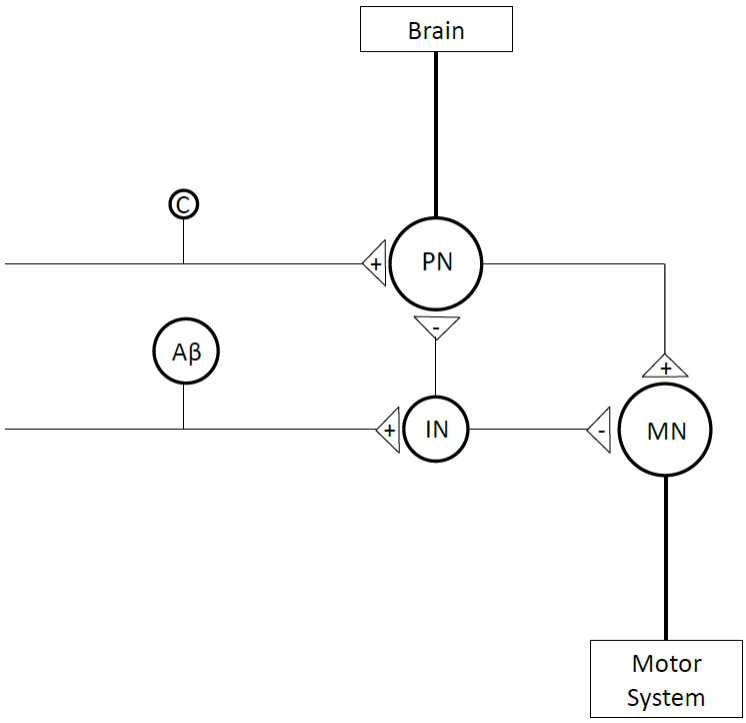

Figure 66: Scheme of connectivity in SC. The nociceptors (here C-fiber) send the signals to projection neurons (PN), which send the information either to the brain or directly to the motor neurons (MN). The Aβ-fibers contain non-noxious information and carry some to the interneurons (IN). This IN can be inhibitory like in this scheme. A loss of this inhibitory action might enhance the reflex.

The biggest interest on calcium channel subunits was put on the α2δ-1 and -2 subunits because both have binding sites for gabapentinoids, a class of drugs used for treatment of neuropathic pain [82, 83]. Looking at the mechanical induced (automatic von Frey test) acute pain after neuropathic pain induction, there was no prominent difference. Although there was a tendency for the mutant for a delayed recovery but it was not significant. After analyzing the data from the manual von Frey test, where single filaments are used, we saw differences for particular filaments. Most differences were found 14 days after injury, showing that the role for the subunit here is more in the recovery phase, meaning without α2δ-3 the recovery is delayed, so the animals stay

more sensitive. For the thermal stimuli we didn't find prominent differences (significance gone after normalization), although the tendency is the same, the deficient animals are more sensitive.

Knowing from literature that the α2δ-1 subunit is strongly up-regulated after injury [44, 84, 85], we wanted to see what happens to α2δ-3 after CCI. With the same approach like for the developmental profiling, we did after injury. And again similarities in profiles appeared. This time $Ca_V2.3$, β-4, α2δ-2 and α2δ-3 go together, raising again the question if this is one composition of calcium channel complex. Same as in the developmental profiling, again β-4 and α2δ-3 show similar profiles, strengthen the possibility of preference. The down regulation of the α2δ-3 after injury fits quite to the timescale of the hypersensitivity induced by CCI. This would strengthen the hypothesis in a way, that after injury α2δ-3 is reduced, and therefore the sensitivity increased (loss of inhibition), same as observed for the Hargreaves test. After recovery happened, when the α2δ-3 is up regulated again, the proper inhibitory circuits are reestablished.

Nowadays it's quite clear that pain elicited by chronic inflammation depends on other mechanisms than neuropathic pain [86]. Inflammation-like processes occur widely in the body, but especially after tissue injury. Chronic inflammations as they happen in neuropathies for example, are still a challenging problem in pain therapy. Because we already saw some effects of α2δ-3 depletion in neuropathic pain we expected to see some in this kind of chronic pain as well. We did the same behavioral experiments as before but this time induced an inflammation. After inflammation it seems like the differences are more in the induction and maintenance phase, which is different from the neuropathic pain results. For the heat induced acute pain there was a difference for the absolute values, but gone after normalization. In the manual von Frey the significant differences are mostly before day 7, meaning during induction and maintenance phase. Same as in the neuropathic pain model the differences occur mostly for 0.07 g or lower. This is a very low range so that it's supposed to be regarded as allodynia.

Taken all this chronic pain data we can say that there is a contribution of α2δ-3 in both forms, but here in different phases. Other support to our hypothesis comes from the already mentioned study by Pirone et al. [52] where an increased tactile startle response was observed. This suggests that the loss of inhibition in the spinal reflexes circuit leads to an increased sensitivity independent from the modality of stimulus (thermal or mechanical).

4.3. Concluding remarks / outlook

To sum up again in brief, the α2δ-3 subunit is expressed in DRG and SC. The α2δ-3 is supposed to have a role in heat sensation, as the deficient animals show deficits. There could be a connection to the TRPV1 heat receptor, shown by cells the express both proteins. Alterations in electrophysiological properties other than from calcium currents point to a possible mechanism, in which the subunit alters the properties via effects on sodium currents.

For future investigations it would be of great interest to further classify the cell-types that express α2δ-3. Also a more detailed look on the innervation pattern in the SC could elicit new insights of possible changes we weren´t able to detect so far. Here viral approaches can be of great opportunity. Injections of retrograde viral-markers into the paw can stain the primary afferents and show the presynaptic innervation pattern. Quantifications and measurements of synaptic boutons can be done in search for alterations.
For the interaction with TRPV1 the co-IP should be optimized with constructs that are easier to detect with commercially available antibodies. If there's no direct interaction found, a mass-spec analysis of the whole captured complex can be done to look for other intermediate proteins.
Having the developmental expression profile in mind there should be some knock-down studies done. In our deficient mice compensatory effects could happen. With knock-down experiments the depletion could be done in cells from adult tissue, which would reflect the acute effect of α2δ-3 in mice. Therefore a more elegant way would be a inducible knock out mouse, raising the possibility to "switch off" the protein at any developmental stage. Speaking about genetic altered mice, conditional knock out lines, having depletions in different tissues might also be a good tool to draw a clearer picture.
Further studies on the effects of α2δ-3 on sodium channels need to be done. Therefore simple co-expression experiments in patch-clamp recordings would be able to show interaction dependent alterations.

In future α2δ-3 might be of interest as a target for pain therapy, and here particularly for heat pain. So far there is no known pharmacological substance targeting α2δ-3 but the investigations haven't been that extensive yet.

5. References

1. Neely, G.G., et al., *A genome-wide Drosophila screen for heat nociception identifies alpha2delta3 as an evolutionarily conserved pain gene.* Cell, 2010. 143(4): p. 628-38.
2. Kandel, E., *Principles of neural science*. 4 ed. 2000, New York United States of America: McGraw-Hill.
3. Smith, E.S. and G.R. Lewin, *Nociceptors: a phylogenetic view.* J Comp Physiol A Neuroethol Sens Neural Behav Physiol, 2009. 195(12): p. 1089-106.
4. Basbaum, A.I., et al., *Cellular and molecular mechanisms of pain.* Cell, 2009. 139(2): p. 267-84.
5. Woolf, C.J., *What is this thing called pain?* J Clin Invest, 2010. 120(11): p. 3742-4.
6. Dib-Hajj, S.D., et al., *The Na(V)1.7 sodium channel: from molecule to man.* Nat Rev Neurosci, 2013. 14(1): p. 49-62.
7. Cummins, T.R., S.D. Dib-Hajj, and S.G. Waxman, *Electrophysiological properties of mutant Nav1.7 sodium channels in a painful inherited neuropathy.* J Neurosci, 2004. 24(38): p. 8232-6.
8. Cox, J.J., et al., *An SCN9A channelopathy causes congenital inability to experience pain.* Nature, 2006. 444(7121): p. 894-8.
9. Akopian, A.N., L. Sivilotti, and J.N. Wood, *A tetrodotoxin-resistant voltage-gated sodium channel expressed by sensory neurons.* Nature, 1996. 379(6562): p. 257-62.
10. Dib-Hajj, S., et al., *NaN/Nav1.9: a sodium channel with unique properties.* Trends Neurosci, 2002. 25(5): p. 253-9.
11. Nockemann, D., et al., *The K(+) channel GIRK2 is both necessary and sufficient for peripheral opioid-mediated analgesia.* EMBO Mol Med, 2013. 5(8): p. 1263-77.
12. Waxman, S.G. and G.W. Zamponi, *Regulating excitability of peripheral afferents: emerging ion channel targets.* Nat Neurosci, 2014. 17(2): p. 153-63.
13. Yan, X., et al., *Endogenous activation of presynaptic NMDA receptors enhances glutamate release from the primary afferents in the spinal dorsal horn in a rat model of neuropathic pain.* J Physiol, 2013. 591(Pt 7): p. 2001-19.
14. Li, J., et al., *Experimental colitis modulates the functional properties of NMDA receptors in dorsal root ganglia neurons.* Am J Physiol Gastrointest Liver Physiol, 2006. 291(2): p. G219-28.
15. Du, J., et al., *N-methyl-D-aspartate-induced excitation and sensitization of normal and inflamed nociceptors.* Neuroscience, 2003. 118(2): p. 547-62.
16. Ilkjaer, S., et al., *Effect of systemic N-methyl-D-aspartate receptor antagonist (dextromethorphan) on primary and secondary hyperalgesia in humans.* Br J Anaesth, 1997. 79(5): p. 600-5.
17. Chen, C.C., et al., *A P2X purinoceptor expressed by a subset of sensory neurons.* Nature, 1995. 377(6548): p. 428-31.
18. Honore, P., et al., *Analgesic profile of intrathecal P2X(3) antisense oligonucleotide treatment in chronic inflammatory and neuropathic pain states in rats.* Pain, 2002. 99(1-2): p. 11-9.
19. Cockayne, D.A., et al., *Urinary bladder hyporeflexia and reduced pain-related behaviour in P2X3-deficient mice.* Nature, 2000. 407(6807): p. 1011-5.
20. Julius, D., *TRP channels and pain.* Annu Rev Cell Dev Biol, 2013. 29: p. 355-84.
21. Vay, L., C. Gu, and P.A. McNaughton, *The thermo-TRP ion channel family: properties and therapeutic implications.* Br J Pharmacol, 2012. 165(4): p. 787-801.

22. Caterina, M.J., et al., *The capsaicin receptor: a heat-activated ion channel in the pain pathway.* Nature, 1997. 389(6653): p. 816-24.
23. Belmonte, C., J.A. Brock, and F. Viana, *Converting cold into pain.* Exp Brain Res, 2009. 196(1): p. 13-30.
24. Story, G.M., et al., *ANKTM1, a TRP-like channel expressed in nociceptive neurons, is activated by cold temperatures.* Cell, 2003. 112(6): p. 819-29.
25. Kwan, K.Y., et al., *TRPA1 contributes to cold, mechanical, and chemical nociception but is not essential for hair-cell transduction.* Neuron, 2006. 50(2): p. 277-89.
26. Caterina, M.J., et al., *Impaired nociception and pain sensation in mice lacking the capsaicin receptor.* Science, 2000. 288(5464): p. 306-13.
27. Goswami, C., et al., *Rapid disassembly of dynamic microtubules upon activation of the capsaicin receptor TRPV1.* J Neurochem, 2006. 96(1): p. 254-66.
28. Liapi, A. and J.N. Wood, *Extensive co-localization and heteromultimer formation of the vanilloid receptor-like protein TRPV2 and the capsaicin receptor TRPV1 in the adult rat cerebral cortex.* Eur J Neurosci, 2005. 22(4): p. 825-34.
29. Zhang, X., L. Li, and P.A. McNaughton, *Proinflammatory mediators modulate the heat-activated ion channel TRPV1 via the scaffolding protein AKAP79/150.* Neuron, 2008. 59(3): p. 450-61.
30. Kim, A.Y., et al., *Pirt, a phosphoinositide-binding protein, functions as a regulatory subunit of TRPV1.* Cell, 2008. 133(3): p. 475-85.
31. Bavassano, C., et al., *Identification of voltage-gated K(+) channel beta 2 (Kvbeta2) subunit as a novel interaction partner of the pain transducer Transient Receptor Potential Vanilloid 1 channel (TRPV1).* Biochim Biophys Acta, 2013. 1833(12): p. 3166-75.
32. Bean, B.P., *Classes of calcium channels in vertebrate cells.* Annu Rev Physiol, 1989. 51: p. 367-84.
33. Bourinet, E., et al., *Calcium-permeable ion channels in pain signaling.* Physiol Rev, 2014. 94(1): p. 81-140.
34. Simms, B.A. and G.W. Zamponi, *Neuronal voltage-gated calcium channels: structure, function, and dysfunction.* Neuron, 2014. 82(1): p. 24-45.
35. Brice, N.L. and A.C. Dolphin, *Differential plasma membrane targeting of voltage-dependent calcium channel subunits expressed in a polarized epithelial cell line.* J Physiol, 1999. 515 (Pt 3): p. 685-94.
36. Letts, V.A., et al., *The mouse stargazer gene encodes a neuronal Ca2+-channel gamma subunit.* Nat Genet, 1998. 19(4): p. 340-7.
37. Rauck, R.L., et al., *Intrathecal ziconotide for neuropathic pain: a review.* Pain Pract, 2009. 9(5): p. 327-37.
38. Cheng, J.K., et al., *Effects of intrathecal injection of T-type calcium channel blockers in the rat formalin test.* Behav Pharmacol, 2007. 18(1): p. 1-8.
39. Catterall, W.A., *Structure and regulation of voltage-gated Ca2+ channels.* Annu Rev Cell Dev Biol, 2000. 16: p. 521-55.
40. Davies, A., et al., *The alpha2delta subunits of voltage-gated calcium channels form GPI-anchored proteins, a posttranslational modification essential for function.* Proc Natl Acad Sci U S A, 2010. 107(4): p. 1654-9.
41. Dolphin, A.C., *The alpha2delta subunits of voltage-gated calcium channels.* Biochim Biophys Acta, 2013. 1828(7): p. 1541-9.
42. Calderon-Rivera, A., et al., *Identification of a disulfide bridge essential for structure and function of the voltage-gated Ca(2+) channel alpha(2)delta-1 auxiliary subunit.* Cell Calcium, 2012. 51(1): p. 22-30.

43. Anantharaman, V. and L. Aravind, *Cache - a signaling domain common to animal Ca(2+)-channel subunits and a class of prokaryotic chemotaxis receptors.* Trends Biochem Sci, 2000. 25(11): p. 535-7.
44. Bauer, C.S., et al., *The increased trafficking of the calcium channel subunit alpha2delta-1 to presynaptic terminals in neuropathic pain is inhibited by the alpha2delta ligand pregabalin.* J Neurosci, 2009. 29(13): p. 4076-88.
45. Eroglu, C., et al., *Gabapentin receptor alpha2delta-1 is a neuronal thrombospondin receptor responsible for excitatory CNS synaptogenesis.* Cell, 2009. 139(2): p. 380-92.
46. Kurshan, P.T., A. Oztan, and T.L. Schwarz, *Presynaptic alpha2delta-3 is required for synaptic morphogenesis independent of its Ca2+-channel functions.* Nat Neurosci, 2009. 12(11): p. 1415-23.
47. Chiu, I.M., et al., *Transcriptional profiling at whole population and single cell levels reveals somatosensory neuron molecular diversity.* Elife, 2014. 3.
48. Cole, R.L., et al., *Differential distribution of voltage-gated calcium channel alpha-2 delta (alpha2delta) subunit mRNA-containing cells in the rat central nervous system and the dorsal root ganglia.* J Comp Neurol, 2005. 491(3): p. 246-69.
49. Ling, F., et al., *The molecular and cellular basis of taste coding in the legs of Drosophila.* J Neurosci, 2014. 34(21): p. 7148-64.
50. Iossifov, I., et al., *De novo gene disruptions in children on the autistic spectrum.* Neuron, 2012. 74(2): p. 285-99.
51. Wong, A.M., et al., *Characterization of CACNA2D3 as a putative tumor suppressor gene in the development and progression of nasopharyngeal carcinoma.* Int J Cancer, 2013. 133(10): p. 2284-95.
52. Pirone, A., et al., *alpha2delta3 is essential for normal structure and function of auditory nerve synapses and is a novel candidate for auditory processing disorders.* J Neurosci, 2014. 34(2): p. 434-45.
53. Schlick, B., B.E. Flucher, and G.J. Obermair, *Voltage-activated calcium channel expression profiles in mouse brain and cultured hippocampal neurons.* Neuroscience, 2010. 167(3): p. 786-98.
54. Zimmermann, K., et al., *Phenotyping sensory nerve endings in vitro in the mouse.* Nat Protoc, 2009. 4(2): p. 174-96.
55. Sakurada, T., et al., *The capsaicin test in mice for evaluating tachykinin antagonists in the spinal cord.* Neuropharmacology, 1992. 31(12): p. 1279-85.
56. Bennett, G.J. and Y.K. Xie, *A peripheral mononeuropathy in rat that produces disorders of pain sensation like those seen in man.* Pain, 1988. 33(1): p. 87-107.
57. Iadarola, M.J., et al., *Enhancement of dynorphin gene expression in spinal cord following experimental inflammation: stimulus specificity, behavioral parameters and opioid receptor binding.* Pain, 1988. 35(3): p. 313-26.
58. Wanajo, A., et al., *Methylation of the calcium channel-related gene, CACNA2D3, is frequent and a poor prognostic factor in gastric cancer.* Gastroenterology, 2008. 135(2): p. 580-90.
59. Barrot, M., *Tests and models of nociception and pain in rodents.* Neuroscience, 2012. 211: p. 39-50.
60. Yeomans, D.C. and H.K. Proudfit, *Nociceptive responses to high and low rates of noxious cutaneous heating are mediated by different nociceptors in the rat: electrophysiological evidence.* Pain, 1996. 68(1): p. 141-50.

61. Yeomans, D.C., V. Pirec, and H.K. Proudfit, *Nociceptive responses to high and low rates of noxious cutaneous heating are mediated by different nociceptors in the rat: behavioral evidence.* Pain, 1996. 68(1): p. 133-40.
62. Thompson, R.J., et al., *PGP 9.5--a new marker for vertebrate neurons and neuroendocrine cells.* Brain Res, 1983. 278(1-2): p. 224-8.
63. Todd, A.J., *Neuronal circuitry for pain processing in the dorsal horn.* Nat Rev Neurosci, 2010. 11(12): p. 823-36.
64. Fremeau, R.T., Jr., et al., *The expression of vesicular glutamate transporters defines two classes of excitatory synapse.* Neuron, 2001. 31(2): p. 247-60.
65. Persson, S., et al., *Distribution of vesicular glutamate transporters 1 and 2 in the rat spinal cord, with a note on the spinocervical tract.* J Comp Neurol, 2006. 497(5): p. 683-701.
66. Mackie, M., et al., *Distribution and colocalisation of glutamate decarboxylase isoforms in the rat spinal cord.* Neuroscience, 2003. 119(2): p. 461-72.
67. Bullitt, E., *Expression of c-fos-like protein as a marker for neuronal activity following noxious stimulation in the rat.* J Comp Neurol, 1990. 296(4): p. 517-30.
68. Liu, M., et al., *TRPV1, but not P2X, requires cholesterol for its function and membrane expression in rat nociceptors.* Eur J Neurosci, 2006. 24(1): p. 1-6.
69. Kilsdonk, E.P., et al., *Cellular cholesterol efflux mediated by cyclodextrins.* J Biol Chem, 1995. 270(29): p. 17250-6.
70. Weiss, D.J., D. Liggitt, and J.G. Clark, *Histochemical discrimination of endogenous mammalian beta-galactosidase activity from that resulting from lac-Z gene expression.* Histochem J, 1999. 31(4): p. 231-6.
71. Liu, Y., et al., *VGLUT2-dependent glutamate release from nociceptors is required to sense pain and suppress itch.* Neuron, 2010. 68(3): p. 543-56.
72. Hippenmeyer, S., et al., *A developmental switch in the response of DRG neurons to ETS transcription factor signaling.* PLoS Biol, 2005. 3(5): p. e159.
73. Gingold, H. and Y. Pilpel, *Determinants of translation efficiency and accuracy.* Mol Syst Biol, 2011. 7: p. 481.
74. Canti, C., A. Davies, and A.C. Dolphin, *Calcium Channel α2δ Subunits: Structure, Functions and Target Site for Drugs.* Current Neuropharmacology, 2003. 1(3): p. 209-217.
75. Liao, M., et al., *Structure of the TRPV1 ion channel determined by electron cryo-microscopy.* Nature, 2013. 504(7478): p. 107-12.
76. Dolphin, A.C., *Calcium channel auxiliary alpha2delta and beta subunits: trafficking and one step beyond.* Nat Rev Neurosci, 2012. 13(8): p. 542-55.
77. Goswami, C., et al., *Identification and characterization of a Ca2+ -sensitive interaction of the vanilloid receptor TRPV1 with tubulin.* J Neurochem, 2004. 91(5): p. 1092-103.
78. Melzack, R. and P.D. Wall, *Pain mechanisms: a new theory.* Science, 1965. 150(3699): p. 971-9.
79. Chen, J.T., et al., *Presynaptic GABAergic inhibition regulated by BDNF contributes to neuropathic pain induction.* Nat Commun, 2014. 5: p. 5331.
80. Draxler, P., et al., *VGluT3(+) primary afferents play distinct roles in mechanical and cold hypersensitivity depending on pain etiology.* J Neurosci, 2014. 34(36): p. 12015-28.
81. Lorenzo, L.E., et al., *Spatial and temporal pattern of changes in the number of GAD65-immunoreactive inhibitory terminals in the rat superficial dorsal horn following peripheral nerve injury.* Mol Pain, 2014. 10: p. 57.

82. Gee, N.S., et al., *The novel anticonvulsant drug, gabapentin (Neurontin), binds to the alpha2delta subunit of a calcium channel.* J Biol Chem, 1996. 271(10): p. 5768-76.
83. Gong, H.C., et al., *Tissue-specific expression and gabapentin-binding properties of calcium channel alpha2delta subunit subtypes.* J Membr Biol, 2001. 184(1): p. 35-43.
84. Newton, R.A., et al., *Dorsal root ganglion neurons show increased expression of the calcium channel alpha2delta-1 subunit following partial sciatic nerve injury.* Brain Res Mol Brain Res, 2001. 95(1-2): p. 1-8.
85. Luo, Z.D., et al., *Upregulation of dorsal root ganglion (alpha)2(delta) calcium channel subunit and its correlation with allodynia in spinal nerve-injured rats.* J Neurosci, 2001. 21(6): p. 1868-75.
86. Guo, D. and J. Hu, *Spinal presynaptic inhibition in pain control.* Neuroscience, 2014. 283: p. 95-106.

6. Acknowledgements

First I would like to thank my supervisor Dr. Jing Hu for the project and the years of very good guidance, as well as the possibility to realize own ideas.
Second I would like to thank my colleagues in our group for all the good conversations and discussions. Having such lovely people around makes work and life much easier.
I also want to thank all the people from other labs in the Werner Reichardt Centre for Integrative Neuroscience (CIN) that helped either with advice or equipment. Wherever I went, people were always friendly and calm.
Huge thanks go to the administrative office of CIN for all the help with the bureaucracy.

For technical support I would like to thank Dr. Hubert Kalbacher (Tübingen) for the help with the α2δ-3 antibody, as well as Dr. Gerald Obermair (Innsbruck) for sharing the α2δ-3-HA construct and giving the possibility to do the qRT-PCR in his lab. Further I want to thank Dr. T. Münch and Prof. Dr. J. Engel for providing the α2δ-3 deficient mouse line.
For the α2δ-3-T7 construct I want to thank Dr. Akiyama (Japan) as well as Dr. P Heppenstall (Italy) for the TRPV1 construct. For the TRPV1 antibody I would like to thank Prof Dr. D. Julius (San Francisco) and Prof. Dr. J Siemens (Heidelberg). Another thank goes to Susanne Tulke, a former rotation Student for the support with the calcium imaging in HEK cells.

I further would like to thank the people from the Graduate School for Cellular & Molecular Neuroscience. The organization is very good and the support always helpful.

At the end I want to thank my parents, because they always supported me and thereby made it possible for me to do all this.